



Carlo Cappello

# **Theory of Decision Based on Structural Health Monitoring**



UNIVERSITY OF TRENTO - Italy  
Department of Civil, Environmental  
and Mechanical Engineering



Doctoral School in Civil, Environmental and Mechanical Engineering  
Topic 1. Civil and Environmental Engineering - 29th cycle

Doctoral Thesis - June 2017

Carlo Cappello

# **Theory of Decision Based on Structural Health Monitoring**

**Supervisor**

Prof. Daniele Zonta, University of Trento, Italy



Except where otherwise noted, contents on this book are licensed under a Creative  
Common Attribution - Non Commercial - No Derivatives  
4.0 International License

University of Trento  
Doctoral School in Civil, Environmental and Mechanical Engineering  
*<http://web.unitn.it/en/dricam>*  
Via Mesiano 77, I-38123 Trento  
Tel. +39 0461 282670 / 2611 - *[dicamphd@unitn.it](mailto:dicamphd@unitn.it)*

*To Valentina*



# Abstract

The average age of strategic constructions in the Western world is becoming higher and higher. Many of these structures need inspection, maintenance or replacement, resulting in significant costs. The accurate estimate of structural condition can make operators optimize the allocation of resources. Nowadays, the progress of technology and machine learning has made structural health monitoring appealing to the agencies that manage important structures. This has encouraged the research community in the study of new structural health monitoring methods. In spite of this, the use of monitoring data is often disregarded by practitioners, who still prefer to gather more information and then act based on experience. Similarly, unlike the design of civil structures, the design of structural health monitoring systems is carried out based on heuristics rather than on rigorous evaluations of the expected monitoring system effectiveness. In this doctoral thesis, I apply expected utility theory for the development of decision support systems to be used in structural health monitoring and I develop a procedure for the design of structural health monitoring systems that follows the scheme of semi-probabilistic structural design. The use of monitoring data in a decision support system that implements expected utility theory financially optimizes the management of civil structures. The proposed monitoring system design method enables practitioners to design monitoring systems using their experience and guarantees that the installation of a monitoring solution is financially convenient. I present the mathematical formulation for monitoring-based decision support systems and monitoring system design. Then, I propose the numerical algorithms for the development of monitoring-based decision support systems and solutions for monitoring data analysis. Finally, the proposed methods are applied to three case studies, which enabled me to discuss the application in real life and the hypotheses. The applications show also the feasibility of the proposed approaches and test the numerical algorithms.



# Acknowledgements

Many professors, graduate students, postdocs and practitioners contributed, directly or indirectly, to my doctoral activity. First, I wish to thank my advisor at the University of Trento, Prof. Daniele Zonta, the finest professor I have ever met. His enthusiasm, inspiration and advices were of great help during my research. Then, I would like to thank also my advisor at Princeton University, Prof. Branko Glisic, for his cooperation and constant support during my activity at the SHMlab. I extend my gratitude also to Prof. Jerome Lynch, University of Michigan, for his words of encouragement and for the interesting conversations that we had during numerous international conferences. My appreciation also goes to Prof. Matteo Pozzi, Carnegie Mellon University, for his countless comments and for the help in the development of this thesis.

Among those at the Department of Civil, Environmental and Mechanical Engineering of the University of Trento, I wish to thank Prof. Oreste S. Bursi for his support during my doctoral program and his cooperation in publishing many scientific papers. Special thanks also go to my colleagues: Denise Bolognani, Dr. Emiliano Debiasi, Dr. Davide Trapani, Andrea Verzobio, Daniel Tonelli, Anna Groff, Claudia Sguazzardo and Angela Beltempo.

I wish to thank also my former colleagues at Princeton University: Dr. Yao Yao, Dr. Dorotea Sigurdardottir, Kaitlyn Kliever, Dr. Hiba Abdel-Jaber, Jack Reilly and Xi Li. For their insightful comments, I am grateful also to the researchers that I had the pleasure to meet during my studies: Prof. Marco Torbol, Dr. Chiara Ferrari, Dr. David Rodenas, Dr. Xuan Zhu (Peter), Dr. Chenhao Jin (Colin), Shanwu Li, Dr. Rosana Martinez, Jay Wu, Dr. Alessandro Cattaneo, Katherine Flanigan, Dr. Gaston Fernandois-Cornejo, Wai Kei Ao (Vincent), Prof. Vito Racic, Dr. Katrien Van Nimmen, Dr. Pedram Hesam, Dr. Francesco Cavalieri, Dr. Andrea Titi, John Mowat, Eric Lee, Kyeongtaek Park, Dr. Thomas Gernay, Dr. George Lederman, Ilaria Capraro, Gabriela Graziani and Dr. Antonio Perazzo.

The decision support system of Colle Isarco Viaduct was carried out under the research agreement between Autostrada del Brennero SpA/Brennerautobahn AG and

the University of Trento. The financial contribution of Autostrada del Brennero is greatly acknowledged. I also wish to thank personally all those who cooperated with me in the design of the Colle Isarco structural health monitoring system: Stefano Vivaldelli, Antonello Cassani, Paolo Joris, Marco Morgante, Gianluca Liberi, Franco Lucchini, Duilio Guizzetti, Dr. Daniele Posenato, Dr. Alessio Bonelli, Alessandro Massarotto, Luca Mazzi, Alessio Vallarini, Klemens Raffl and Francesca Parolini.

The monitoring project of Adige Bridge was funded by the Department of Public Works of the Autonomous Province of Trento. For this project, I would like to thank specifically Luciano Martorano, Stefano Ravis, Matteo Pravda, Paolo Nicolussi Paolaz, Dr. Nicola Tondini and Saulo Maestranzi.

The research project of Wayne Overpass was in part supported by SMARTEC SA, Switzerland, the USDOT-RITA UTC Program, grant no. DTRT12-G-UTC16, enabled through the Center for Advanced Infrastructure and Transportation (CAIT) at Rutgers University, and the National Science Foundation under grant no. CMMI-1362723. The project was also supported by the International Bridge Study (IBS) within the Long-Term Bridge Performance (LTBP) Program put forth by the Federal Highway Administration (FHWA) in the United States. The opinions and conclusions expressed in this thesis are those of the author and do not necessarily reflect the views of USDOT-RITA or the National Science Foundation. This project was realized with the important support and great help of: Drexel University, Emin Aktan, Frank Moon, Jeff Weidner, New Jersey Department of Transportation (NJDOT), Eddy Germain, PB Americas Inc., Michael Morales, Rutgers University, Ali Maher, Nenad Gucunski, IBM partners and Joseph Vocaturo.

Last but not least, I wish to express my sincere gratitude to my family, Giovanna, Tiziano and my girlfriend Valentina, for their unconditional support, understanding and love. I could not have been surrounded by better people.

---

# Table of contents

Abstract .....	i
Acknowledgements .....	iii
List of abbreviations.....	ix
1 Introduction .....	1
1.1 Motivation .....	2
1.2 Decision theory for structural health monitoring .....	2
1.3 Decision theory for the design of structural health monitoring systems .....	4
1.4 Overview .....	5
2 State of the art .....	9
2.1 Data acquisition and structural health monitoring .....	9
2.2 Bayesian logic for structural health monitoring .....	11
2.3 Expected utility theory for structural health monitoring .....	14
2.3.1 Expected utility theory for societal decision-making .....	16
2.3.2 Criticisms to expected utility theory .....	19
2.3.3 Expected utility theory for the value of information .....	20
2.3.4 Optimal sensor placement based on expected utility theory .....	24
2.3.5 Risk-based inspection planning and infrastructure management .....	25
2.4 Conclusions about the analysis of the state of the art.....	27
3 Decision-making based on structural health monitoring data .....	29
3.1 Problem of structural health monitoring .....	29
3.2 Glossary.....	31

3.3 Bayesian inference.....	34
3.3.1 Bayes’ theorem for parameter estimation.....	36
3.3.2 Bayes’ theorem for model selection .....	37
3.4 Expected utility theory for SHM-based decisions .....	39
3.5 Solution of the structural health monitoring problem.....	44
3.6 Summary of the chapter.....	45
4 Software for decision support systems .....	47
4.1 Storing the data.....	48
4.2 Preparing the samples .....	49
4.2.1 Filter for morning measurements.....	51
4.2.2 Temperature compensation without temperature measurements.....	52
4.2.3 Temperature compensation with temperature measurements.....	53
4.3 Computational Bayesian inference .....	54
4.4 Importance sampling .....	56
4.5 Summary of the chapter.....	59
5 Structural health monitoring system design .....	61
5.1 Problem of structural health monitoring system design .....	61
5.2 Value-of-information-based monitoring system design .....	63
5.3 Performance-based monitoring system design .....	67
5.3.1 Demand.....	70
5.3.2 Capacity .....	72
5.3.3 Capacity of the monitoring system concept versus prior information....	73
5.3.4 Capacity of the monitoring system concept versus demand.....	74
5.3.5 Calculation of the expected covariance using uncertainty propagation..	74
5.3.6 Monte Carlo algorithm for the expected covariance matrix .....	76
5.4 Summary of the chapter.....	78
6 Decision support system for Colle Isarco Viaduct .....	79

---

6.1 Colle Isarco Viaduct.....	79
6.2 Monitoring system.....	86
6.2.1 Topographic network .....	86
6.2.2 Resistance thermometers.....	96
6.2.3 Fiber-optic sensors .....	102
6.2.4 Networking.....	107
6.3 Temperature data.....	109
6.4 Temperature compensation .....	113
6.5 Displacement data .....	120
6.6 Decision support system.....	126
6.6.1 Single-stage decisions .....	126
6.6.2 Multi-stage decisions.....	132
6.7 Discussion of results and conclusions .....	137
7 Single-parameter monitoring system design: the case study of Adige Bridge....	141
7.1 Adige Bridge .....	141
7.2 Monitoring system concept .....	146
7.3 Structural model and distributions .....	147
7.4 Pre-posterior analysis and results.....	149
7.5 Discussion of results and conclusions .....	151
8 Multi-parameter monitoring system design: the case study of Wayne Overpass	153
8.1 Wayne Overpass.....	153
8.2 Monitoring system concept .....	157
8.3 Structural model and distributions .....	158
8.4 Pre-posterior analysis and results.....	162
8.5 Discussion of results and conclusions .....	164
9 Summary and conclusions.....	169
References .....	173



# List of abbreviations

ADC	analog-to-digital converter
AMH	adapting Metropolis-Hastings
CM	condition monitoring
COV	coefficient of variation
CSV	comma-separated value
CVSI	conditional value of sample information
DSS	decision support system
ENGS	expected net gain of sampling
EUT	expected utility theory
EVSI	expected value of sample information
FBG	fiber Bragg grating
FEM	finite element model
FFT	fast Fourier transform
FIM	Fisher information matrix
FOS	fiber-optic sensor
GDP	gross domestic product
IM	infrastructure management
KDE	kernel density estimation
LQI	life quality index
LVDT	linear variable differential transformer
MCMC	Markov chain Monte Carlo
MIS	most informative subset
OSP	optimal sensor placement
RC	reinforced concrete
RTD	resistance temperature detector
RUC	road user cost
SD	standard deviation
SHM	structural health monitoring
SQL	structured query language

TMCMC	transitional Markov chain Monte Carlo
TSV	tab-separated value
UPS	uninterruptible power supply
VOI	value of information
VSL	value of statistical life

# 1 Introduction

The definition of *structural health monitoring* (SHM) is still debated by the academic community and there is not a unique view of the SHM paradigm. Sohn *et al.* [1] refer to SHM as “the process of implementing a damage detection strategy for aerospace, civil and mechanical engineering infrastructure”. The monitoring process can be periodic or continuous. In some cases, SHM is implemented to monitor the long-term behavior of a structure; in others, SHM seeks information about a structure immediately after extreme events such as earthquakes or structural rehabilitation. SHM of civil structures has been increasingly studied since the early 1980s [2] due to the financial benefits that may result from obtaining precise information on the structural state. Major applications of SHM include offshore installations, buildings, towers, nuclear installations, tunnels and bridges [3]. In 2010, 69,223 out of 604,485 (11.5%) bridges longer than 20 ft in the US were structurally deficient [4]. As the average age of bridges and strategic constructions in the Western world becomes higher, many of these structures need frequent inspections, maintenance and replacement. Whereas, in the past, maintenance and repair were performed on as-needed basis [5], an accurate estimate of the structural condition can assist operators in a better allocation of the available resources and save money as a result. SHM can be used to evolve from the current *time-based maintenance* philosophies into the more cost effective *condition-based maintenance* philosophies [2]. Moreover, SHM can expedite the current slow post-earthquake risk assessment procedures [6]. However, SHM of civil structures is also challenging. Monitoring of rotating and reciprocating machinery, known as *condition monitoring* (CM), is easier mostly due to minimal environmental variability and well-defined damage types [2]. Monitoring of civil structures is difficult because of the complexity of the structural elements, variability of the damage scenarios and uncertainty that affects the properties of materials. Instrumenting strategic constructions usually requires a large number of sensors and expensive instrumentation, while the monitoring data will be inevitably affected by the uncertainties due to the operational and environmental conditions [7].

Nowadays, progress in technology and new methods for data analysis have made SHM appealing to operators of important structures and have encouraged the academic community in research. After the development of robust sensor technology, the aim of research is now to integrate SHM into more comprehensive processes such as damage prognosis [6] and to interpret structural performance while supplementing the subjective human element [3].

## 1.1 Motivation

In SHM, decision-making is usually regarded as something that automatically follows a prediction of the structural state (e.g. “damaged” or “undamaged”). However, the output of monitoring systems is always affected by severe uncertainty, which is not always quantified. Thus, operators and technicians often employ precious resources to acquire further information on the monitored structure and eventually take decisions disregarding the output of the monitoring system. Instead, in order to optimize the use of monitoring data, the acquisition of measurements should be followed by an analysis that considers the costs of the available management policies and of the outcomes.

A similar inconvenience also affects the design process of SHM systems. The decision to implement SHM, the type of sensors and the number of sensors in the monitoring system concept are usually chosen based on the designer’s experience and heuristics. Instead, the identification of the SHM strategy to apply should follow a quantitative evaluation of the tentative monitoring systems.

In this thesis, I formalize a model of *decision support system* (DSS) that optimizes the use of monitoring data and drives decision-making based on SHM. Moreover, I develop a novel approach to the design of SHM systems (*monitoring system design*), which follows the scheme of semi-probabilistic structural design and enables practitioners to quantitatively predict the effectiveness of a monitoring system concept.

## 1.2 Decision theory for structural health monitoring

DeGroot, in 1970, defined *decision theory* as “the class of statistical problems in which the statistician must gain information about certain critical parameters in order

to be able to make effective decisions in situations where the consequences of his decisions will depend on the values of these parameters” [8]. In SHM, we acquire information to improve our capabilities of taking optimal decisions about the monitored structure, where the term “optimal decisions” usually stands for financially optimal choices. From this perspective, it seems logic that an application of decision theory must follow the acquisition of data from any monitoring system. Nevertheless, in the SHM community, optimal strategies are often considered as implicitly provided by the probabilistic analysis of the data, without the need to consider the financial outcomes of each possible scenario that concerns the monitored structure.

In the development of the SHM-based DSS that I propose in §3 of this dissertation, I apply *expected utility theory* (EUT) after Bayesian inference in order to identify financially optimal decisions. As a result, the optimal actions are identified not only based on the condition of the monitored structure, but also on the direct and indirect costs that would follow the realization of each possible structural state. By implementing EUT along with Bayesian inference, we obtain a function – a classifier – that correlates the measurements provided by the monitoring system to financially optimal actions. With this classifier, SHM-based DSSs identify the actions that have to be suggested to operators immediately after the measurements coming from the monitoring system become available.

The paradigm of SHM proposed by Farrar *et al.* [9] includes:

1. operational evaluation;
2. data acquisition, normalization and cleansing;
3. feature selection and information condensation;
4. statistical model development for feature discrimination.

*Operational evaluation* is performed before the installation of the monitoring system and it analyzes the condition in which SHM will be implemented. In *data normalization*, changes in the measurements due to damage are separated from the effects of operational and environmental conditions. In *data cleansing*, we select the data that will be considered in the following steps. *Feature selection* and *feature discrimination* are processes in which damage sensitive features are calculated from the monitoring data in order to identify possible damages. The proposed SHM-based DSS takes the monitoring data as an input after normalization and cleansing, and suggests financially optimal actions as an output.

In continuous monitoring, the proposed DSS is included in the SHM process as depicted by Figure 1.1. The measurements, which are observations provided by the monitoring system, come from the sensors installed on the monitored structure. The reading units control the sensors and acquire the raw monitoring data, which are stored in a database. Then, an algorithm performs data normalization and cleansing. Finally, the DSS identifies the optimal action the agent should undertake.

### 1.3 Decision theory for the design of structural health monitoring systems

Monitoring design is a decision problem in which we have to choose a monitoring system concept among different alternatives, including the option of not to do SHM at all. Since the purchase and installation of a monitoring system always come with a cost, we may think that the optimal choice will be always the decision to install the cheapest monitoring system or not to install any system. However, SHM improves our capabilities of taking wiser choices, and repeatedly taking wiser choices leads to an average reduction in our expenditure. With EUT, we can quantify the *value of information* (VOI) a monitoring system concept is expected to produce by calculating the change in the expected utility due to the measurements. This approach was proposed by Raiffa and Schlaifer [10] for the design of experiments and requires an estimate of the financial outcomes that follow each combination of actions and structural conditions, besides the definition of a utility function that encodes the risk aversion of the decision-maker. These outcomes usually include direct and indirect costs of structural damages, which are difficult to calculate before damages actually occur. Practitioners need a more straightforward approach, similar to that of semi-probabilistic structural design in which they calculate the capacity of the structure and compare the capacity with a value of demand prescribed by a design code.

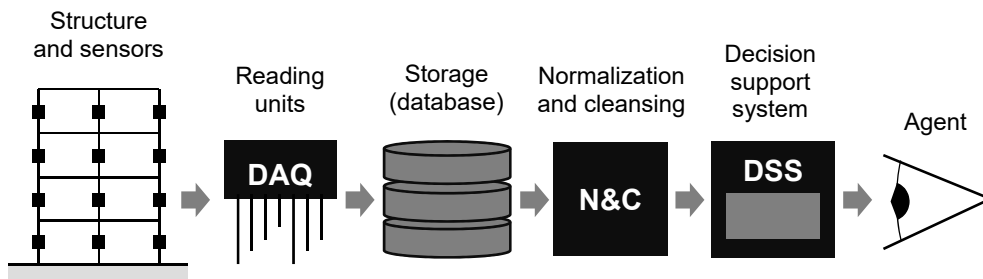


Figure 1.1. Holistic view of structural health monitoring with decision support system.

In §5 of this dissertation, I start from the Raiffa and Schlaifer's VOI-based experiment design approach and I develop a performance-based monitoring system design method, whose scheme reproduces that of semi-probabilistic structural design. In the proposed formulation, the VOI is used to calculate the required monitoring effectiveness, which I call *demand*. However, the demand can be prescribed by design codes for groups of monitoring problems. Instead, the calculation of the effectiveness of a monitoring system concept, which I call *capacity*, can be done through pre-posterior analysis using only Bayesian logic. Demand and capacity can be assessed in the design stage, before actually installing the monitoring system. Demand and capacity are defined as the covariance matrix that characterize the distribution of the state parameters *a posteriori*, i.e. after the acquisition of the monitoring data. These parameters are damage sensitive features of the monitored structure such as stiffness or natural frequencies, which usually have a physical meaning. Therefore, besides the proposed performance-based monitoring system design follows an approach that is similar to semi-probabilistic structural design, it also lets designers judge the calculated values of capacity and demand with their experience, as they do in structural design.

## 1.4 Overview

In the second chapter of this thesis, I review the current state of the art that regards the implementation of Bayesian logic and EUT in SHM. The analysis of the literature evidenced the need to formalize the application of EUT to decision-making based on monitoring data and the need for a method of monitoring system design applicable by practitioners in real life.

In §3 of this thesis, I introduce the reader to the problem of SHM-based decision-making, define the variables involved in the analysis of monitoring data, present Bayesian inference and describe the application of EUT to SHM. The result of the implementation of Bayesian inference and EUT in SHM is a classifier that provides the financially optimal action based on any possible combination of the measurements. In the next chapter, I present some considerations on data normalization, data cleansing and on the development of SHM-based DSS programs working with real-life data. Then, I propose the algorithms for Bayesian inference and Monte Carlo simulation that are contained in the literature.

In §5 of this thesis, I develop the performance-based monitoring system design method. After the formal definition of capacity and demand, I propose: (1) a criterion for the comparison of capacity and demand; (2) a Monte Carlo simulation that can be used to predict the capacity of a monitoring system concept based only on information *a priori*; (3) an approach based on the propagation of uncertainty that can be used in some circumstances instead of the Monte Carlo simulation for the calculation of capacity.

In §6 of this dissertation, I show the development of a SHM-based DSS for a real-life case study – Colle Isarco Viaduct. The viaduct, located in northern Italy, was instrumented with prisms for topographic measurements, resistance thermometers (RTDs) and fiber-optic sensors (FOSs) for the measurement of strain. The technical specifications and the architecture of the monitoring system is presented. Then, I present the measurements of displacement acquired from the topographic network and the temperature measurement obtained using the RTDs. The strain measurements of the FOSs were not available when this thesis was written. Finally, I show the equation of the classifier that defines the DSS and present some results.

In §7 and §8 of this thesis, I apply the performance-based monitoring system design method to two real-life case studies. In the first example, the case study regards SHM of the cables of Adige Bridge, a cable-stayed bridge located in northern Italy. The monitoring system design was aimed to predict the uncertainty that would affect the tension of the stay cables, if the tension were calculated from the orthogonal accelerations provided by a single accelerometer. Since the tension can be calculated based only on the first mode of the cable, I could calculate the expected standard deviation of the tension through both the Monte Carlo simulation and uncertainty propagation.

In §8 of this dissertation, the case study is the monitoring problem of Wayne Overpass. The neutral axis and the curvature of one of the bridge steel girders had to be calculated based on two measurements of strain acquired from FOSs. In this case, the expected performance of the monitoring system concept could not be calculated using uncertainty propagation. However, I could use the Monte Carlo simulation to implement performance-based monitoring system design and I could apply the method for the comparison of capacity and demand that I proposed for multi-parameter monitoring system design.

A summary and a discussion of the results are presented at the end of each chapter except in this introduction. Finally, the last chapter presents comprehensive

conclusions, discusses the outcome of the research project and predict the impact of the findings.



## 2 State of the art

SHM is a research topic that has gained a lot of interest by academia and industry in the last decades. Some definitions and approaches to SHM are universally accepted by the research groups in the field, others change from school to school. There is a strong tradition of research in sensor technology and in damage identification techniques, but some groups also focus on probabilistic data analysis and *optimal sensor placement* (OSP). In this chapter, I introduce the terms that are commonly used in SHM and the SHM techniques that mostly influenced the current state of the art.

During my research project, I used EUT to define a framework for the development of SHM-based DSSs and a performance-based monitoring system design procedure. My literature review is focused on those approaches that were closely related to my research interests and on those contributions that were based on the same theories. In the first section, I present the meaning of *structural monitoring* of civil structures. Then, I introduce Bayesian logic in the form recognized by most of the literature sources and, finally, I present the current state of the art, the issues and the criticisms that regard the implementation of EUT in SHM.

### 2.1 Data acquisition and structural health monitoring

SHM should not be regarded as the mere use of a *monitoring system*. Whereas running a monitoring system just indicates the acquisition of data through the sensor and the physical devices installed on the structure, SHM includes the acquisition of data as well as the analysis performed in order to assist the agent who manages the monitored structure.

Every monitoring system includes sensors and reading units, which are the components that affect the precision of the raw measurements. Sensors are sources of information and are considered as objects that convert physical quantities (e.g. displacements, strains, temperatures and accelerations) into a signal that can be

acquired by the reading units. Depending on the quantity that needs to be measured, there are different types of sensors that can be employed. A monitoring system can have one or more reading units, depending on the number of sensors that need to be connected and on how many types of sensors are in the system. The reading units acquire the signal (e.g. voltage or light spectrum) from the sensors and usually encode the signal into a stream of bits that is sent to a computer. Reading units and computers communicate through an interface. Examples of interfaces are *Ethernet*, *universal serial bus* (USB), *Wi-Fi* and *RS-232*. The choice of sensors and reading units influences the type and precision of measurements. In the following, I present the well-established definitions of the most important specifications of monitoring systems [11].

- *Sensitivity*. The sensitivity is the ratio between the variations in the encoded measurements and the variations of the measured quantity.
- *Resolution*. The resolution is the minimum variation in the measured quantity that can be detected by the monitoring system.
- *Accuracy*. The accuracy is defined as the difference between the measurements and the true values of the measured quantity. In statistical terms, it represents a systematic error or bias.
- *Precision*. The precision is the random error that affects each measurement. It can be quantified, for example, by repeating the measurement without changing the measured quantity and can be expressed with the standard deviation of the resulting distribution. The precision indicates the magnitude of noise introduced by a particular combination of sensors and reading units.
- *Dynamic range*. It is the ratio between the maximum and the minimum magnitude of the measured quantity that can be read by the monitoring system.
- *Stability*. It is the property of the monitoring system to provide the same measurement in time, without variations in the measured quantity. If a monitoring system configuration is not stable, the measurements may experience a drift in time and their accuracy decreases.

After data are collected by the reading units, the raw measurements are stored in a database and are ready for the analysis.

What should happen to the monitoring data after the acquisition depends on the approach. There is not a unique opinion on if SHM should include also techniques for *damage prognosis* [6], the calculation of the probability of failure, or the calculation of a classifier for the automatic identification of financially optimal decisions. Lynch [12] distinguishes SHM from *structural monitoring* based on whether the *structural health* is actually assessed. Sigurdardottir, in her doctoral thesis [13], analyzed [2], [14] and [15], and formulated this general definition of SHM: “SHM is the process of periodically or continuously measuring structural parameters over time and the analysis of these measurements with the ultimate aim of providing actionable information of structural health and performance for engineers, managers and decision-makers”. These views forecast that comprehensive SHM approaches should include the estimation of structural reliability and support decision-making. However, this is in contrast to what happens in real life.

Herein, I propose a general framework for SHM-based DSSs that implement well-established probability theories in order to analyze monitoring data and identify optimal management strategies. In the development of SHM-based DSSs, first, monitoring data are analyzed by application of Bayesian logic for the identification of the structural condition. Then, EUT is used to identify the financially optimal action that the decision-maker should take. In the next section, I present and discuss the state of the art regarding Bayesian inference, focusing on the application to SHM. Then, I present the contributions in the field of SHM that already uses EUT for bridge management and OSP.

## **2.2 Bayesian logic for structural health monitoring**

For a long time, the SHM community studied techniques for damage identification from the deterministic standpoint. The effort of researchers focused on the development of novel sensor technologies and accurate models, while damage identification was performed based on heuristics or using non-probabilistic classifiers such as *support vector machines* [16]. Although the use of accurate models and effective sensors is crucial, all the deterministic approaches are useless if we need to know the uncertainty of the results (e.g. the probability of failure) or if we need to take decisions based on monitoring data. Moreover, we cannot judge whether a SHM

method is worth the costs simply by quantifying model and sensor precision. Instead, we need to take into account all the sources of uncertainty and study how much the uncertainties together affect the damage sensitive features.

The application of Bayesian logic enables us to take into account different sources of information about the monitored structure in order to estimate the most probable structural state and the probability of misclassification, i.e. the confusion matrix [17] of the structural states. In SHM based on Bayesian logic, the information about a monitored structure may come from one or more of the following sources:

1. measurements acquired by sensors;
2. documents that are produced during the structural design of the monitored structure;
3. reports containing results of inspections and tests performed on the monitored structure;
4. engineering experience.

With Bayesian logic, we can merge all the sources above and obtain the most precise estimate of the structural condition, which is provided by means of probability distributions. Using the Bayes' theorem [18], the probability of the *state* of the structure after acquiring *data* is proportional to the product between the probability of observing the *data*, given the *state*, and the probability of the *state* before acquiring the *data*:

$$p(\textit{state}|\textit{data}) \propto p(\textit{data}|\textit{state}) \cdot p(\textit{state}). \quad (2.1)$$

The probability  $p(\textit{state}|\textit{data})$  is called *posterior probability*,  $p(\textit{data}|\textit{state})$  is called *likelihood function* and  $p(\textit{state})$  is called *prior probability*. The *data* are usually a vector or matrix with the measurements coming from sensors, tests or inspections. The *state* is usually a class that represents the condition of the structure (e.g. “damaged” and “undamaged”) or a set of parameters that represent the structural condition (e.g. stiffness and natural frequencies).

Bayesian logic has been increasingly implemented in SHM techniques during the last decade. Vanik *et al.* [19] showed how Bayesian statistics can be used to estimate, from modal parameters, the probability that the stiffness of a structure is less than a predefined value. Where the “predefined value” was a fraction of the model

stiffness corresponding to the pristine condition of the structure. Vanik *et al.* assumed that a high value of probability of reduction in the stiffness indicates a damage. A later paper by Beck and Au [20] proposed an adaptive *Markov chain Monte Carlo* (MCMC) simulation, based on the Metropolis-Hastings algorithm, to perform Bayesian inference for system identification based on SHM data. Enright and Frangopol [21] showed how engineering judgement and data from inspections performed on *reinforced concrete* (RC) bridges can be combined to assess the bridge conditions. Enright and Frangopol studied how inspections influence the estimate of time-variant bridge reliability. Sohn and Law [22] present a Bayesian probabilistic approach for damage detection, with application to multi-storey frame structures. In their work, they applied Bayesian logic to assess the modal parameters of structures and then to identify the locations of multiple damages.

In 2015, I published a paper [23], in which we showed how data from a SHM system can be combined with knowledge coming from different sources, including *finite element model* (FEM) analysis results, topographic surveys and engineering experience. Sources other than measurements were included through prior probabilities in the Bayesian inference. We analyzed the strain data of the cables of Adige Bridge, a cable-stayed bridge built in 2008 near Trento, Italy. The aim of the analysis was to study the results provided by Bayesian inference when the Bayes' theorem is implemented in SHM for the calculation of both the parameters that characterize the structural behavior and the structural state class. In the paper, we showed that the influence of the information considered through prior probabilities is big when we take into account little data and decreases as more measurements are included in the Bayesian inference.

Despite the effectiveness in the identification of the most probable structural state, the output of Bayesian inference *per se* does not help operators in managing a structure. Indeed, decision-making does not depend only on the probability of the different scenarios that may occur; decisions are affected also by the consequences that may result from different combinations of actions and scenarios. When a bridge manager evaluates the option of closing a bridge that may be damaged with a certain probability, he considers also the loss due to a possible structural failure and the loss due to a possible bridge downtime. This is the reason why SHM-based DSSs that provide suggestions for structure management must be based on a model that takes into account losses and gains that may result from all the possible scenarios. EUT does exactly this and it has been employed already in medicine and finance, in which

the estimation of costs and probabilities is easier due to a large amount of available data.

### 2.3 Expected utility theory for structural health monitoring

In order to develop SHM-based DSSs that assist operators by providing actions regarding the management of the monitored structure (e.g. “do nothing”, “close the bridge”, “send inspector”), we need to implement EUT and take into account the losses that may result from all the possible combinations of actions and structural states. With EUT, the weight of each available action depends on:

1. the probability of the scenarios that may occur after the action is taken;
2. the quantification of the consequences of each possible scenario;
3. the risk aversion of the stakeholders.

In SHM, scenarios are defined by structural states, and their probability can be calculated using Bayesian inference, as presented in the preceding section. The quantification of the consequences is called *outcome* and is usually expressed in monetary terms, i.e. with a currency such as EUR or USD. Outcomes usually include direct costs, like the cost of repairing the structure or sending an inspector to take more information about the structural state, and indirect costs, which include the impact of events on environment and society. The stakeholders can be identified in structure owners, infrastructure operators, technicians or in the society. Their risk aversion is considered by using a function called *utility function*, which takes an outcome as an argument and provides the corresponding *utility* as an output. More formally, if each  $state_i$  occurs with a probability  $p(state_i)$  and results in  $cost_i$  after that action  $a$  is taken, the *expected utility* of  $a$  is

$$EU_a = \sum_{i=1}^N p(state_i) \cdot utility(cost_i), \quad (2.2)$$

where  $N$  is the number of states that may occur after action  $a$ . The *utility* decreases as its argument – the *cost* – increases.

EUT can improve risk-based management [24] by taking into account the risk aversion of the stakeholders. In classic risk-management, decisions are driven by *risk*,

which is the expected monetary value associated with a given action  $a$  [25] [26]. The technical definition of risk is:

$$risk_a = \sum_{i=1}^N p(state_i) \cdot cost_i . \quad (2.3)$$

The use of expected utility instead of risk enables us to identify management policies that better satisfy the stakeholders when the consequences of some events are extreme. Therefore, since the structural failure of a bridge or a building involves major direct and indirect costs, EUT is more appropriate in the management of civil engineering facilities.

EUT was born as an attempt to model people's preferences in presence of uncertain consequences. Daniel Bernoulli, in his article of 1738 [27] [28], argued that people in risk-taking situations did not seek the maximum monetary expected value. Instead, he suggested that the choices must have been based on the utility of the monetary consequences rather than the monetary consequences themselves [29]. He also defined the expected utility as "moral expectation". The promising Bernoulli's hypothesis evolved in the von Neumann-Morgenstern utility theory [30] presented in 1947. The literature contains many contributions showing applications of EUT, but also criticisms to the axiomatic hypotheses of the theory. The most suitable formulation of EUT for the application to SHM is that proposed by Raiffa and Schlaifer [10], in 1961. The axiom of the von Neumann-Morgenstern utility theory, represented by (2.2), was used also in civil engineering and SHM. However, a rigorous framework that implements EUT in SHM for the development of SHM-based DSSs is still missing.

The civil engineering community has implicitly recognized EUT for years. For example, Melchers, in his seminal book *Structural Reliability Analysis and Prediction* [31] published in 1999, states that "the objective of structural engineering design may be taken reasonably to be the maximization of the total expected utility of the structure [...]". The formulation of VOI proposed by Raiffa and Schlaifer [10] has attracted those operating in SHM because it enables us to assign a monetary value to the measurements acquired through a monitoring system. Therefore, it enables who designs the system to optimize his monitoring strategy [32]. The use of VOI for assessing the advantages of monitoring has been extensively recognized by the SHM community [33] [34].

EUT has been applied also to the optimization of *infrastructure management* (IM) policies. However, although the approaches to IM available in the literature appear to be rigorous and might be successfully applied for major structures, the feasibility of implementing complex models in SHM-based DSSs for operational civil structures still remains to be proven. For its practical application, I found very inspiring the methodology proposed by Mussi [35] in his article “Putting value of information theory into practice: a methodology for building sequential decision support systems”. Mussi proposed a method in which a DSS is built by extending a Bayesian network with nodes representing the utility. In this way, the solution of the network automatically provides the expected value of each choice, because each choice affects the variables in the system that in turn provide the optimal action. Although Mussi’s method is very straightforward and looks promising for application in real life, it is not in a form that can be implemented in SHM. Due to the high magnitude of *aleatory* and *epistemic* uncertainties [36] involved in the SHM problems, any DSS that is based on SHM data needs a general robust framework for the quantification of the probability of each structural state. Moreover, the probabilistic analysis of structures usually requires complex models that need to be studied with numerical algorithms or, when they are very complex, with approximated metamodels [37].

In the following sections, I present the issues that may arise from the application of EUT to SHM and the tentative solutions that are proposed by the literature. Finally, I review the contributions in which EUT was applied to civil engineering and SHM.

### **2.3.1 Expected utility theory for societal decision-making**

Decision-making in civil engineering should “serve society and hence the individuals of society to maintain or even improve their quality of life” [38]. One of the questions that usually arises when we implement EUT in civil engineering problems regards the consideration of the impact of structural failure on the environment, society and of intergenerational effects. Faber and Maes [38] identified the classes of consequences that concern civil engineering structures, such as buildings or bridges. An event may occur with a certain probability that can be calculated using either Bayesian inference or a simple frequentist approach. If the considered event occurs, the structure, the environment and the society may be positively or negatively

affected. This happens also with a certain probability, given that the event occurs. Faber and Maes [38] call these types of events *exposure events*, and they identify three type of consequences: one direct and two indirect. They define *vulnerability* the probability of an event that results in direct consequences. *Direct consequences* are: immediate casualties, physical damage of the assets and damage of the environment. They define *robustness* the capability of the structure to avoid indirect consequences. Indirect consequences are of two types. The first type are “event-imposed consequences”, which are loss of performance and costs due to the impossibility of using the structure or part of the structure. The second type are “societal-imposed consequences”, which occur due to the change of the public perception about the exposure events. Whereas direct consequences are relatively easy to assess, it is difficult to quantify the indirect costs that stem from the impossibility of using a structure, and it is even more difficult to quantify the impact of damages on the environment or the losses due to a change in the public opinion.

SHM is usually performed for the management of bridges and other strategic structures, whose behavior is of huge impact on the environment and society. Therefore, I reviewed the methods that can be used to estimate the indirect costs that result from closing a road bridge and address the indirect costs of casualties. The indirect costs of a bridge downtime are the sum of the *road user costs* (RUCs). The cost of human life is estimated by evaluating the impact of deaths or major injuries on the society’s *gross domestic product* (GDP).

### **Road user costs**

Closing a bridge forces the infrastructure operator to reroute the traffic that was going to use the structure. The costs of forced traffic flow due to lane closures, road closure and posted speed are not direct costs to the manager’s budget, but affect the society because are costs to the road users. In sustainable decision-making, the total expected cost to the road users stemming from an action of the infrastructure operator should be considered.

There are reliable procedures to calculate the RUCs due to road or lane closures that may result from altering the traffic flow on a monitored bridge. These RUCs can be used in SHM-based decision-making to calculate the utility of those conditions in which the traffic on the monitored structure is limited.

According to the *Road User Cost Manual* of the *New Jersey Department of Transportation* [39], the RUCs depend on the vehicle class. For simplicity, traffic can

be divided in cars and trucks. For all traffic, five major sources of RUCs can be reliably assessed.

- *Work zone delay.* The cost due to work zone delay stems from the additional time required to traverse a work zone. This cost usually occurs because a speed lower than normal speed is posted in the work zone.
- *Queue delay.* The cost from queue delay is due to the additional time required to creep through a queue when the traffic flow is forced.
- *Queue idling vehicle operating costs.* Queue idling vehicle operating costs are those costs that are due to the irregular driving (“stop and go”) throughout the queue. These operating costs depend on the cost of fuel, oil, maintenance and depreciation [39].
- *Circuity vehicle operating costs.* These costs occur when the traffic flow is forced in a detour. Circuity vehicle operating costs are those costs that stem from the additional distance imposed by the detour.
- *Circuity delay.* The cost from circuity delay is due to the time required to drive throughout the excess distance imposed by a detour.

### Life quality and cost of casualties

Faber and Rackwitz [40] proposed to use the *life quality index* (LQI) in order to account for human life in decision-making. Assuming a GDP pro capita  $g$ , a life expectancy  $l$ , and that  $w$  is the fraction of  $l$  devoted to paid work, the LQI  $L_q$  is

$$L_q = \frac{g^q \cdot l}{q}, \quad q = \frac{w}{1-w}. \quad (2.4)$$

By following the approach of Faber and Rackwitz [40], we can maximize the LQI and obtain that, in the stationary point, small variations  $\delta g$  in the pro-capita GDP and small variations  $\delta l$  in the life expectancy are related through the equation

$$-\delta g = \frac{g}{q} \cdot \frac{\delta l}{l}. \quad (2.5)$$

Now, let me say that a choice of costs  $z$  changes the life expectancy of  $\Delta l$ , but does not change  $w$  and  $g$ . Based on (2.5), we can conclude that it improves the overall life quality of a society if

$$z < \frac{g}{q} \cdot \frac{\Delta l}{l}. \quad (2.6)$$

Otherwise, the same choice worsens the overall life quality of a society. The right-hand term of (2.6) can be used in EUT application as a quantification, in monetary terms, of variations in the life expectancy.

The presented approach is a simplified model, which assumes that the value of a human life in a society is quantified through the contribute of an individual to the GDP. Equation (2.6) also assumes that the contribute to the GDP of an individual decreases in proportion to the life expectancy. This results from the fact that  $g$  and  $q$  are constants in (2.6). To me, this is reasonable for small values of  $\Delta l$ , and (2.6) cannot be used to calculate the costs of casualties. Instead, the cost of human losses should be regarded as the *value of statistical life* (VSL), which ideally represents the amount of money that a society evaluates a human life. The VSL mostly depends on the country. Faber and Rackwitz [40] report that, for societies in the western world, the VSL is in the range of €4 million to €6 million. The US Food and Drug Administration estimated the VSL in US\$7.9 million; the US Department of Transportation estimated the VSL in UD\$6 million [41]. In spite of this estimates, the analysis of society decision-making often results in much lower VSL. Ashenfelter and Greenstone [42], found that, in 1987, the US government raised the speed limit from 55 mph to 65 mph. This increased the fatality rate by 35%, but also resulted in saving of 125,000 hours per lost life. If the saved time were evaluated in terms of average hourly wage and assuming that the government had correctly forecasted the fatality rate increment, we would obtain that the VSL implicitly assumed during the decision of rising the speed limit was US\$1.54 million (in 1997 USD).

### 2.3.2 Criticisms to expected utility theory

The application of EUT, even with complex utility functions, leads to financially optimal choices but may not reproduce the behavior of actual decision-makers. Thus, implementing EUT makes agents maximize the overall utility, but may not satisfy

them. This inconvenience has several reasons. First, there are some aspects of decision-making that cannot be reproduced by a decision tree. Kahneman and Tversky [43], in 1979, found that people usually disregard the components of a choice that are shared among the alternatives. When their subjects took an action, they implicitly followed a decision tree that is different from the tree that we would have built to solve the decision problem using EUT. This phenomenon, called *isolation effect*, may be observed when decision-makers have to choose an alternative that will be effective after the realization of a state that is still unknown. In this situation, the decision-makers usually imagine that the state has been already observed, instead of taking into account the probabilities of the different realizations.

People also attribute a weight to each choice that is non-linear with respect to the actual probability. They underweight outcomes that are probable (i.e. may or may not occur), whereas they overweight outcomes whose probability is extreme. This phenomenon, called *certainty effect*, is exploited in gambling because people overestimate little probabilities of getting huge rewards. In *prospect theory* [43] and *cumulative prospect theory* [44], proposed by Kahneman and Tversky, the *isolation effect* and the *certainty effect* are taken into account by: (1) editing the decision tree according to four editing rules (*coding*, *combination*, *segregation* and *cancellation*); (2) using a weighting function that is non-linear with respect to probabilities. By applying the prospect theory or the cumulative prospect theory, the behavior of decision-makers toward risk depends both on a *value function* that plays the role of the utility function used in EUT and on a *weighting function*, which takes the probabilities as an argument.

Unlike isolation and certainty effect, a phenomenon that can hardly be considered in a quantitative analysis of a decision problem is *formulation effect* [45]. Formulation effect results in inconsistent choices when the same decision problem is proposed to the decision-maker in terms of gain rather than losses. With the formulation effect, the attitude of the decision-maker towards the same decision problem can turn from risk aversion to risk seeking.

### 2.3.3 Expected utility theory for the value of information

One of the most common applications of EUT to SHM is done to assign a monetary value to the information provided by monitoring systems. In science and engineering, *information* is a statistical concept. In information theory, the information is usually

measured with *entropy* [46] [47], which quantifies the uncertainty of a random variable. When one or more parameters are random variables with a statistical distribution, we can quantify the magnitude of the uncertainty that affects those parameters by calculating the corresponding entropy. For example, let me say that we defined the prior probability  $p(S)$  of a state class  $S$ . The entropy that quantifies our information on the state class *a priori* is

$$H(S) = -\sum_{\Omega_S} p(S) \log_2 p(S). \quad (2.7)$$

In a similar way, the entropy of  $k$  state parameters  $\theta$  characterized *a priori* by a multivariate normal distribution of covariance  $\Sigma_\theta$  is

$$H(\theta) = \frac{1}{2} \log \left[ (2\pi)^k \exp(k) \det(\Sigma_\theta) \right]. \quad (2.8)$$

For two random variables, we can also define *conditional entropy* and *mutual information*. The value of conditional entropy is the entropy of a variable, given the complete knowledge of another variable. The value of mutual information represents the reduction in the uncertainty of a variable due to the knowledge of the other. The latter also quantifies the dependence between the two random variables [48].

We may be tempted to measure the effectiveness of a monitoring solution using the entropy. However, if we observe (2.8), we notice that the entropy of the state parameters depends on the unit of the parameters themselves – it is not dimensionless. Therefore, it would be very difficult to define a general metric for the quantification of monitoring effectiveness based on entropy. Moreover, if we quantify the monitoring effectiveness with entropy, there would be no way to check whether a monitoring solution is worth the costs. To overcome these issues, we must use the VOI instead. The concept of VOI follows an application of the EUT and was introduced by Raiffa and Schlaifer [10] with the aim of assessing the value of an experiment. In simple words, the VOI corresponding to an experiment, which is formally identical to monitoring, is the difference between the expected utility of the situation in which we know the results of an experiment (or monitoring data) and the expected utility of the situation in which we do not have monitoring data but only prior information. The latter situation is that in which no experiment is performed and in the literature is sometimes called *null experiment* or *dummy experiment*. VOI

measures in monetary terms how much our decision capability improves after we acquire data with the experiment (or monitoring).

The VOI is a concept that has been employed in engineering since the late 1990s. Back in 1999, Papazoglou [49] used the VOI to define the optimum sampling strategy for the certification of the reliability of single- and multi-component systems. In Papazoglou's method, the reliability of the system components is modeled with simple equations. He defines a utility function that takes the reliability of the entire system as an argument. Thus, in this case, the utility is not a function of costs or gains, but it is a function of the reliability. Then, Papazoglou applies pre-posterior analysis [10] to calculate the *expected value of sample information* (EVSI) corresponding to a given sampling strategy. Although Papazoglou does not evaluate the VOI of a sampling strategy in monetary terms, his approach follows the rigorous pre-posterior analysis method originally proposed by Raiffa and Schlaifer [10].

More recently, some research groups have used the concept of VOI to quantify the value of SHM techniques. The calculation of the VOI due to a SHM technique has been subject to several studies because, in principle, it can prove that the installation of a monitoring system leads to a net monetary gain. More generally, according to [34], the VOI can be employed in SHM in order to:

1. compare the VOI corresponding to a SHM solution with the monitoring costs and drawbacks;
2. compare different monitoring systems, i.e. rank different SHM strategies;
3. compare the choice of performing SHM with other available actions like inspection, maintenance and rehabilitation.

Zonta *et al.* [33], in 2014, showed with a simple example the formal difference between decision-making based on the mere output of Bayesian inference and decision-making that strictly follows EUT. If SHM-based decision-making follows the principle of EUT, Zonta *et al.* showed that the thresholds in the measurements that identify the decision of closing a bridge does not correspond to the values for which the probability of damage exceeds 50%, which would be the threshold in a mere probabilistic approach. In the same paper, Zonta *et al.* calculate the EVSI that resulted from performing SHM with Bayesian pre-posterior analysis.

In 2014, six working groups from both academia and industry in the European region established the network *COST Action TU1402: Quantifying the Value of Structural Health Monitoring*, supported by the *European Framework Program Horizon 2020*. The aim of COST Action TU1402 is the quantification of the value of SHM solutions in monetary terms. COST Action TU1402 recognizes that the calculation of the SHM value must be based on EUT [32] [50]. In this context, Bayesian pre-posterior analysis is not used specifically to design a monitoring system, but it is used to evaluate the benefits of a SHM strategy. The calculation of the SHM value requires:

1. a probabilistic model of the structure, which is possibly time-dependent;
2. a probabilistic model that takes into account the uncertainties of the structural model and the uncertainties that are introduced by the monitoring system;
3. the monetary outcomes of the structural states that may occur;
4. a utility function or the assumption that the stakeholders are risk-neutral.

COST Action TU1402 indicates the *JCSS Probabilistic Model Code* [51], developed by the Joint Committee on Structural Safety, for the definition of the uncertainties. The definition of the utility function is usually avoided in favor of the assumption that the stakeholders are risk-neutral and that the utility is the opposite of costs.

Despite the methods proposed by the academic community to calculate the value of SHM strategies, these applications are still confined to academic examples. Indeed, in practice the actual VOI may be hard to obtain because the expected utility of structural states is based on: (1) the probability of each structural state; (2) the costs of the consequences following each state. The former, (1), involves complex numerical models of the monitored structure, while the latter, (2), is mostly influenced by indirect costs (e.g. impact of the consequences on the environment and society) that are hard to estimate.

### 2.3.4 Optimal sensor placement based on expected utility theory

Many successful approaches to OSP are based on the minimization of *information entropy*, which is a scalar measurement of uncertainty [52]. Provided that the state parameters to be estimated do not change, ranking different monitoring solutions based on information entropy can be useful to compare different sensor configurations [53]. Papadimitriou and Lombaert [54] showed how the information entropy corresponding to any sensor configuration decreases as more and more sensors are installed on a structure. This property is extremely important in practice, because it guarantees that the efficiency with which we identify the structural state can only improve as more information is taken into account. The principle of minimizing the information entropy was also used by Papadimitriou and Lombaert in order to define computationally-efficient heuristic algorithms for sequential sensor placement.

As an alternative approach, Udawadia [55] proposed to carry out OSP by maximizing a norm (either trace or determinant) of the *Fisher information matrix* (FIM). The use of the determinant of the FIM instead of the trace is justified when a large amount of data is available [54]. Heredia-Zavoni and Esteva [56] showed that minimizing the expected value of the trace of the FIM is equivalent to minimizing the function defined by the sum of the squared errors in the parameter space.

A different method was proposed by Fedorov and Hackl [57]. Their technique, called *most informative subset* (MIS), is based on the coefficients of the covariance matrix. According to the MIS technique, the best sensor configuration is the one that minimizes the determinant of the covariance matrix. An evolution of the MIS technique, called *variance method*, was implemented in a case study by Meo and Zumpano [58].

OSP based on EUT has been broadly studied by Flynn and Todd, with applications to guided-wave damage detection [59] [60]. In [61], Flynn and Todd proposed a method that finds the optimal configuration of sensors by minimizing either the expected global type I error (false positive/false alarm) or type II error (false negative). In [59], the two authors extend their approach and present a criterion to find the sensor configuration that minimizes the Bayes risk [62] of an entire structure subjected to monitoring. Briefly, the approach proposed by Flynn and Todd can be summarized as follows:

1. iterative choice of a sensor arrangement through a genetic algorithm [63], with the aim of minimizing the global Bayes risk;
2. for a given sensor arrangement, calibration of the thresholds in the detector to minimize the Bayes risk;
3. calculation of local detection and false alarm rate for the given sensor arrangement based on the thresholds in the detector;
4. computation of the global Bayes risk based on the local detection rate, local false alarm rate and the costs of misclassification.

The Bayes risk is similar to the expected utility, but it is calculated as the product between costs and probabilities. Flynn and Todd assumed that the monitored system is divided in regions and that each region is monitored with a sensor that may or may not correctly classify the state of the region, with a given probability. The global Bayes risk is calculated without using a utility function, i.e. assuming that the stakeholder is risk-neutral. The sensor configuration is changed in order to find the configuration of minimum global risk. For each tentative configuration, the thresholds used for the classification are changed to minimize the risk for that configuration.

The framework of Flynn and Todd is rigorous and extremely effective when the type and number of sensor is given, i.e. it is efficient to optimize the sensor configuration of a given monitoring strategy. However, it does not formalize how different monitoring systems should be compared and how to calculate the required monitoring effectiveness.

### **2.3.5 Risk-based inspection planning and infrastructure management**

EUT has been implemented also to optimize the schedule of inspections in IM. In this case, it is usually necessary to define *performance models* [64], i.e. models that provide the condition of the structure given information including: the age of the structure, the loads and the history of maintenance and rehabilitation. In risk-based inspection planning, we usually assume that the life of a structure can be divided in stages and that at the beginning of each stage an operator can take an action that may affect the future state of the structure, with some uncertainty.

Madanat, in 1993, published a paper entitled “Optimal infrastructure management decisions under uncertainty” [64]. In his contribution, he proposed a

technique aimed to the optimization of maintenance and rehabilitation that takes into account the presence of uncertainty in the acquisition of data. He defined his formulation a *latent Markov decision process*, because the management policy of the structure is optimized every year based on annual inspections, while the actual state of the system is hidden by the uncertainty of the inspection results. Madanat assumes that the operator in charge of the structure observes in each stage (e.g. each year) only measurements that are probabilistically related to the actual state of the structure. Based on these measurements the operator can predict the condition of the structure in the next stages, with some uncertainty. In the current stage, the agent can also take an action among those available that will affect the future condition. Madanat defined what he calls a *dynamic programming formulation*, which provides a prediction of the total cost for the entire remaining life of the structure. In Madanat's formulation, the expected costs are calculated assuming that the stakeholders are risk-neutral and include: (1) the expected cost of maintenance and repair; (2) the cost of inspections; (3) the expected user costs. The optimal action in each stage is the one that minimizes the total future expected costs.

In a more recent contribution entitled "Framework for risk-based planning of operation and maintenance for offshore wind turbines" [65], Sorensen implemented EUT to optimize structural maintenance planning at the beginning of service life and to optimize sequential decision-making during the service life itself. In his work, he considers a limited probability of damage detection, a time-variant probability of structural failure, and the chance of performing corrective and preventive actions whose costs are capitalized using a rate of interest. The application of Sorensen's approach requires: (1) a damage model that considers uncertainty; (2) a decision rule that links the outcome of inspection or monitoring to the appropriate maintenance policy; (3) a stochastic model to treat the uncertainties; (4) the costs. Sorensen defined a function that returns the total expected benefits minus the total costs over the entire lifetime of the structure. This function can be maximized both in the design stage for optimal design and afterwards to optimize inspection and service. The function includes expected costs of inspection/service, maintenance/repair and failure, with the assumption of risk-neutral stakeholders. Each component of the function is a cost for the entire lifetime of the structure and requires the definition of a rate of interest. The probability of failure in time and the probability of incurring repair costs are required to calculate the expected costs. The probability of failure is calculated based

on a damage model using techniques of structural reliability such as FORM/SORM [66], and can be updated by the outcomes of inspections and SHM.

In “On the value of SHM in the context of service life and integrity management” [67], Qui *et al.* propose a framework for the evaluation of SHM information based on a technique that is similar to Sorensen’s. However, they assume that there is chance to perform only a single inspection within the entire service life of the structure. After the inspection, the operator has to choose whether the considered structure should be repaired or not, in order to minimize the Bayes risk. On the other hand, they assume that there is chance also of performing continuous monitoring to observe the annual deterioration of resistance. A time-dependent ultimate limit state function is considered in a probabilistic model and finally the VOI due to monitoring is calculated through application of EUT, based on the costs of structural failure, inspection and repair. The rate of interest is used to account for the costs.

A comprehensive approach to VOI-based IM has been proposed also by Memarzadeh and Pozzi in “Value of information in sequential decision-making: component inspection, permanent monitoring and system-level scheduling” [68]. In their contribution, they recognize that the optimal management policy follows a trade-off between *exploration* and *exploitation*. When an exploratory action is taken, we pay a price in order to reduce the uncertainty by acquiring information on the structure. We can then exploit the acquired information by improving the efficiency of the management policy. Memarzadeh and Pozzi used a model that implements a *partially observable Markov decision process* and optimizes management strategies that possibly include component-level inspections, system-level inspections and permanent monitoring. The hypotheses were: (1) risk neutrality; (2) no constraint in the budget; (3) infinite time horizon; (4) free inspections. However, assumption (4) does not mean that the operator is allowed to take an infinite number of inspections because the time is discretized (e.g. in years) and only one uncertain observation is available at each stage.

## 2.4 Conclusions about the analysis of the state of the art

The analysis of the current state of the art evidenced that in the last decades the research on SHM-based decision-making and monitoring system design has often implemented approaches based on EUT and Bayesian pre-posterior analysis.

Although often these applications rigorously followed the Raiffa and Schlaifer's formulation [10], a definition of DSS based on monitoring data is still missing. None of the SHM methods that I analyzed gives specific indications for the development of SHM-based DSSs that use information provided by monitoring systems. Moreover, the literature lacks a method for the design of monitoring systems that enables practitioners to compare different monitoring system concepts and to check whether a tentative monitoring solution is expected to provide the financial benefits that justify the costs.

# 3 Decision-making based on structural health monitoring data

The SHM process does not end with the acquisition of data from the sensor installed on the monitored structure. The mere probabilistic evaluation of the structural reliability is also useless when SHM is performed to help decision-makers in the management of civil structures. The analysis of the current state of the art evidenced the need to define a formulation for the development of DSSs that suggest the best actions operators should take based on the measurements acquired through a monitoring system. In this chapter, I formalize the problem that must be solved in SHM-based decision-making. Then, I apply Bayesian logic and EUT to define a classifier that provides financially optimal actions based on monitoring data. Bayesian inference is implemented to use all the available information in order to obtain a precise estimate of the structural state. EUT is implemented to use the output of Bayesian inference, the losses that may result from the possible structural states and the stakeholders' risk profile, in order to identify financially optimal choices. The function obtained through the implementation of Bayesian inference and EUT is a map, or classifier, that can be used to drive the management of structures.

## 3.1 Problem of structural health monitoring

In both academia and industry, SHM is regarded as a process that helps civil structure operators in taking decisions about the management of constructions. However, the relationship between monitoring data and financially optimal decisions has never been formalized. The paradigm of real-life SHM is:

1. acquisition of data from the sensors installed on the monitored structure;

2. analysis of the measurements obtained from the sensors;
3. assessment of the structural state through probabilistic methods, deterministic methods or heuristics;
4. choice of the action to take.

The analysis of the current state of the art evidenced that most of the times decision-making is considered as a process that automatically occurs after that the most probable state of the structure is identified. In real life, the agents who are in charge of the management of civil structures are very skeptical about the SHM capabilities of identifying the correct structural state. Thus, they often disregard the output of monitoring and they prefer to interpret directly the raw measurements based on their experience or even completely ignore SHM, before taking decisions. This inconvenience is due to the fact that decision-making is actually a complex process that should not be confused with the mere assessment of the structural state. Whereas SHM usually provides only the most probable structural state, decision-making is the identification of optimal decisions based on the probability of the possible structural states and on the consequences of each state.

The research community has recognized that EUT can be used to identify financially optimal decisions based on the probability of the states of the nature that may occur and on the outcome that follows the realization of each state [10]. For the last decades, EUT has been implemented in finance and medicine decision problems, in which the calculation of probabilities and outcomes is relatively simple [62]. Herein, I use EUT to select the actions that operators of civil structures should take.

In order to apply EUT, we need to calculate the probability of each possible structural state. Bayesian logic is the most effective tool for the probabilistic analysis of monitoring data. In Bayesian inference, we merge prior information, such as information included in design documents or in the results of sampling campaigns, with the measurements provided by the monitoring system in order to obtain a precise estimate of the structural state. In other words, Bayesian logic is a tool that converts information provided through measurements and prior beliefs into information about the structural condition.

By implementing Bayesian logic and EUT in SHM, I formalize the SHM-based DSS depicted by Figure 3.1. In this formulation, the input are the monitoring observations  $\mathbf{y}$  and the prior knowledge about the structural state. The prior knowledge is introduced by defining the prior probability  $P(\mathbf{S})$  of the structural state

$\mathbf{S}$  and  $p(\boldsymbol{\theta}|\mathbf{S})$  of the state parameters  $\boldsymbol{\theta}$ . For example: the structural state  $\mathbf{S}$  can be a scalar  $S$  that can take two values:  $S_1 = \text{“damaged”}$  and  $S_2 = \text{“pristine”}$ . The state parameters  $\boldsymbol{\theta}$  are usually damage sensitive features such as material properties or structural stiffness. Bayesian inference enables us to calculate precise probability distributions of the state parameters  $\boldsymbol{\theta}$  and the probability of the structural state  $\mathbf{S}$ . These are the posterior probability  $P(\mathbf{S}|\mathbf{y})$  of the structural state  $\mathbf{S}$  and  $p(\boldsymbol{\theta}|\mathbf{y},\mathbf{S})$  of the state parameters  $\boldsymbol{\theta}$ . The posterior probabilities will be used in a model based on EUT, in order to calculate the financially optimal action  $a_{\text{opt}}$ . The decision model requires also the outcomes  $\mathbf{Z}$  of the possible combinations of actions and structural states. These outcomes are usually direct and indirect losses or gains, expressed in monetary terms (e.g. EUR or USD). In conclusion, this SHM-based DSS is a classifier that suggests us the most convenient action  $a_{\text{opt}}$ , given a realization of the monitoring observations  $\mathbf{y}$ .

Below, I define the entities involved in SHM-based decision-making. Then, I formalize the implementation of Bayesian logic and EUT for the definition of the proposed SHM-based DSS. The algorithms that should be employed for the development of SHM-based DSSs in real life are presented in the next chapter.

## 3.2 Glossary

There are different definitions for each entity involved in the SHM process, even within the SHM community. In this section, I present a list of definitions that describes the function of the entities used in the proposed SHM-based DSS. Each definition comes with one or more hypotheses.

### Sensor

Herein, I use the term “sensor” to define “any device which functions as a source of information” [69]. Sensors are transducers that enable us to measure a physical quantity like length, strain, temperature and voltage, and provide a piece of uncertain information, which I call “observation” or “measurement”. Working sensors are usually connected to *reading units*, which control the sensors during the acquisition of data and transmit the measurements. Example of sensors are thermocouples, RTDs, strain gauges, FOSs and accelerometers.

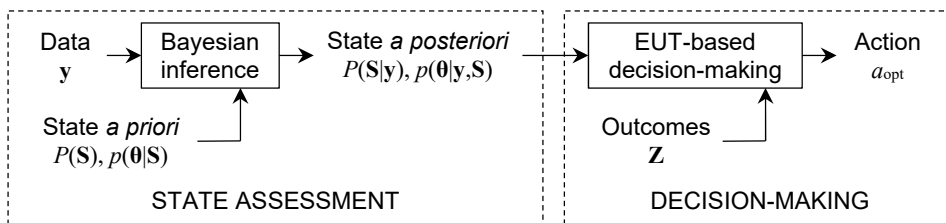


Figure 3.1. Framework for SHM-based DSSs.

### Observation/measurement

In this dissertation, I do not distinguish “observation”, “measurement” and “monitoring data”. They are data collected by sensors, usually through reading units. In order to be handled by humans or machines, the observations must be subjected to *signal conditioning*, in which the measured quantity is converted into a number with a finite precision. If this process is done by an electronic system, an *analog-to-digital converter* (ADC) turns the analog signal provided by sensors into a binary number, causing a little loss of information [70]. Here, I consider observations the value of the physical quantities provided by the data acquisition process, after signal conditioning. I also assume that the observations are affected by a certain magnitude of noise, which makes the observations uncertain. In this dissertation, when I describe data analysis occurring at time  $t$ , I assume that all the observations collected beforehand are available and contained in a vector  $\mathbf{y}(t)$ . I define  $\Omega_{\mathbf{y}}$  as the domain of  $\mathbf{y}(t)$ .

### State

I call “state” the set of one or more variables representing the condition of the structure involved in the analysis. I use  $\mathbf{S}$  to indicate a set of *state classes* defined in the domain  $\Omega_{\mathbf{S}}$ , which is a discrete hyperspace. For example,  $\mathbf{S}$  can be made of only one class describing the severity of damage,  $\mathbf{S} = S \in \{\text{“severe”}, \text{“moderate”}, \text{“null”}\}$ , or it could be made of several classes, for example, when we analyze the state of a system or a group of structural elements. In SHM, the probability of state classes  $\mathbf{S}$  usually expresses the reliability of a structure or a system. I use  $\boldsymbol{\theta}$  to indicate a set of *state parameters*, defined in a generic hyperspace  $\Omega_{\boldsymbol{\theta}}$ , which are usually damage sensitive features, i.e. they represent the structural performance. For example, for a concrete element,  $\boldsymbol{\theta}$  can be the collection of the exposure class  $\theta_1 \in \mathbb{N}$ , material strength  $\theta_2 \in \mathbb{R}^+$ , crack size  $\theta_3 \in \mathbb{R}^+$  and load  $\theta_4 \in \mathbb{R}^+$ .

When we use probabilities to identify decisions based on EUT, the definition of structural states is important and cannot be made based on heuristics. A different structural state must be assigned to each condition that results in a different outcome. From this perspective, the use of multiple damage states (e.g. “severe”, “moderate” and “null”) has to occur if different losses may result from the damage. In other words, when EUT is employed, the magnitude of damage has to be defined based on the financial consequences of the damage itself, which will be considered in the analysis of the decision problem.

### Model

In *model-driven methods* for data analysis, we use a “model”  $g(\mathbf{x}, \boldsymbol{\theta})$  to calculate a value  $\hat{\mathbf{y}}$  of the physical quantities that are observed from the state parameters  $\boldsymbol{\theta}$  and possibly some deterministic variables  $\mathbf{x}$ . The model can be an analytic or a numerical function, and can have a mechanical or heuristic background. In general, the relationship between the observations  $\mathbf{y}$  and the state parameters  $\boldsymbol{\theta}$  is uncertain. Thus, we must distinguish the model output  $\hat{\mathbf{y}}$  from the observations  $\mathbf{y}$  obtained through the monitoring system. The difference between  $\hat{\mathbf{y}}$  and  $\mathbf{y}$  is called *residual*  $\boldsymbol{\varepsilon}$ , and depends on *aleatory* and *epistemic* uncertainties. Whereas aleatory uncertainties are due to an intrinsic randomness of the observed phenomenon (e.g. sensor noise), the epistemic uncertainties are due to lack of knowledge (e.g. error of the structural model) [36]. The model  $g(\mathbf{x}, \boldsymbol{\theta})$  should not be confused with the *predictive model* [36]:

$$\mathbf{y} = g(\mathbf{x}, \boldsymbol{\theta}) + \boldsymbol{\varepsilon} . \quad (3.1)$$

For example, let me assume that the deflection of a concrete cantilever changes in time because of creep and shrinkage according to a linear trend whose slope must be estimated through SHM. In this case, the model  $g(\mathbf{x}, \boldsymbol{\theta})$  is heuristic and is a line function in which  $\mathbf{x} = \mathbf{t}$  are time intervals,  $\theta_1$  is the intercept and  $\theta_2$  is the slope:

$$\hat{\mathbf{y}} = \theta_1 + \theta_2 \cdot \mathbf{x} .$$

In reality, the trend is non-linear and the measured deflection  $\mathbf{y}$ , which is taken, say, using a linear variable differential transformer (LVDT), is affected by random noise. Therefore, we must introduce the residual  $\boldsymbol{\varepsilon} = \theta_1 + \theta_2 \cdot \mathbf{x} - \mathbf{y}$ , which will be a realization of a random variable.

In this thesis, I assume that data analysis is always model-driven. However, it is also possible to do data analysis for SHM without using a model having a physical or heuristic background. In this case, the model would be a statistical representation of the system and the approach would be called *data-driven* [71].

## Outcome

Here, an “outcome”  $z$ , also known as “consequence” or “reward”, is a variable that quantifies the direct and indirect consequences of a possible combination of an action  $a$  and structural state  $\mathbf{S}$ . In real life, an outcome can be of various nature. In civil engineering, outcomes are usually the sum of direct costs, indirect costs, and rewards to the stakeholders. For example, for a structure, the state of failure will be followed by direct costs due to the need to perform structural rehabilitation or, in the worst case, removal of debris, and indirect costs such as the impact of failure on the society. The outcomes used in the proposed SHM-based DSS should be measured with a currency. Herein, I use  $\mathbf{Z}$  to indicate a set of outcomes to be used in the implementation of EUT, and I use  $\Omega_z^{(i)}$  to indicate the outcomes of the  $i$ th decision stage.

## Action

An “action”  $a$  is an option the decision-maker can take at a decision point. The set  $\Omega_a^{(i)}$  indicates the actions available in the  $i$ th decision stage. The set  $\Omega_a^{(i)}$  can be discrete or continuous. If  $\Omega_a^{(i)}$  is discrete, examples of actions concerning a monitored structure are:  $a_1 =$  “do nothing”,  $a_2 =$  “repair” and  $a_3 =$  “replace”. If  $\Omega_a^{(i)}$  is continuous, the action could be the choice of the frequency with which a bridge is subjected to ordinary maintenance. An action can be either *terminal* or *non-terminal*. If an action is terminal, there will not be a chance to take any another decision after that it is taken. If an action is non-terminal, the decision-maker will possibly move to another decision stage –  $i$  will change – and he will need to take another action. Any action can affect the condition of the monitored structure and change the future outcomes.

## 3.3 Bayesian inference

Structures are characterized by the configuration of their elements (e.g. beams, columns and bricks) whose mechanics depends on the material and geometry. In

structural design, we need to show that the structure is expected to satisfy its functions during the entire service life. Therefore, we use the values of the geometrical features and the material properties along with a model of the structure to observe the predicted behavior (e.g. resistance or displacements).

Unlike structural design, in SHM we observe the true behavior of the monitored structure through sensors, while we are interested in the properties and in the state of the structure. Usually, the state parameters are the random variables that we want to assess through SHM. They are the parameters that control the structural model used during the analysis. If we could develop a model that perfectly reproduces the structural behavior and our sensors were infinitely precise, we could calculate the exact value of the state parameters and the structural state from a limited set of observations. Of course, this never happens in real life because both the model and the observations are affected by uncertainty. Thus, the estimate of the state parameters is also affected by a certain amount of uncertainty.

Structural design is governed by deductive logic because we try to predict the outcomes of a phenomenon (the structural behavior) based on the corresponding causes (the properties of the structure). Instead, SHM is governed by inductive logic because we try to identify the causes of an observed behavior. In order to solve the problem of assessing the structural state from the observed behavior, the best we can do is to use the prior knowledge about the structural state, a model that approximates the structural behavior and the observations in Bayesian inference [72] [18]. When a structural model is used in Bayesian inference along with prior knowledge about the structure and monitoring data, we use all the information we have and we obtain the most precise estimate of the state, given the monitoring system in use. In Bayesian inference, we can use heuristic models instead of structural models, or even trained *artificial neural networks* [73] [74]. A heuristic model is usually an analytical function that fits the data. For example, if we are interested in the deformation trend (in  $\mu\epsilon/\text{year}$ ) of a concrete column based on strain measurements (in  $\mu\epsilon$ ), we could simply use as a model the equation of a straight line. In this case, the state parameters to be estimated would be the slope (in  $\mu\epsilon/\text{year}$ ) and the constant term (in  $\mu\epsilon$ ) of the line equation.

Since I want to develop a DSS for SHM-based decision-making, Bayesian logic is used in order to merge prior information with monitoring data for the calculation of the probability of the structural states, which will influence decision-making. In [75], I showed how Bayesian logic can be used in combination with EUT

in order to identify financially optimal actions in the management of structures. Below, the formulation of Bayesian logic is already specialized for the application to SHM. In the next two sections, first I show how the Bayes' theorem is employed for *parameter estimation*, i.e. to assess the state parameters  $\boldsymbol{\theta}$ , and then how Bayesian *model selection* is used to calculate the probability of the state classes  $\mathbf{S}$ .

### 3.3.1 Bayes' theorem for parameter estimation

The well-known Bayes' theorem is a corollary of the *sum rule* and *product rule*, which form the basic algebra of probability theory [18] [76]. The joint probability  $p(\boldsymbol{\theta}, \mathbf{y} | \mathbf{x})$  of state parameters  $\boldsymbol{\theta}$  and observations  $\mathbf{y}$ , given some deterministic variables  $\mathbf{x}$ , can be written as

$$p(\boldsymbol{\theta}, \mathbf{y} | \mathbf{x}) = p(\mathbf{y} | \boldsymbol{\theta}, \mathbf{x}) \cdot p(\boldsymbol{\theta} | \mathbf{x}) = p(\boldsymbol{\theta} | \mathbf{y}, \mathbf{x}) \cdot p(\mathbf{y} | \mathbf{x}). \quad (3.2)$$

From (3.2), we can write the Bayes' theorem:

$$p(\boldsymbol{\theta} | \mathbf{y}, \mathbf{x}) = \frac{p(\mathbf{y} | \boldsymbol{\theta}, \mathbf{x}) \cdot p(\boldsymbol{\theta} | \mathbf{x})}{p(\mathbf{y} | \mathbf{x})}, \quad \boldsymbol{\theta} \in \Omega_{\boldsymbol{\theta}}, \quad (3.3)$$

where  $p(\mathbf{y} | \boldsymbol{\theta}, \mathbf{x})$  is the probability of the observations  $\mathbf{y}$  given the state parameters  $\boldsymbol{\theta}$ , called *likelihood function*, and  $p(\boldsymbol{\theta} | \mathbf{x})$  is a mere probability of the state parameters  $\boldsymbol{\theta}$ , called *prior probability*. When the observations  $\mathbf{y}$  are available, the probability  $p(\mathbf{y} | \mathbf{x})$ , called *evidence*, is a constant that can be calculated by marginalization:

$$p(\mathbf{y} | \mathbf{x}) = \int_{\Omega_{\mathbf{y}}} p(\mathbf{y}, \boldsymbol{\theta} | \mathbf{x}) \cdot d\mathbf{y} = \int_{\Omega_{\boldsymbol{\theta}}} p(\mathbf{y} | \boldsymbol{\theta}, \mathbf{x}) \cdot p(\boldsymbol{\theta} | \mathbf{x}) \cdot d\boldsymbol{\theta}. \quad (3.4)$$

Although  $p(\mathbf{y} | \boldsymbol{\theta}, \mathbf{x})$  gives the probability of  $\mathbf{y}$ , its argument are the state parameters  $\boldsymbol{\theta}$  while the value of  $\mathbf{y}$  is fixed to that of the observations. In other words,  $p(\mathbf{y} | \boldsymbol{\theta}, \mathbf{x})$  tells us the probability of observing  $\mathbf{y}$  for the value of  $\boldsymbol{\theta}$  that we are testing,  $p(\mathbf{y} | \mathbf{x})$  tells us what the probability of  $\boldsymbol{\theta}$  was before acquiring  $\mathbf{y}$ , and  $p(\boldsymbol{\theta} | \mathbf{y}, \mathbf{x})$  is proportional to the product of the two.

In some cases, the state parameters  $\boldsymbol{\theta}$  are only a subset of the parameters involved in the Bayesian parameter estimation. Thus, the remaining parameters  $\boldsymbol{\phi} \in \Omega_{\boldsymbol{\phi}}$ , called *nuisance parameters* [77], need to be marginalized out. The

probability  $p(\boldsymbol{\theta}|\mathbf{y},\mathbf{x})$  becomes a marginal posterior probability, and is calculated by solving

$$p(\boldsymbol{\theta}|\mathbf{y},\mathbf{x}) = \int_{\Omega_{\boldsymbol{\varphi}}} p(\boldsymbol{\theta},\boldsymbol{\varphi}|\mathbf{y},\mathbf{x}) \cdot d\boldsymbol{\varphi}, \quad (3.5)$$

where  $p(\boldsymbol{\theta},\boldsymbol{\varphi}|\mathbf{y},\mathbf{x})$  is the joint posterior probability of the state parameters  $\boldsymbol{\theta}$  and nuisance parameters  $\boldsymbol{\varphi}$ . The chance of marginalizing out the nuisance parameters is one of the advantages of Bayesian inference over the frequentist approach [77].

### 3.3.2 Bayes' theorem for model selection

The posterior probability of the state classes  $\mathbf{S}$  is easily obtained as

$$p(\mathbf{S}|\mathbf{y},\mathbf{x}) = \frac{p(\mathbf{y}|\mathbf{S},\mathbf{x}) \cdot p(\mathbf{S}|\mathbf{x})}{p(\mathbf{y}|\mathbf{x})}, \quad \mathbf{S} \in \Omega_{\mathbf{S}}, \quad (3.6)$$

where

$$p(\mathbf{y}|\mathbf{x}) = \sum_{\mathbf{S} \in \Omega_{\mathbf{S}}} p(\mathbf{y}|\mathbf{S},\mathbf{x}) \cdot p(\mathbf{S}|\mathbf{x}). \quad (3.7)$$

The probability  $p(\mathbf{y}|\mathbf{S},\mathbf{x})$  is the *global likelihood* for the state classes  $\mathbf{S}$  and is calculated by

$$p(\mathbf{y}|\mathbf{S},\mathbf{x}) = \int_{\Omega_{\boldsymbol{\theta}}} p(\mathbf{y}|\mathbf{S},\boldsymbol{\theta},\mathbf{x}) \cdot p(\boldsymbol{\theta}|\mathbf{S},\mathbf{x}) \cdot d\boldsymbol{\theta}, \quad (3.8)$$

where  $p(\mathbf{y}|\mathbf{S},\boldsymbol{\theta},\mathbf{x})$  is the likelihood of the state parameters  $\boldsymbol{\theta}$  corresponding to the state class  $\mathbf{S}$ , and  $p(\boldsymbol{\theta}|\mathbf{S},\mathbf{x})$  is the prior distribution of the state parameters  $\boldsymbol{\theta}$  for the state class  $\mathbf{S}$ .

In (3.6), the global likelihood  $p(\mathbf{y}|\mathbf{S},\mathbf{x})$  can also contain direct observations  $\mathbf{S}_y$  of the structural state  $\mathbf{S}$ , or condition-rating information. If condition rating was performed using state classes  $\mathbf{S}_{cr}$  that are different from  $\mathbf{S}$ , we need to define a likelihood function that probabilistically links  $\mathbf{S}_{cr}$  to  $\mathbf{S}$ . In mathematical terms, the global likelihood of (3.8) would become

$$\begin{aligned}
 & p(\mathbf{S}_y, \mathbf{y}, \mathbf{S}_{cr} | \mathbf{S}, \mathbf{x}) = \\
 & = \int_{\Omega_0} p(\mathbf{S}_y | \mathbf{S}, \boldsymbol{\theta}, \mathbf{x}) \cdot p(\mathbf{S}_{cr} | \mathbf{S}, \boldsymbol{\theta}, \mathbf{x}) \cdot p(\mathbf{y} | \mathbf{S}, \boldsymbol{\theta}, \mathbf{x}) \cdot p(\boldsymbol{\theta} | \mathbf{S}, \mathbf{x}) \cdot d\boldsymbol{\theta}. \quad (3.9)
 \end{aligned}$$

In SHM, (3.6) is usually employed for two purposes: (1) to identify by *model comparison* which model has the greatest probability of fitting the observations  $\mathbf{y}$ ; (2) to identify the probability of damage based on the observations  $\mathbf{y}$ . However, from the statistical standpoint, problem (1) is the same as problem (2) because the latter is solved by comparing the probability of the model including the damages with the probability of the model of the pristine structure.

When we compare two classes (or models)  $\mathbf{S}_i$  and  $\mathbf{S}_j$  using (3.6), we can calculate the odds ratio  $O_{ij}$  in favor of  $\mathbf{S}_i$  as follows:

$$O_{ij} = \frac{p(\mathbf{S}_i | \mathbf{y}, \mathbf{x})}{p(\mathbf{S}_j | \mathbf{y}, \mathbf{x})} = \frac{p(\mathbf{y} | \mathbf{S}_i, \mathbf{x}) \cdot p(\mathbf{S}_i | \mathbf{x})}{p(\mathbf{y} | \mathbf{S}_j, \mathbf{x}) \cdot p(\mathbf{S}_j | \mathbf{x})} = \frac{p(\mathbf{S}_i | \mathbf{x})}{p(\mathbf{S}_j | \mathbf{x})} \cdot B_{ij}, \quad \mathbf{S}_i, \mathbf{S}_j \in \Omega_S, \quad (3.10)$$

where  $B_{ij}$  is the *Bayes factor*. The probability  $p(\mathbf{y} | \mathbf{S}, \boldsymbol{\theta}, \mathbf{x})$  is the likelihood of the observations  $\mathbf{y}$ , function of the parameters  $\boldsymbol{\theta}$ , and the more the model corresponding to  $\mathbf{S}$  fits  $\mathbf{y}$ , the higher  $p(\mathbf{y} | \mathbf{S}, \boldsymbol{\theta}, \mathbf{x})$ ; no matter if the complication of the model is not justified. However, the prior probability  $p(\boldsymbol{\theta} | \mathbf{S}, \mathbf{x})$  accounts for the plausibility of the parameters  $\boldsymbol{\theta}$  corresponding to  $\mathbf{S}$ , regardless the observations  $\mathbf{y}$ . This distribution penalizes overcomplicated models because the parameters of overcomplicated models, with possibly little physical justification, have prior probability distributions containing little information (if the parameters are continuous, their distribution would be very flat and wide). Thus, (3.10) contains an *Occam's razor*, which tends to act in favor of classes  $\mathbf{S}$  containing simple models. The global likelihood of (3.8) is also used to define [77] the total *Occam penalty*  $\Theta$  as follows:

$$\Theta = \frac{p(\mathbf{y} | \mathbf{S}, \mathbf{x})}{\max_{\boldsymbol{\theta} \in \Omega_0} p(\mathbf{y} | \mathbf{S}, \boldsymbol{\theta}, \mathbf{x})}. \quad (3.11)$$

### 3.4 Expected utility theory for SHM-based decisions

In general, when we apply EUT, we assign a probability and an outcome to each state of the nature. Then, we calculate a value of *utility* for each outcome, which represents the impact of the outcome on the stakeholders. Different actions can lead to different states of the nature, can change the probability of each state and can change the outcomes. Thus, each action corresponds to a different expected utility. Formally, each terminal action  $a$  in  $\Omega_a$  leads to a state  $\mathbf{S}$  in  $\Omega_s$ , which result in a monetary outcome  $z$  in  $\Omega_z$  and in the corresponding utility  $u(z|\mathbf{S},a)$ . The relationship between the outcome  $z$  and the utility  $u(z|\mathbf{S},a)$  is a function, called *utility function*, that encodes the risk aversion of the stakeholders. For risk-neutral decision-makers  $u(z|\mathbf{S},a) \propto z$ .

In a decision problem, any arbitrary linear transformation of a utility function leads to the same preferences [62]. However, the preferences depends on the utility function. With the utility function, we can suggest actions that better satisfy the stakeholders by encoding their risk aversion. Risk aversion corresponds to concave utility functions. Conversely, a decision maker is risk seeking if the utility function that satisfies him the most is convex. If the utility function is a straight line, the decision maker is risk neutral.

In single-stage decision problems, every available action is a terminal action, which means that no other actions will be available after that the decision-maker makes his choice. An action  $a$  can be defined either in a discrete space  $\{a_1, \dots, a_J\}$  (e.g.  $a_1 =$  “close the bridge”,  $a_2 =$  “send inspector”,  $a_3 =$  “do nothing”) or in a continuous space such as  $\mathbb{R}^+$  (e.g. when the choice is the definition of a threshold). Each decision problem can be graphically represented by a *decision tree*, in which actions and states are logically linked. In decision trees, *decision nodes* are displayed as squares, while *chance nodes* are displayed as circles. Figure 3.2 shows a single-stage decision problem involving a discrete set of actions  $\{a_1, \dots, a_n, \dots, a_N\}$ . After action  $a_n$  is taken, the state may evolve in a realization included in a discrete set  $\{\mathbf{S}_1, \dots, \mathbf{S}_m, \dots, \mathbf{S}_M\}$ . Each combination of state  $\mathbf{S}_m$  and action  $a_n$  leads to an outcome  $z_m$  and consequently to an utility  $u(z_m|\mathbf{S}_m, a_n)$ .

The use of single-stage decision problems is mostly academic. In real life, there is no such thing because usually other actions become available after the first one is taken. When we want to solve these multi-stage decision problems using EUT, we have to analyze the decision tree from the terminal actions all the way up to the options available at the beginning of the decision tree. Herein, when I study multi-

stage decision problems, I distinguish the actions available in different stages using superscripts:  $a^{(1)}$  is for actions available in the first stage,  $a^{(2)}$  in the second, *etc.* I also define  $u(z | \mathbf{S}, a^{(j)}, \dots, a^{(1)})$  as the utility resulting from outcome  $z$  and state  $\mathbf{S}$  after the specific combination of actions  $a^{(1)}, \dots, a^{(j)}$ . Figure 3.3 shows a two-stage decision problem in which action  $a_n^{(1)}$  leads to an uncertain stage in which a second action  $a^{(2)}$  is taken. If the terminal action  $a_n^{(2)}$  is taken in the second stage, the state may evolve in  $\mathbf{S}_m$ , leading to the outcome  $z_m$  and utility  $u(z_m | \mathbf{S}_m, a_n^{(2)}, a_n^{(1)})$ .

After we model a decision problem using a decision tree, we need a principle that enables us to rank the actions of a decision node. Let me say that we are solving a single-stage decision problem in which a choice  $a$  may lead to different states  $\mathbf{S}$  with probability  $p(\mathbf{S} | \mathbf{y}, \mathbf{x})$ , which depends on the observations  $\mathbf{y}$  and some deterministic variables  $\mathbf{x}$ . According to EUT, the metric to rank each action  $a$  is the expected utility:

$$u^*(a, \mathbf{y}) = E_{\mathbf{S} | \mathbf{y}, a} [u(z | \mathbf{S}, a)]. \quad (3.12)$$

The operator  $E_{\mathbf{S} | \mathbf{y}, a}$  calculates the expected value, i.e. the mean, of its argument based on the probability of  $\mathbf{S}$ , given the observations  $\mathbf{y}$  and following action  $a$ . Since I assumed that  $\Omega_{\mathbf{S}}$  is a discrete space, then

$$u^*(a, \mathbf{y}) = \sum_{\mathbf{S} \in \Omega_{\mathbf{S}}} u(z | \mathbf{S}, a) \cdot p(\mathbf{S} | \mathbf{y}, \mathbf{x}). \quad (3.13)$$

The optimal action  $a_{\text{opt}}(\mathbf{y})$  is the action that maximizes the expected utility:

$$a_{\text{opt}}(\mathbf{y}) = \arg \max_{a \in \Omega_a} u^*(a, \mathbf{y}), \quad (3.14)$$

where  $\Omega_a$  can be either a continuous or a discrete space. Taking action  $a_{\text{opt}}(\mathbf{y})$  leads to the maximum expected utility of the considered decision node:

$$u_{\text{max}}^*(a, \mathbf{y}) = \max_{a \in \Omega_a} u^*(a, \mathbf{y}) = u^*(a_{\text{opt}}(\mathbf{y}), \mathbf{y}). \quad (3.15)$$

Risk aversion can be expressed in formal mathematical terms. A decision maker is risk averse if and only if

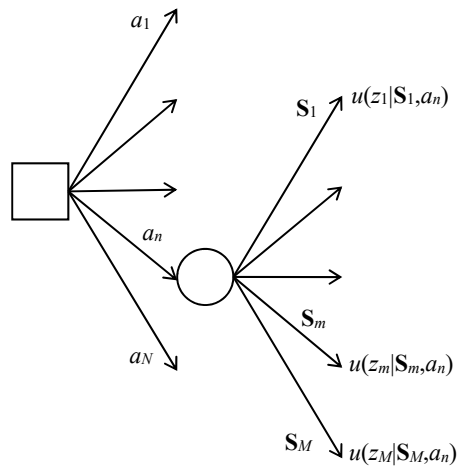


Figure 3.2. Decision tree of a single-stage decision problem; action  $a_n$  leads to an uncertain state of the world  $\mathbf{S}$ , which may take the realization  $\mathbf{S}_m$  corresponding to outcome  $z_m$  and utility  $u(z_m | \mathbf{S}_m, a_n)$ .

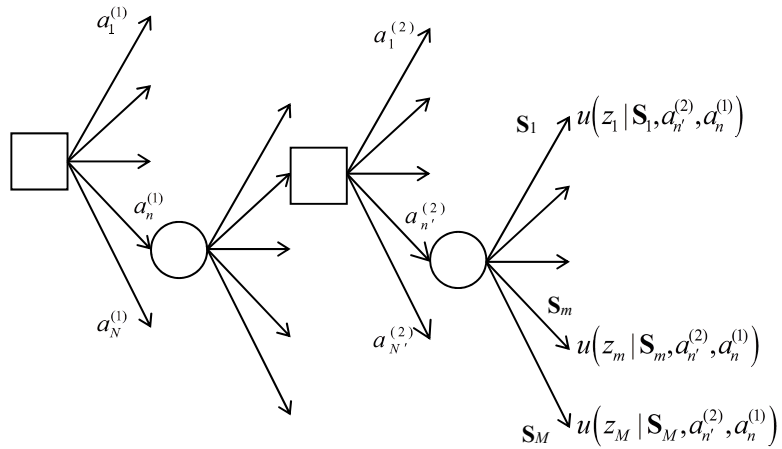


Figure 3.3. Decision tree of a multi-stage decision problem; action  $a_n^{(1)}$  leads to an uncertain state of the world; then, a second choice  $a_{n'}^{(2)}$  leads to another uncertain state  $\mathbf{S}$ , which may take the realization  $\mathbf{S}_m$  corresponding to outcome  $z_m$  and utility  $u(z_m | \mathbf{S}_m, a_{n'}^{(2)}, a_n^{(1)})$ .

$$u\left(\sum_{\mathbf{S} \in \Omega_{\mathbf{s}}} z(\mathbf{S}, a) \cdot p(\mathbf{S} | \mathbf{y}, \mathbf{x})\right) > \sum_{\mathbf{S} \in \Omega_{\mathbf{s}}} u(z | \mathbf{S}, a) \cdot p(\mathbf{S} | \mathbf{y}, \mathbf{x}). \quad (3.16)$$

In other words, we can say that a decision maker is strictly risk averse if he always prefers to get the sure outcome

$$\bar{z}(\mathbf{y}) = \sum_{\mathbf{S} \in \Omega_{\mathbf{s}}} z(\mathbf{S}, a) \cdot p(\mathbf{S} | \mathbf{y}, \mathbf{x}). \quad (3.17)$$

rather than any uncertain scenario with the same expected monetary outcome.

Now, let me say that we want to solve a multi-stage decision problem and we need to calculate the expected utility of action  $a^{(j)}$  available in a generic  $j$ th terminal decision node. Unlike the single-stage case, we have to consider *when* we calculate the expected utility. The expected utility of the same action can change if we calculate it in a different node because the information used to calculate the state probabilities can change. I put a superscript  $(k)$  on expected utilities, probabilities and expected value operators, to indicate that the information used to calculate the state probabilities is that of node  $k$ . With this assumption, the expected utility of action  $a^{(j)}$ , available in node  $j$ , calculated with the information available in node  $k$ , is

$$u^{*(k)}(a^{(j)}, \mathbf{y}) = E_{\mathbf{S} | \mathbf{y}, a^{(j)}, \dots, a^{(1)}}^{(k)} \left[ u(z^{(j)} | \mathbf{S}, a^{(j)}, \dots, a^{(1)}) \right], \quad (3.18)$$

which reads

$$u^{*(k)}(a^{(j)}, \mathbf{y}) = \sum_{\mathbf{S} \in \Omega_{\mathbf{s}}} u(z^{(j)} | \mathbf{S}, a^{(j)}, \dots, a^{(1)}) \cdot p^{(k)}(\mathbf{S} | \mathbf{y}, \mathbf{x}). \quad (3.19)$$

The value of  $p^{(k)}(\mathbf{S} | \mathbf{y}, \mathbf{x})$  may be different from  $p^{(k')}(\mathbf{S} | \mathbf{y}, \mathbf{x})$ , with  $k \neq k'$ , because in node  $k'$  we may have information that are different from that in node  $k$ .

We are now ready to calculate the optimal action of a terminal node  $j$ , using the information of node  $k$ :

$$a_{\text{opt}}^{(j,k)}(\mathbf{y}) = \arg \max_{a^{(j)} \in \Omega_a^{(j)}} u^{*(k)}(a^{(j)}, \mathbf{y}). \quad (3.20)$$

Equation (3.20) can be easily solved when  $j$  is a terminal node because the outcomes  $z^{(j)}$  of (3.19) are available. The complexity in solving multi-stage decision problems arises when node  $j$  is not a terminal node, because in this case node  $j$  is followed by another decision node. In this case we need to assign an expected utility to decision nodes that are reached after other actions are taken. The expected utility of an entire decision node  $j$ , which I call  $u_{\text{node}}^{(j,k)}(\mathbf{y})$ , depends on the node  $k$  from which I take the information that affects the state probabilities and on the observations  $\mathbf{y}$ , but also requires that we assume a *decision rule*. Assuming a decision rule defines how the decision-maker will behave when he has to take action  $a^{(j)}$ . In this dissertation, I always assume that decision-makers act in order to maximize the expected utility using all the information available when they have to make the choice. With this assumption, I can define the expected utility  $u_{\text{node}}^{(j,k)}(\mathbf{y})$  of a terminal node as

$$u_{\text{node}}^{(j,k)}(\mathbf{y}) = \max_{a^{(j)} \in \Omega_a^{(j)}} E_{\mathbf{S}|\mathbf{y}, a^{(j)}, \dots, a^{(1)}}^{(k)} \left[ u \left( z^{(j)} \mid \mathbf{S}, a^{(j)}, \dots, a^{(1)} \right) \right]. \quad (3.21)$$

Since now we can calculate the expected utility of each terminal decision node using (3.21), we can solve decision problems that include non-terminal actions, provided the actions that follow are terminal. Intuitively, we can see that this makes possible to calculate the expected utility corresponding to each of these decision nodes and enables us to proceed until we solve the entire decision tree. However, it is complex to propose a general formulation for multi-stage decision problems in civil engineering because we would have to account for any possible event that occurs after the actions that may lead to decision node  $j$  are taken and before decisions  $\Omega_a^{(j)}$  become available. Herein, I propose the expression below. It formalizes the calculation of the optimal choice  $a_{\text{opt}}^{(w,k)}$  belonging to  $\Omega_a^{(w)}$  and available in a generic decision node  $w$ , which is placed before and connected to a generic decision node  $j$  through a single chance node. The prior probability that characterizes the chance node between decision node  $w$  and  $j$  is crucial but it is difficult to define herein because we do not know what it regards. Here, I just assume that the probability of ending up in decision node  $j$  from decision node  $w$ , given a generic action  $a^{(w)}$ , is  $p^{(k)} \left[ \text{node}_w \rightarrow \text{node}_j \mid a^{(w)} \right]$  and I call  $\text{node}_j$  a *child* of  $\text{node}_w$ . With these assumptions, we can say that the optimal action  $a_{\text{opt}}^{(w,k)}(\mathbf{y})$  of  $\text{node}_w$  is

$$a_{\text{opt}}^{(w,k)}(\mathbf{y}) = \arg \max_{a^{(w)} \in \Omega_a^{(w)}} u^{*(k)} \left( a^{(w)}, \mathbf{y} \right), \quad (3.22)$$

where

$$u^{*(k)}(a^{(w)}, \mathbf{y}) = \sum_{j \in \text{children}(w)} u_{\text{node}}^{(j,k)}(\mathbf{y}) \cdot p^{(k)}[\text{node}_w \rightarrow \text{node}_j | a^{(w)}], \quad (3.23)$$

and  $\text{children}(w)$  gives a set containing the indexes of the decision nodes connected after decision node  $w$  through a single chance node. The expected utility  $u_{\text{node}}^{(w,k)}(\mathbf{y})$  can be simply calculated as

$$u_{\text{node}}^{(w,k)}(\mathbf{y}) = \max_{a^{(w)} \in \Omega_a^{(w)}} u^{*(k)}(a^{(w)}, \mathbf{y}). \quad (3.24)$$

The reader can now see that the problem is completely formalized because (3.19) to (3.21) can be used to solve terminal decision nodes, and (3.22) to (3.24) can be used to solve any other decision node.

### 3.5 Solution of the structural health monitoring problem

The financially optimal action  $a_{\text{opt}}(\mathbf{y})$  calculated with (3.14) is a function of the observations  $\mathbf{y}$  because the probability  $p(\mathbf{S}|\mathbf{y}, \mathbf{x})$  in (3.13) is a posterior probability, which depends on both the observations and the prior probabilities. The function of (3.22) is either an analytical expression or a function that can be solved with numerical methods. The solution has to be obtained with a numerical algorithm when we have to use a numerical method to calculate the posterior distribution  $p(\mathbf{S}|\mathbf{y}, \mathbf{x})$  or the probability  $p^{(k)}[\text{node}_w \rightarrow \text{node}_j | a^{(w)}]$ . When the observations  $\mathbf{y}$  come from a monitoring system, function (3.14) is the classifier that can be implemented for the development of SHM-based DSSs. SHM-based DSSs must take the observations  $\mathbf{y}$  from a database and present to the operator of the monitored structure the suggested action (usually along with a comprehensive report containing the monitoring data). In general, the calculation of  $p(\mathbf{S}|\mathbf{y}, \mathbf{x})$  requires a long time because a numerical algorithm for Bayesian inference must be carried out. Therefore, the DSS should not solve the (3.14) every time the observations  $\mathbf{y}$  change. Instead, when we develop SHM-based DSSs we should calculate a *lookup table* that approximates the entire map defined by (3.14) and implement only the lookup table in the DSS. In this way, when the DSS is in use, each time the observations  $\mathbf{y}$  are updated, the set  $\mathbf{y}$  is compared with the lookup table to instantly obtain the optimal action  $a_{\text{opt}}$ .

Equation (3.14) is a classifier, or a map, which correlates any possible set of observations  $\mathbf{y}$  to the optimal action  $a_{\text{opt}}(\mathbf{y})$  to take:

$$a_{\text{opt}}(\mathbf{y}): \Omega_{\mathbf{y}} \rightarrow \Omega_a. \quad (3.25)$$

Herein, I assume that the set of possible actions  $\Omega_a$  is discrete, while the measurements can be of any nature and size. If the measurements are one or two, we can represent (3.14) with a graph. Figure 3.4a shows a classifier that defines the relationship between two measurements  $\mathbf{y} = \{y_1, y_2\}$  (e.g. two measurements of strain) and three optimal actions  $\{a_1, a_2, a_3\}$  (e.g.  $a_1 =$  “do nothing”,  $a_2 =$  “repair” and  $a_3 =$  “close the bridge”). In Figure 3.4a, the map has a general form. In some other cases, like that depicted in Figure 3.4b, the domains in which each action is optimal can be rectangular with respect to the observations  $\mathbf{y}$ . In those lucky cases, the map can be defined through a set of thresholds. For example, in the case of Figure 3.4b:

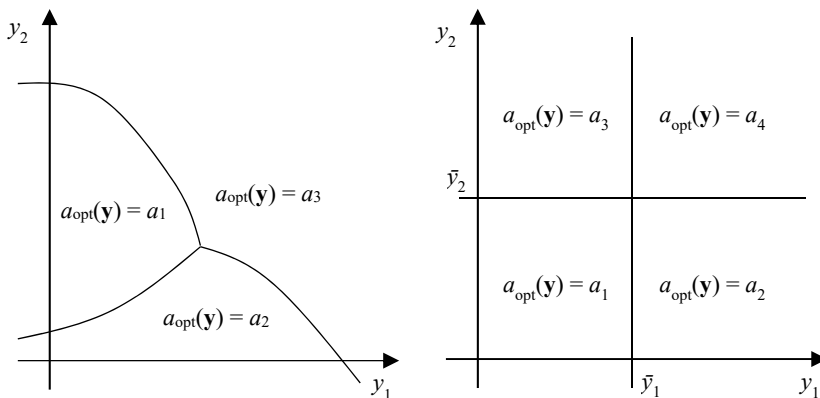
$$a_{\text{opt}}(\mathbf{y}) = \begin{cases} a_1 & y_1 \leq \bar{y}_1 \cap y_2 \leq \bar{y}_2, \\ a_2 & y_1 > \bar{y}_1 \cap y_2 \leq \bar{y}_2, \\ a_3 & y_1 \leq \bar{y}_1 \cap y_2 > \bar{y}_2, \\ a_4 & y_1 > \bar{y}_1 \cap y_2 > \bar{y}_2, \end{cases} \quad (3.26)$$

where  $\bar{y}_1$  and  $\bar{y}_2$  are the two thresholds.

### 3.6 Summary of the chapter

In this chapter, I presented a formulation for the development of DSSs that work with SHM data. SHM-based DSSs are regarded as functions that map the monitoring data and identify, for each value of the observations, the financially most convenient action. In the proposed approach, SHM-based DSSs are based on a classifier in which the measurements are analyzed with Bayesian logic in order to calculate a precise probability of each possible structural state (e.g. “damaged” and “undamaged”). Bayesian statistics enables us to merge information from both monitoring data and sources available *a priori* (e.g. reports of inspections and laboratory test results). After Bayesian inference, an application of EUT uses the outcomes (direct and indirect costs) of each possible structural state and the probability of the states in order to identify the most convenient action. The risk aversion of the stakeholders is

encoded using a utility function that provides a value of utility for each outcome. The most convenient action is the action that corresponds to the maximum expected utility. The calculation of the optimal action for each possible realization of the measurements enables to develop efficient SHM-based DSSs that suggest the optimal management strategy to the operator as soon as new monitoring data become available.



(a) Example of a classifier like that defined in (3.14);  $a_{\text{opt}}(\mathbf{y})$  defines a map of the optimal actions  $\{a_1, a_2, a_3\}$  in the space of the observations  $\mathbf{y} = \{y_1, y_2\}$

(b) A case in which  $a_{\text{opt}}(\mathbf{y})$  can be expressed in terms of two thresholds,  $\bar{y}_1$  and  $\bar{y}_2$

Figure 3.4. Examples of classifiers.

# 4 Software for decision support systems

When we want to develop a DSS that relies on SHM data, we need to use the observations provided by the monitoring system along with a model of the monitored structure to calculate the probability of the structural state and finally suggest an action to the decision-maker. Let me assume now that: (1) the model that encode the relationship between the structural state and the observations has been defined; (2) the uncertainties that affect the model and the measurements have been quantified; (3) the costs and gains that follow each possible structural state have been calculated; (4) the utility function that represents the risk aversion of the stakeholders has been defined. Then, the implementation in real-life settings of the framework proposed in §3 usually requires us to:

1. apply data normalization [2] and cleansing [78] to the raw measurements;
2. build an algorithm that performs Bayesian inference;
3. build an algorithm that solves the decision problem of (3.23).

In (1), data normalization is the process of separating the changes in the data that are due to damage from those due to varying operational and environmental conditions [2] [79]. Usually, in data normalization we manipulate the raw measurement in order to remove the effects of the temperature. In §6 of this dissertation, I will present the case study of Colle Isarco Viaduct, whose deck displacements are severely affected by temperature changes. In general, temperature can affect both the structural behavior and the measurement process – sensors are sensitive to temperature. However, the effects of temperature on sensors are usually taken into account by the corresponding reading unit or by installing additional temperature sensors near the measurement points. The displacements of the deck of Colle Isarco Viaduct are measured through topographic prisms, whose position is monitored by automatic

total stations. Unpredictable environmental conditions affect the topographic measurements so that the effect of temperature is negligible with respect to the measurement noise. Nevertheless, the effects of temperature on the deck displacements have to be reproduced in order to study the structural behavior. In Colle Isarco Viaduct, the temperature of concrete is recorded through resistance thermometers. This enables us to estimate the temperature sensitivity, which can be considered a state parameter, and to separate the temperature-induced deck behavior from the effects of loads.

Data cleansing is the process of choosing if a measurement will or will not be included in the analysis of data. Usually, in data cleansing we remove outliers or undefined values generated by measurement failure. In (2), we need a numerical algorithm for Bayesian inference because usually we cannot calculate the parameters (e.g. mean vector and covariance matrix) of the posterior probability distribution using an analytical expression. In (3), the calculation of probability  $p^{(k)}[\text{node}_w \rightarrow \text{node}_j | a^{(w)}]$ , which is necessary to solve (3.23), may require a Monte Carlo simulation. When we have to perform Bayesian inference with a numerical algorithm, we usually employ the Metropolis-Hastings algorithm, or a similar MCMC. If a Monte Carlo simulation is implemented in order to solve (3.23), the developer should investigate whether *importance sampling* is needed. Importance sampling is a well-established sampling technique, which is usually required when we have to sample from the tails of probability distributions.

In this chapter, I first present how data should be stored before being analyzed by SHM-based DSSs. Then, I show how to compensate the observations in order to reduce the uncertainty due to temperature variations – the major source of errors and biases. Next, I review the current approaches to Bayesian inference proposed by the literature, and, finally, I briefly present importance sampling.

## 4.1 Storing the data

The configuration of the computer network used to store the raw monitoring data should depend on the monitoring problem and on the reliability of the monitoring system that is required. In any case, we should make sure that a first copy of the monitoring data is automatically saved in a computer as close as possible to the reading units. This computer acts as a buffer in case the connection between the reading units and the database that is used in normal conditions is temporarily lost.

Then, we should make automatic frequent backups of all the raw monitoring data on a computer that (1) is not the computer containing the database used in normal operations and (2) can be accessed only using unique credentials – not those of the other computers in the network.

Every device that is used to acquire and save monitoring data, including computers, Ethernet switches, routers and reading units, should be connected to an uninterruptible power supply (UPS) unit in order to avoid loss of data in case of power loss. The UPS should also have an IP address to be controlled remotely. These requirements become crucial when the structure is not accessible after the installation of the monitoring system or when doing maintenance to the monitoring system results in significant direct and indirect costs.

For a single monitoring system, data should be stored in a single *relational database*. The commercial programs that can be used to control the reading units usually include only the option of storing data in: comma-separated values (CSV) files, tab-separated values (TSV) files and proprietary formats. Files that are coded using either the CSV or the TSV format can be read by almost any computer program or with few lines of programming language. Nevertheless, a single CSV or TSV file is not a relational database. Moreover, the order and type of the fields in these files are arbitrary. This makes difficult to read these files when data regard different quantities and comes from different type of sensors. When data can come only with files that are not a relational database, we should build a program that merges all the monitoring data in a single relational database (e.g. MySQL, PostgreSQL). Data should be retrieved in read-only mode from the relational database using Structured Query Language (SQL) through the network. Our DSS should be installed on a computer that is not the one that contains the relational database, so that the DSS can also check the status of the database.

## **4.2 Preparing the samples**

Raw monitoring data may be affected by severe uncertainty. Some of this uncertainty cannot be reduced because it is due to random sensor noise or other environmental conditions that cannot be reproduced even with a numerical model. Some uncertainty can be reduced by acquiring more information or using a more detailed model for the analysis of data. In SHM for civil structures, one of the most severe sources of uncertainty is that due to the effect of temperature variations. For example, some

bridges showed a variation of the first natural frequency of approximately 5% during 24 hours, and 10% during one year [80]. The effect of temperature is usually linear, or bilinear, with a different sensitivity when temperature is below 0 °C [81]. The other sources of uncertainty include wind and humidity. Operating conditions such as mass loading may also affect the measurements. Kim *et al.* [82] observed that heavy traffic caused a variation of 5.4% in the natural frequency of a 46 m-long simply-supported plate girder bridge. Other studies on the effects of mass loading are [83] and [84]. Abe *et al.* [85] observed that wind induces a reduction of the first natural frequency of suspension bridges. However, it appears that data normalization for the reduction of the uncertainty due to environmental and operational conditions depends on the monitoring problem [80].

There are two strategies to reduce the uncertainty due to temperature the choice depends on whether we have temperature measurements or not. In any case, if the objective is to monitor the long-term behavior of the structure, we should consider for each sensor only one measurement per day, at the same instant, when the temperature in our structure is mostly homogenous. The Sun heats up by radiation some parts of the structure during the day while the parts of the structure that are exposed to the sky during the night are cooled down. Quintana *et al.* [86] studied the temperature gradient of a 180 mm-thick concrete slab exposed to sunlight. The slab was located on a Mexican highway and was instrumented with fiber-optic temperature sensors, accelerometers and strain gauges. They found out that usually the temperature was uniform in the slab at 6 PM, whereas the gradient was extreme between 12 PM and 3 PM. The temperature difference measured between the top and the bottom of the slab was up to 8 °C in 120 mm. The temperature of the top of the slab changed in the range between 16 °C (at 7 AM) and 32 °C (at 3 PM). The temperature of the bottom of the slab changed in the range between 20 °C (at 7 AM) and 25 °C (at 5 PM). That study highlights the importance of accurately measure the temperature field in structures subjected to SHM.

Let me assume we found that the temperature gradient in the monitored structure is minimum at hour  $t_h \in [0, 24)$  hour. Below, I present an algorithm that, for each sensor, enables us to select one measurement per day, the closest to  $t_h$ , if a measurement between  $t_h - 1$  hour and  $t_h + 1$  hour exists.

We should consider in the analysis only one measurement per day for each sensor if the objective is monitoring the long-term behavior of the structure. Then, regardless we are using all the measurements or one measurement per day, we need

to compensate the data to remove the remaining effects of temperature. If we have few temperature sensors or we cannot calculate the temperature gradient in our structural elements, we can build a thermal model of the structure to predict the temperature field in the structural elements. If we have no temperature measurements, we must consider temperature effects based on our experience or on a heuristic model.

#### 4.2.1 Filter for morning measurements

Let me assume that the input of the algorithm are the vector  $t' = \{t'_1, \dots, t'_N\}$  of timestamps in days and the matrix of all the measurements  $\mathbf{y}' = \{\mathbf{y}'_1, \dots, \mathbf{y}'_N\}$ . The following algorithm (a pseudocode) can be used to obtain the corresponding cleaned vectors and matrix,  $\mathbf{t} = \{t_1, \dots, t_M\}$ ,  $\mathbf{y} = \{\mathbf{y}_1, \dots, \mathbf{y}_M\}$ ,  $\mathbf{v} = \{v_1, \dots, v_M\}$ .

If  $(t'_1 - \lfloor t'_1 \rfloor) > (t_h + 1) / 24$ ,  $t_F \leftarrow \lfloor t'_1 \rfloor + (24 + t_h) / 24$ , else  $t_F \leftarrow \lfloor t'_1 \rfloor + t_h / 24$ .

If  $(t'_N - \lfloor t'_N \rfloor) < (t_h - 1) / 24$ ,  $t_L \leftarrow \lfloor t'_N \rfloor - (24 - t_h) / 24$ , else  
 $t_L \leftarrow \lfloor t'_N \rfloor + t_h / 24$ .

Calculate the maximum number of measurements  $M \leftarrow t_L - t_F + 1$ .

Initialize a vector  $\mathbf{v} \leftarrow \{0, \dots, 0\}$ .

Initialize  $\tau \leftarrow t_F$ ,  $j \leftarrow 1$ ,  $k \leftarrow 1$ .

While  $\tau \leq t_L$ ,

$\Delta t_{\max} \leftarrow 1 / 24$ ,

while  $t'_j \leq \lfloor \tau \rfloor + (t_h + 1) / 24$ ,

$\Delta t \leftarrow |t'_j - \tau|$ ,

if  $\Delta t < \Delta t_{\max}$ ,

$\Delta t_{\max} \leftarrow \Delta t$ ,

$v_k \leftarrow j$ ,

end of if,

$j \leftarrow j + 1$ ,

end of while,

if  $v_k > 0$ ,

$$t_k \leftarrow t'_{v_j},$$

$$y_k \leftarrow y'_{v_j},$$

end of if,

$$\tau \leftarrow \tau + 1,$$

$$k \leftarrow k + 1,$$

end of while.

When the algorithm ends,  $\mathbf{t}$  and  $\mathbf{y}$  have null values for those days in which a valid measurement does not exist. However, those values can be identified and purged.

#### 4.2.2 Temperature compensation without temperature measurements

If we use daily measurements and we have one year of data or more, we can assume that the effect of temperature on the measurements is sinusoidal with unknown amplitude and phase. The period will be, on average, 365.25 days. Thus, in order to take into account the effects of temperature on the structural behavior, it is reasonable to add the sine function to the model output. In this case, we can assume that the model  $g(\mathbf{x}, \boldsymbol{\theta})$  defined in (3.1) is a function of a model  $g'(\mathbf{x}', \boldsymbol{\theta}')$  that does not consider the temperature effect and a sine function:

$$g(\mathbf{x}, \boldsymbol{\theta}) = g'(\mathbf{x}', \boldsymbol{\theta}') + \theta_a \sin\left(\frac{2\pi(\mathbf{t} - \theta_\phi)}{8,766 \text{ hour}}\right), \quad \mathbf{x} = \{\mathbf{x}', \mathbf{t}\}, \quad \boldsymbol{\theta} = \{\boldsymbol{\theta}', \theta_a, \theta_\phi\}, \quad (4.1)$$

where  $\mathbf{t}$  is in hours. Amplitude and phase of the sine must be among those state parameters that are estimated through Bayesian inference. Usually, a fixed period of 365.25 days works well; however, the period can be also considered a state parameter. When we use the sine function we make the assumption that the amplitude of the temperature effects and the period are constant every year. Whether this hypothesis is valid or not can be checked by observing the data after removing the sine component; if the data still show an oscillation with period of about one year, the effect of annual temperature variations has not been completely removed.

### 4.2.3 Temperature compensation with temperature measurements

If the monitoring system acquires the temperature gradients in the structure, we can use a model to improve our analysis thanks to the temperature data. Temperature is usually measured with a good precision and therefore it can be included among the deterministic variables  $\mathbf{x}$  of the model. Type J (iron-constantan) thermocouples and Pt100 resistance thermometers usually provide temperature measurements with noise of standard deviation lower than 0.5 °C. For steel and concrete, this temperature variation corresponds to a variation in strain of about 6  $\mu\epsilon$ , which is in the order of the noise that affects strain measurements provided by FOSs. Thus, for simplicity temperature is usually considered among the deterministic variables  $\mathbf{x}$  of the model, while the uncertainty that is brought into the analysis by the temperature measurements is added to the model uncertainty. In general, when temperature measurements are available, we can assume that the model  $g(\mathbf{x}, \boldsymbol{\theta})$  defined in (3.1) is a function of a model  $g'(\mathbf{x}', \boldsymbol{\theta}')$ , which does not consider the temperature effects, and a function  $g''(\boldsymbol{\theta}_T, \mathbf{T})$  that models only the temperature effects:

$$g(\mathbf{x}, \boldsymbol{\theta}) = g'(\mathbf{x}', \boldsymbol{\theta}') + g''(\boldsymbol{\theta}_T, \mathbf{T}), \quad \mathbf{x} = \{\mathbf{x}', \mathbf{T}\}, \quad \boldsymbol{\theta} = \{\boldsymbol{\theta}', \boldsymbol{\theta}_T\}, \quad (4.2)$$

where  $\boldsymbol{\theta}_T$  are state parameters that control the sensitivity of the measurements to the temperature and  $\mathbf{T}$  are the temperature measurements.

In case we decide to acquire the temperature, the position of the temperature sensors is important. Temperature sensors should be placed according to the following recommendations, which I formulated based on my experience:

1. temperature sensors should be placed where the temperature is expected to influence the structural behavior most.
2. their configuration should accurately detect the temperature gradients within the structure;
3. the active parts of the sensors must be in contact with the structure, not with the air that surrounds the structure;
4. since temperature sensors usually provide analog electrical signals that are subjected to interferences, thus, they should be placed as close as possible to their reading units;

5. the installation of temperature sensors should not change the temperature field in the structure and the temperature of the material in contact with the sensor must be the same temperature of the structural part on which the sensor is installed;
6. temperature sensors should be installed so that they can be easily replaced.

After the raw monitoring data have been normalized so that the measurements can be compared with the output of the model, we are ready to implement Bayesian inference. Performing Bayesian inference may require a numerical algorithm of those presented in the next section when we cannot calculate the parameters of the posterior distribution using an analytical expression.

### 4.3 Computational Bayesian inference

Equations (3.3) and (3.6) provide the analytical expression for the posterior distribution, respectively for the case of parameter estimation and model selection. In (3.3), the numerator is a function of the state parameters and defines the shape of the posterior probability. Instead, the evidence is a normalization constant. In practice, the calculation of this constant in (3.3) is difficult, particularly if the state parameters are a lot, because it requires an integration over the domain of the state parameters [87]. The numerical calculation of integrals for Bayesian inference is demanding and usually requires importance sampling [88] [89] [90]. However, in parameter estimation we can use the unscaled posterior distribution – the product between the likelihood function and the prior distribution. Using the unscaled posterior distribution, we can obtain samples from the true posterior distribution using different algorithms. MCMC methods are among the most efficient methods to obtain samples from the posterior probability distribution  $p(\boldsymbol{\theta}|\mathbf{y},\mathbf{x})$ , which in this context is called *target distribution*. These methods generate a random series of samples in the parameter domain such that each sample  $\boldsymbol{\theta}^{(n)}$  depends only on the previous sample  $\boldsymbol{\theta}^{(n-1)}$ . This process is based on a *proposal distribution*  $p_p(\boldsymbol{\theta}'|\boldsymbol{\theta}^{(n-1)})$ , which is used to get a candidate sample  $\boldsymbol{\theta}'$  in the  $n$ th step. Metropolis *et al.* [91] formulated a method to build a MCMC using symmetric proposal distributions; Hastings [92] generalized the algorithm presented by Metropolis *et al.* for the use of asymmetric proposal distributions. In the so called Metropolis-Hastings algorithm, a candidate sample  $\boldsymbol{\theta}'$

is included in the chain if a random variable  $u$ , drawn from a distribution uniform in the interval  $[0,1]$ , is smaller than

$$\alpha(\boldsymbol{\theta}^{(n-1)}, \boldsymbol{\theta}') = \min \left[ 1, \frac{p(\boldsymbol{\theta}' | \mathbf{y}, \mathbf{x}) \cdot p_p(\boldsymbol{\theta}^{(n-1)} | \boldsymbol{\theta}')}{p(\boldsymbol{\theta}^{(n-1)} | \mathbf{y}, \mathbf{x}) \cdot p_p(\boldsymbol{\theta}' | \boldsymbol{\theta}^{(n-1)})} \right], \quad (4.3)$$

which is called *acceptance probability* [87], otherwise,  $\boldsymbol{\theta}^{(n)} = \boldsymbol{\theta}^{(n-1)}$ . In summary, assuming that the required number of samples is  $N$ , the steps of the Metropolis-Hastings algorithm are the following.

- Start with an assumed sample  $\boldsymbol{\theta}^{(1)}$  and  $n \leftarrow 1$ ;
- Draw the sample candidate  $\boldsymbol{\theta}'$  from  $p_p(\boldsymbol{\theta}' | \boldsymbol{\theta}^{(n-1)})$ ;
- Calculate  $\alpha(\boldsymbol{\theta}^{(n-1)}, \boldsymbol{\theta}')$  with (4.3);
- Draw  $u$  from an uniform distribution in  $[0,1]$ ;
- If  $u < \alpha(\boldsymbol{\theta}^{(n-1)}, \boldsymbol{\theta}')$ ,  $\boldsymbol{\theta}^{(n)} \leftarrow \boldsymbol{\theta}'$ , else  $\boldsymbol{\theta}^{(n)} \leftarrow \boldsymbol{\theta}^{(n-1)}$ ;
- If  $n = N$ , stop, else,  $n \leftarrow n + 1$  and draw another sample.

The aforementioned Metropolis-Hastings algorithm is probably the simplest approach to computational Bayesian inference for parameter estimation. It enables us to obtain samples from the true posterior distribution, but it has some disadvantages, listed in the following.

1. It does not calculate the *evidence*, which is required to compare different models that may be implemented in the likelihood function for parameter estimation. This drawback forces us to find another solution if we have to do model selection or if we want to find a state class.
2. The required number of samples  $N$  is sensitive to the proposal distribution  $p_p(\boldsymbol{\theta}' | \boldsymbol{\theta}^{(n-1)})$ ; if the shape of the proposal distribution is very different from the true posterior distribution,  $N$  must be huge.
3. A variable number of samples at the beginning of the chain depends on sample  $\boldsymbol{\theta}^{(1)}$ , which is assumed. Thus, we have to identify and remove these samples from the chain before making inference. The

number of samples in the chain that must be removed is called *burn-in period* [87].

4. It cannot be applied if the true posterior distribution is multimodal, because the chain may converge to a single peak.

In order to overcome the issues above, Ching and Chen [93], in 2007, proposed the *transitional Markov chain Monte Carlo* (TMCMC) method based on the *adapting Metropolis-Hasting* (AMH) method presented by Beck and Au [20]. The method of Ching and Chen can be used for model selection, with multimodal target distributions, and does not require the definition of the proposal distribution nor the removal of the samples in the burn-in period. In the TMCMC, the proposal distribution change in different steps as it approaches the target distribution. A comparison between the Metropolis-Hastings algorithm and the TMCMC that proved the advantaged of the latter was presented in 2016 by Ching and Wang [94].

Besides the TMCMC proposed by Ching and Chen [93], other approaches has been studied and presented in the literature. For example, Angelikopoulos *et al.* [95] proposed the X-TMCMC, which minimizes the computational costs required to produce the Markov chain without losing efficiency.

If we choose the basic Metropolis-Hastings algorithm but we also need to calculate the global likelihood of the state classes, we have to calculate the integral of (3.8). When the analytical expression of (3.8) is not available, a Monte Carlo simulation must be carried out. In this case, if the probability of one or more state classes is very little, the number of samples required to obtain a reliable estimate of the probabilities is huge and may lead to long CPU times. A method that can be followed to reduce the required number of samples in a Monte Carlo simulation is *importance sampling*. This technique, which is described in the next section, may also be used to calculate the probability  $p^{(k)}[\text{node}_w \rightarrow \text{node}_j | a^{(w)}]$ , which is necessary to solve (3.23).

## 4.4 Importance sampling

Monte Carlo simulations can be performed in order to approximate probabilities or integrals, which can be expressed in the general form of

$$I_q = \int_{\Omega_0} q(\boldsymbol{\theta}) \cdot p(\boldsymbol{\theta}) \cdot d\boldsymbol{\theta}, \quad (4.4)$$

where  $q(\boldsymbol{\theta})$  is any function of some parameters  $\boldsymbol{\theta}$  (even a model that provides only numerical results) and  $p(\boldsymbol{\theta})$  is a probability density function of  $\boldsymbol{\theta}$ . The integral of (4.4) can be approximated by computing

$$I_q \cong \frac{1}{N} \sum_{n=1}^N q(\boldsymbol{\theta}^{(n)}), \quad \boldsymbol{\theta}^{(n)} \sim p(\boldsymbol{\theta}), \quad (4.5)$$

where  $N$  is the total number of samples  $\boldsymbol{\theta}^{(n)}$  of the Monte Carlo simulation, drawn from  $p(\boldsymbol{\theta})$ .

In some problems such as those of Bayesian statistics,  $q(\boldsymbol{\theta})$  can be small or nearly constant over most of the domain  $\Omega_0$  except a small portion. In these problems, it is not efficient to sample from the whole space of  $p(\boldsymbol{\theta})$  and it is better to concentrate the samples  $\boldsymbol{\theta}^{(n)}$  where  $q(\boldsymbol{\theta})$  varies [96]. With importance sampling [97], we can approximate any integral in the form of (4.4) using samples drawn from a probability distribution of our choice,  $p_s(\boldsymbol{\theta})$ , and focus only on the regions in which  $q(\boldsymbol{\theta})$  is significant for our problem [98] [99]:

$$I_q \cong \frac{1}{N} \sum_{n=1}^N q(\boldsymbol{\theta}^{(n)}) \cdot w_s(\boldsymbol{\theta}^{(n)}), \quad w_s(\boldsymbol{\theta}^{(n)}) = \frac{p(\boldsymbol{\theta}^{(n)})}{p_s(\boldsymbol{\theta}^{(n)})}, \quad \boldsymbol{\theta}^{(n)} \sim p_s(\boldsymbol{\theta}). \quad (4.6)$$

The effect of the choice of  $p_s(\boldsymbol{\theta})$  on the estimated value of  $I_q$  are taken into account by the weights  $w_s(\boldsymbol{\theta}^{(n)})$ .

In structural reliability analysis, the parameters  $\boldsymbol{\theta}$  are the random variables that characterize the structural behavior and the structural properties. The probability of failure of the structure can be calculated as

$$p_f = \int_{\Omega_{0,f}} p(\boldsymbol{\theta}) \cdot d\boldsymbol{\theta}, \quad (4.7)$$

where  $\Omega_{0,f}$  is the region in which the values of the parameters  $\boldsymbol{\theta}$  lead to failure, and  $\Omega_{0,f} \subset \Omega_0$ . The integral of (4.7) can be formulated also as

$$p_f = \int_{\Omega_0} \zeta(\Omega_{0,f}, \boldsymbol{\theta}) \cdot p(\boldsymbol{\theta}) \cdot d\boldsymbol{\theta}, \quad (4.8)$$

where  $\zeta(\Omega_{0,f}, \boldsymbol{\theta})$  is the failure indicator function,

$$\zeta(\Omega_{0,f}, \boldsymbol{\theta}) = \begin{cases} 1, & \boldsymbol{\theta} \in \Omega_{0,f}, \\ 0, & \boldsymbol{\theta} \notin \Omega_{0,f}. \end{cases} \quad (4.9)$$

Since  $p_f$  can be often in the order of  $10^{-6}$ , we need at least  $10^6$  samples to calculate  $p_f$  using (4.5). However, since the calculation of  $\zeta(\Omega_{0,f}, \boldsymbol{\theta})$  usually requires long CPU times, the mere use of (4.5) is impossible in real-world structural reliability problems [100]. With importance sampling, we can concentrate the samples in the domain  $\Omega_{0,f}$  and reduce the required number as a result:

$$p_f \cong \frac{1}{N} \sum_{n=1}^N \zeta(\Omega_{0,f}, \boldsymbol{\theta}^{(n)}) \cdot w_s(\boldsymbol{\theta}^{(n)}), \quad w_s(\boldsymbol{\theta}^{(n)}) = \frac{p(\boldsymbol{\theta}^{(n)})}{p_s(\boldsymbol{\theta}^{(n)})}, \quad \boldsymbol{\theta}^{(n)} \sim p_s(\boldsymbol{\theta}). \quad (4.10)$$

Importance sampling can be also implemented in Bayesian inference to solve (3.8),

$$p(\mathbf{y} | \mathbf{S}, \mathbf{x}) = \int_{\Omega_0} p(\mathbf{y} | \mathbf{S}, \boldsymbol{\theta}, \mathbf{x}) \cdot p(\boldsymbol{\theta} | \mathbf{S}, \mathbf{x}) \cdot d\boldsymbol{\theta}.$$

In this case, the shape of  $p(\boldsymbol{\theta} | \mathbf{S}, \mathbf{x})$  may provide samples that correspond to insignificant values of  $p(\mathbf{y} | \mathbf{S}, \boldsymbol{\theta}, \mathbf{x})$ , making the estimate of the probability  $p(\mathbf{y} | \mathbf{S}, \mathbf{x})$  unreliable. This happens, for example, if, for most of the samples  $\boldsymbol{\theta}^{(n)}$ ,  $\mathbf{y}$  ends up in the tails of  $p(\mathbf{y} | \mathbf{S}, \boldsymbol{\theta}, \mathbf{x})$ . However, we can force the samples  $\boldsymbol{\theta}^{(n)}$  in a portion of the domain of our choice by implementing importance sampling:

$$p(\mathbf{y} | \mathbf{S}, \mathbf{x}) \cong \frac{1}{N} \sum_{n=1}^N p(\mathbf{y} | \mathbf{S}, \boldsymbol{\theta}^{(n)}, \mathbf{x}) \cdot w_s(\boldsymbol{\theta}^{(n)} | \mathbf{S}, \mathbf{x}), \quad \boldsymbol{\theta}^{(n)} \sim p_s(\boldsymbol{\theta}), \quad (4.11)$$

where

$$w_s(\boldsymbol{\theta}^{(n)} | \mathbf{S}, \mathbf{x}) = \frac{p(\boldsymbol{\theta}^{(n)} | \mathbf{S}, \mathbf{x})}{p_s(\boldsymbol{\theta}^{(n)})}. \quad (4.12)$$

Equation (4.11) represents the algorithm for a Monte Carlo simulation with importance sampling that is performed to calculate the global evidence of state class  $\mathbf{S}$ .

## 4.5 Summary of the chapter

This chapter presented the indications and the algorithms for the development of SHM-based DSSs based on the formulation of §3 of this thesis. I explained the hardware and software system that should be built to effectively acquire and store monitoring data from the sensors installed on a monitored structure. Monitoring data should be acquired using hardware connected to UPS units; data should be saved both on-site and remotely, in multiple backup copies; data should be stored in a relational database and retrieved using SQL. In the other sections, I presented the methods and the algorithms that can be implemented in order to perform data normalization and to reduce the variations in the monitoring data that are due to temperature. Then, I reviewed the algorithms proposed by the literature for computational Bayesian inference: the Metropolis-Hastings algorithm and the TMCMC algorithm. In the last section, I presented the formulation of Monte Carlo simulation with importance sampling, which can be implemented when we need to calculate small probabilities with a small number of samples.



# 5 Structural health monitoring system design

The design of monitoring systems is one of the most pioneering challenges of the academic studies on SHM. Nowadays, practitioners often design monitoring systems based on experience and the producers of technology for SHM provide little help in the development of monitoring system concepts. There is evidence that monitoring system design will always be asked to operators of structures, who usually rely on consulting companies or civil engineers.

Practitioners who operate in civil engineering are used to semi-probabilistic structural design. When engineers design a structure like a bridge, they follow a common rigorous procedure in which the expected performance of the concept is calculated through structural analysis and compared to the target performance prescribed by the design codes. Unlike in structural design, there is not a code for monitoring system design; there is still the need to define a common procedure similar to that of structural design.

In this chapter, I formalize a performance-based monitoring system design process that follows the scheme of semi-probabilistic structural design. After introducing the problem of monitoring system design, I apply the approach proposed by Raiffa and Schlaifer [10] for the design of experiments to monitoring system design. Their method consists in the application of EUT to ensure that performing the experiment (or installing the monitoring system) actually produces financial benefits. Then, from the Raiffa and Schlaifer's framework, I develop the proposed performance-based monitoring system design.

## 5.1 Problem of structural health monitoring system design

The design of systems for SHM includes the following choices, which are usually subjected to a budget constraint:

1. identification of the purpose of monitoring, which in general is the evaluation of the structural reliability to improve the management of the structure;
2. choice of the quantity to measure (e.g. strain of the columns, accelerations of the girders, drift of the storeys);
3. choice of the position, number and type of sensors to be employed for monitoring;
4. choice of the system used for data acquisition: number and type of reading units, UPS units, networking devices and computers;
5. choice of the type of software that will be used to record the measurements and perform data normalization and cleansing;
6. development of the algorithm that will be carried out to analyze the monitoring observations.

When monitoring system design is based on experience, the choices above are taken once. However, in a more rigorous design approach, the designer should always provide financial justification for performing monitoring [101]. He should evaluate the effectiveness of the monitoring system concept using a quantitative metric and rethink his choices if the monitoring solution appears not to be satisfactory.

The design of a monitoring system is like the design of an experiment. According to Raiffa and Schlaifer [10], experiments can be designed using EUT. With EUT, we can design an experiment by evaluating if the expected utility of doing the experiment is greater than the expected utility of acting based only on prior information. In this evaluation, we calculate the value of the information provided by the experiment and we compare this value with the cost of the experiment. This approach can be applied also to monitoring system design. I call the design process resulting from this application *value-of-information-based monitoring system design* (VOI-based monitoring system design). In VOI-based monitoring system design, the designer calculates the value of the measurements provided by the monitoring system and compare it with the cost of installing the tentative monitoring solution.

This approach to monitoring system design would be a rigorous process, but it would be more similar to structural optimization rather than the common semi-probabilistic design method. Real-life SHM needs a straightforward procedure. In the next section, I formalize VOI-based monitoring system design using EUT. Then, I

develop my *performance-based monitoring system design* and show how performance-based monitoring system design can be as effective as VOI-based monitoring system design. The proposed approach is a process that is the counterpart of the semi-probabilistic structural design and is relatively simple compared to VOI-based monitoring system design. Two examples of application of the proposed method are presented in the next chapters.

## 5.2 Value-of-information-based monitoring system design

In this section, I show how VOI can be used to design a monitoring system that provides measurements  $\mathbf{y}$ . Before the agent in charge of the management of the structure takes any action, the designer of the monitoring system wonders whether installing a monitoring system is convenient. If a monitoring system is installed, the observations  $\mathbf{y}$  will be used along with a model to update the information on the structural state  $\mathbf{S}$ , and a utility  $u(z|\mathbf{S})$  corresponding to an outcome  $z$  will follow each state  $\mathbf{S}$ . Figure 5.1 shows the decision tree in which the designer evaluate the installation of the monitoring system. This decision tree can be used to calculate the EVSI [10] of the observations  $\mathbf{y}$  and therefore predict whether the SHM system is worth installing.

Regardless monitoring data are available or not, the agent will have to choose an action  $a_n^{(2)} \in \Omega_a^{(2)}$  concerning the management of the structure. Each action taken by the agent may have different monetary outcomes  $z_m$ , which depends on the action itself and on the realization of the state  $\mathbf{S}_m$ . In general, the probability of each state  $\mathbf{S}_m$  is affected by the decision  $a_n^{(2)}$  that precedes the realization. I assume that the monetary outcome  $z_m$  accounts for both direct and indirect costs due to the realization of state  $\mathbf{S}_m$ . The utility of each outcome is simply calculated using the utility function  $u(z_m)$ . The branch that follows  $a_0^{(1)}$  in the decision tree of Figure 5.1 includes all the actions  $\Omega_a^{(2)}$  that the agent can take to manage the structure. Before the agent takes his decision, the designer has the option of installing a SHM system that would provide a set of observations  $\mathbf{y}$ . If the monitoring system is not installed, action  $a_0^{(1)}$  is taken in the first stage, node<sub>1</sub>, and the agent proceeds without SHM. Instead, if SHM is performed, action  $a_{\text{SHM}}^{(1)}$  is taken in node<sub>1</sub> and the agent can use the monitoring observations  $\mathbf{y}$  before taking any decision. In this case, I assume that the agent must take an action  $a_n^{(3)} \in \Omega_a^{(3)}$ , in node<sub>3</sub>, among the same set of actions available in node<sub>2</sub>, hence  $\Omega_a^{(2)} = \Omega_a^{(3)}$  and  $a_n^{(3)} = a_n^{(2)}$  for any  $n$ . In the second branch, we have the same

monetary outcomes  $z_m$  for each state  $S_m$ , but here the utility takes into account also the costs of installing and configuring the monitoring system, namely  $z_{SHM}$ . Using (3.19) to (3.24), we can put  $z_{SHM} = 0$  and calculate the EVSI of  $\mathbf{y}$ , or put  $z_{SHM}$  equal to the actual costs of SHM and calculate the *expected net gain of sampling* (ENGs). According to the EUT fundamentals, the choice of monitoring  $a_{SHM}^{(1)}$  is worth taking if  $ENGs > 0$ .

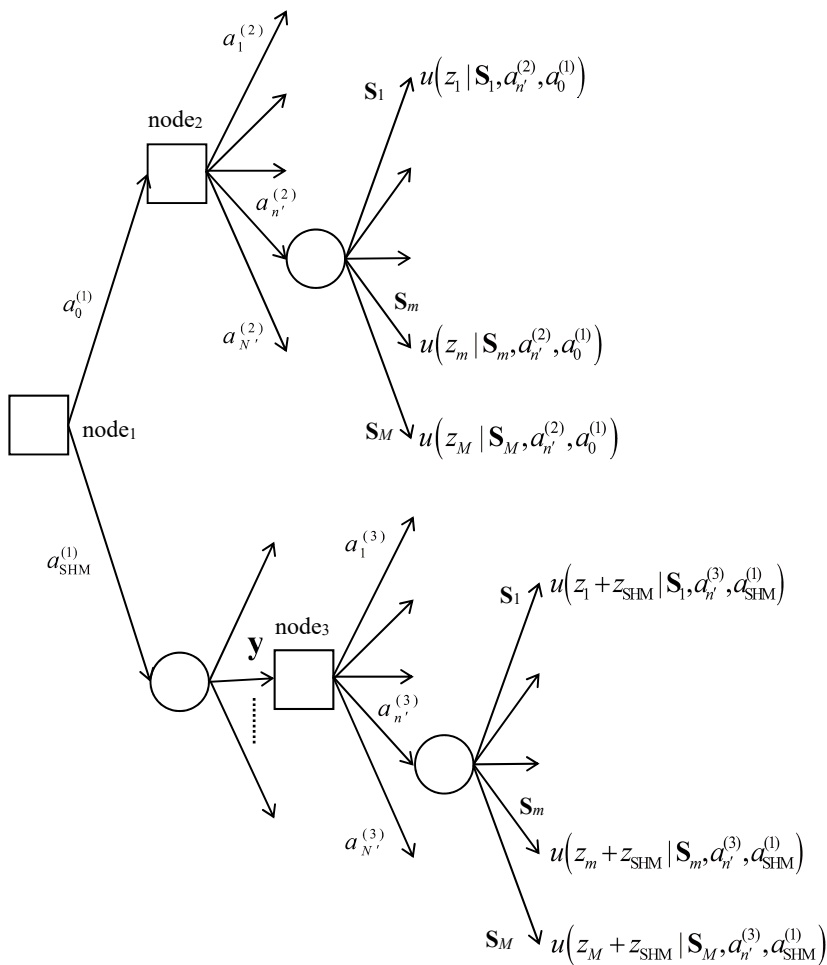


Figure 5.1. Decision tree used to calculate the EVSI of  $\mathbf{y}$ ; action  $a_{SHM}^{(1)}$  is installing a SHM system that provides  $\mathbf{y}$  and action  $a_0^{(1)}$  is the option of proceeding without SHM information.

Assuming that the agent will act always in order to maximize the expected utility of his actions, we can use (3.21) to calculate the expected utility of node<sub>2</sub>, which is also the expected utility of  $a_0^{(1)}$ :

$$u^{*(1)}(a_0^{(1)}) = u_{\text{node}}^{(2,1)} = \max_{a^{(2)} \in \Omega_a^{(2)}} E_{\mathbf{S}|\mathbf{y}, a^{(2)}, a_0^{(1)}}^{(1)} \left[ u(z | \mathbf{S}, a^{(2)}, a_0^{(1)}) \right]. \quad (5.1)$$

With the assumption that  $\mathbf{S}$  is defined in a discrete space, (5.1) becomes

$$u^{*(1)}(a_0^{(1)}) = \max_{a^{(2)} \in \Omega_a^{(2)}} \sum_{m=1}^M u(z_m | \mathbf{S}_m, a^{(2)}, a_0^{(1)}) \cdot p^{(1)}(\mathbf{S}_m), \quad (5.2)$$

because, if the designer takes  $a_0^{(1)}$ , the only information on  $\mathbf{S}$  the agent will have is the prior probability  $p^{(1)}(\mathbf{S})$ .

Unlike action  $a_0^{(1)}$ , the expected utility of action  $a_{\text{SHM}}^{(1)}$  needs to include the observations  $\mathbf{y}$ . If we knew the observation  $\mathbf{y}$ , which we do not, we could calculate the expected utility of action  $a_{\text{SHM}}^{(1)}$  as

$$u^{*(1)}(a_{\text{SHM}}^{(1)}, \mathbf{y}) = \max_{a^{(3)} \in \Omega_a^{(3)}} \sum_{m=1}^M u(z_m + z_{\text{SHM}} | \mathbf{S}_m, a^{(3)}, a_{\text{SHM}}^{(1)}) \cdot p^{(1)}(\mathbf{S}_m | \mathbf{y}), \quad (5.3)$$

where  $p^{(1)}(\mathbf{S}_m | \mathbf{y})$  is obtained through the Bayes' theorem:

$$p^{(1)}(\mathbf{S}_m | \mathbf{y}) = \frac{p^{(1)}(\mathbf{y} | \mathbf{S}_m) \cdot p^{(1)}(\mathbf{S}_m)}{p^{(1)}(\mathbf{y})}. \quad (5.4)$$

By putting  $z_{\text{SHM}} = 0$  and calculating the difference between (5.3) and (5.2), we can calculate the *conditional value of sample information* (CVSI) [10]:

$$\begin{aligned} \text{CVSI}(\mathbf{y}) = & \max_{a^{(3)} \in \Omega_a^{(3)}} \sum_{m=1}^M u(z_m | \mathbf{S}_m, a^{(3)}, a_{\text{SHM}}^{(1)}) \cdot p^{(1)}(\mathbf{S}_m | \mathbf{y}) + \\ & - \max_{a^{(2)} \in \Omega_a^{(2)}} \sum_{m=1}^M u(z_m | \mathbf{S}_m, a^{(2)}, a_0^{(1)}) \cdot p^{(1)}(\mathbf{S}_m), \end{aligned} \quad (5.5)$$

which is of course function of the observations  $\mathbf{y}$ . It should also be noticed that  $p^{(1)}(\mathbf{S}_m | \mathbf{y})$  is a probability density, function of both  $\mathbf{y}$  and  $\mathbf{S}_m$ .

In order to obtain the EVSI, we need to calculate the expected value of CVSI( $\mathbf{y}$ ). Thus, we need to use our prior information on the observations  $\mathbf{y}$ ,  $p^{(1)}(\mathbf{y})$ , and apply the expected value operator:

$$EVSI = \int_{\Omega_{\mathbf{y}}} CVSI(\mathbf{y}) \cdot p^{(1)}(\mathbf{y}) \cdot d\mathbf{y}. \quad (5.6)$$

If we set  $z_{SHM}$  equal to the cost of installing and running the SHM system, we can calculate the ENGS:

$$\begin{aligned} ENGS = & \int_{\Omega_{\mathbf{y}}} \left[ \max_{a^{(3)} \in \Omega_a^{(3)}} \sum_{m=1}^M u(z_m + z_{SHM} | \mathbf{S}_m, a^{(3)}, a_{SHM}^{(1)}) p^{(1)}(\mathbf{S}_m | \mathbf{y}) \right] p^{(1)}(\mathbf{y}) \cdot d\mathbf{y} + \\ & + \int_{\Omega_{\mathbf{y}}} \left[ \max_{a^{(2)} \in \Omega_a^{(2)}} \sum_{m=1}^M u(z_m | \mathbf{S}_m, a^{(2)}, a_0^{(1)}) p^{(1)}(\mathbf{S}_m) \right] p^{(1)}(\mathbf{y}) \cdot d\mathbf{y}. \end{aligned} \quad (5.7)$$

Since the expected utility of  $a_0^{(1)}$  does not depend on  $\mathbf{y}$  and  $\int_{\Omega_{\mathbf{y}}} p^{(1)}(\mathbf{y}) \cdot d\mathbf{y} = 1$ , (5.7) can be simplified:

$$\begin{aligned} ENGS = & \int_{\Omega_{\mathbf{y}}} \left[ \max_{a^{(3)} \in \Omega_a^{(3)}} \sum_{m=1}^M u(z_m + z_{SHM} | \mathbf{S}_m, a^{(3)}, a_{SHM}^{(1)}) p^{(1)}(\mathbf{S}_m | \mathbf{y}) \right] p^{(1)}(\mathbf{y}) \cdot d\mathbf{y} + \\ & - \max_{a^{(2)} \in \Omega_a^{(2)}} \sum_{m=1}^M u(z_m | \mathbf{S}_m, a^{(2)}, a_0^{(1)}) \cdot p^{(1)}(\mathbf{S}_m). \end{aligned} \quad (5.8)$$

The calculation of the EVSI requires the calculation of the probability of each possible structural state  $\mathbf{S}_m$ . This sometimes requires a Monte Carlo simulation of the structural behavior using a FEM, which may take a long CPU time. For example, if we need to calculate the probability of failure of a structure that is expected to be in the order of  $10^{-6}$ , we will have to run the FEM more than  $10^6$  times, each time with a different set of state parameters  $\boldsymbol{\theta}$  randomly drawn from a distribution of  $\boldsymbol{\theta}$ . The number of iterations can be reduced using importance sampling [102] [96], i.e. by pushing the samples to the limit state – the so-called *design point*. Nevertheless, we would still need a large number of samples, in the order of at least  $10^2$  samples.

Pozzi [34] and Straub [103] proposed an efficient algorithm for the computation of the EVSI. Their algorithm can be employed when a complex numerical model of the structure is used to estimate the EVSI. The numeric solution of (5.6) proposed by Straub [103] (with a change of notation) reads

$$\begin{aligned}
 \text{EVSI} = & \sum_{i=1}^{N_y} \max_{a^{(3)} \in \Omega_a^{(3)}} \frac{\sum_{m=1}^M u(z_m | \mathbf{S}_m, a^{(3)}, a_{\text{SHM}}^{(1)}) \sum_{j=1}^{N_{MC}} p^{(1)}(\mathbf{y}_i | \mathbf{S}_m, \boldsymbol{\theta}_{j,m}) p^{(1)}(\mathbf{S}_m)}{\sum_{m=1}^M \sum_{j=1}^{N_{MC}} p^{(1)}(\mathbf{y}_i | \mathbf{S}_m, \boldsymbol{\theta}_{j,m}) \cdot p^{(1)}(\mathbf{S}_m)} + \\
 & - \max_{a^{(2)} \in \Omega_a^{(2)}} \sum_{m=1}^M u(z_m | \mathbf{S}_m, a^{(2)}, a_0^{(1)}) \cdot p^{(1)}(\mathbf{S}_m),
 \end{aligned} \tag{5.9}$$

where  $\boldsymbol{\theta}_{j,m}$  is generated from a prior distribution,  $p^{(1)}(\boldsymbol{\theta} | \mathbf{S}_m)$ , that may depend on  $\mathbf{S}_m$ , and  $\mathbf{y}_i$  is generated based on the conditional distribution  $p^{(1)}(\mathbf{y} | \mathbf{S}_m, \boldsymbol{\theta}_{j,m})$ , for a sample of  $\boldsymbol{\theta}_{j,m}$ .

### 5.3 Performance-based monitoring system design

The design of structural health monitoring systems, or, briefly, *monitoring system design*, is equivalent to the decision problem proposed by Raiffa and Schlaifer [10] in which a decision-maker has to design an experiment to obtain information. This problem has to include also the null experiment, i.e. the situation in which we do not perform any experiment. According to Raiffa and Schlaifer, this decision problem is solved by maximizing the ENGS, formulated here in (5.8). Designing a monitoring system using a VOI-based approach would require to find the optimal monitoring system concept  $e_{\text{opt}}$  out of a set of possible solutions  $\Omega_e$ . In mathematical terms, this would be solving

$$e_{\text{opt}} = \arg \max_{e \in \Omega_e} \text{ENGS}(e), \tag{5.10}$$

where the  $\text{ENGS}(e)$  is a generalization of (5.8) for any monitoring system concept  $e$ :

$$\begin{aligned}
 \text{ENGS}(e) = & \\
 = & \int_{\Omega_y} \left[ \max_{a^{(3)} \in \Omega_a^{(3)}} \sum_{m=1}^M u(z_m + z_{\text{SHM},e} | \mathbf{S}_m, a^{(3)}, a_{\text{SHM},e}^{(1)}) p_e^{(1)}(\mathbf{S}_m | \mathbf{y}) \right] p_e^{(1)}(\mathbf{y}) d\mathbf{y} + \\
 & - \max_{a^{(2)} \in \Omega_a^{(2)}} \sum_{m=1}^M u(z_m | \mathbf{S}_m, a^{(2)}, a_0^{(1)}) \cdot p^{(1)}(\mathbf{S}_m).
 \end{aligned} \tag{5.11}$$

Equation (5.11) is worth discussing. The second term on the right-hand side is the expected utility of node<sub>2</sub> in the decision tree of Figure 5.1. This is the expected utility that we get if we choose not to install the monitoring system. When the agent has to take action  $a^{(2)}$ , he will simply maximize the value of expected utility calculated using the prior probability of each scenario  $\mathbf{S}_m$ , because no data will have been collected to update the probability of  $\mathbf{S}_m$ . The expected utility of node<sub>2</sub> does not depend on the precision of the monitoring system nor on its cost. It is a quantity one can calculate regardless the tentative monitoring system concept. What is affected by the monitoring system is the first term on the right-hand side of (5.11), i.e. the expected utility of node<sub>3</sub>, which is the expected utility we get if the designer chooses to install the monitoring system. If SHM is performed, each monetary outcome is increased by the cost  $z_{\text{SHM}}$  of purchasing and installing the monitoring system. Then, the monitoring system influences the probability distributions  $p_e^{(1)}(\mathbf{S}_m | \mathbf{y})$  and  $p_e^{(1)}(\mathbf{y})$ . This can be intuitively understood because the more the precision of the monitoring system in acquiring the measurements, the more precise our estimate of the state  $\mathbf{S}_m$  and the less uncertainty in  $p_e^{(1)}(\mathbf{y})$ . In other words, if the measurements are affected by a little uncertainty, they will give more information about the state, we will be more confident in our prediction of  $\mathbf{S}_m$  and the distribution  $p_e^{(1)}(\mathbf{y})$  of the observations will be sharper.

Performing monitoring system design using (5.10) is complicated and burdensome because it requires the knowledge of the monetary consequences  $z_m$  of each state  $\mathbf{S}_m$  as well as to assume the utility function. Indeed, this design philosophy is the counterpart of structural optimization. If we were designing a structure, instead of a SHM system, we would not choose the dimension of each structural element and the structural configuration by following a semi-probabilistic method, but by maximizing the overall expected utility calculated based on the cost of the structure, the monetary consequences of structural failure and the probability of failure. If we designed every structure in this way, we would have to estimate the aforementioned costs and use a probabilistic model of the structure rather than a deterministic one. I do not need to mention that this is not what happens in real life. In everyday structural design, we use a performance-based approach in which we compare the capacity of the structure (function of the material strength) with the demand (function of the loads). Usually, design codes prescribe the use partial factors for the calculation of structural capacity and demand; we do not use nominal mean values to check if the structural reliability is satisfactory. In principle, those partial factors ought to be

calibrated in order to translate a requirement that was set in terms of risk to a comparison in terms of design values. Melchers [31] recognizes that “the objective of structural design may be taken reasonably to be the maximization of the total expected utility of the structure [...]”. However, Melchers also recognizes that, if every structural design were carried out using a refined probabilistic approach, the results would not be satisfactory because different outcomes may result from different choices of the probability distributions [31]. In structural design codes such as the Eurocodes (EN 1990:2002: *Eurocode – Basis of structural design*, Annex B and C), the target risk is guaranteed by setting different target values of probability of failure, or *reliability index*, for each class of consequences. In order to keep the target risk constant, a lower probability of failure is required if high consequences of collapse are expected. However, the target reliability is often confined in the annexes of the design codes, while the safety check usually relies on deterministic frameworks like the partial factor method. The target reliability is ensured by proper calibration of the partial factors.

While in the SHM community monitoring system design is often regarded as solving (5.10), here I provide a formulation of monitoring system design that is the counterpart of the everyday structural design – a performance-based procedure. The objective is to rewrite the formulation of VOI-based monitoring system design and obtain a design process based on the comparison between the expected precision of the state parameters  $\theta$  after monitoring and the precision that ensures that performing SHM is convenient. Herein, I provide a methodology in which designers of monitoring systems can identify a satisfactory monitoring system concept based only on the specifications of the concept itself. With this approach, the complexity of VOI-based monitoring system design is removed from the evaluation of a tentative monitoring system and is moved to the calculation of the required precision of monitoring, which I call *demand*. The big advantage is that, like in the structural design codes, the demand can be calculated once for different monitoring problems. For example, SHM of different wind turbines using FOSs will involve similar monitoring costs and similar outcomes due to the misclassification of the structural state. This enables us to calculate the demand for monitoring system design that can be used for different structures. Table 5.1 shows the analogy between semi-probabilistic structural design and the proposed monitoring system design process. The formulation of demand and capacity for performance-based monitoring system design is presented in this section. Demand is the precision of the state parameters

that the monitoring system must provide to be convenient; capacity is the precision of the monitoring system concept that is actually expected.

### 5.3.1 Demand

If we require the tentative concept  $e$  be satisfactory, we have to ensure

$$\text{ENGS}(e) \geq 0. \tag{5.12}$$

Let me assume that the state is represented by a combination of the state parameters  $\theta$ , whose posterior distribution is assumed a multivariate normal distribution  $p^{(1)}(\theta, \Sigma_{\theta|y} | y) = \mathcal{N}(\mu_{\theta|y}, \Sigma_{\theta|y})$ , with mean vector  $\mu_{\theta|y}$  and covariance matrix  $\Sigma_{\theta|y}$ . Let me also assume that the cost of monitoring  $z_{\text{SHM}}(\Sigma_{\theta|y})$  can be defined as a function of the precision provided by the monitoring solution, represented by the covariance matrix of the posterior distribution  $\Sigma_{\theta|y}$ . With the aforementioned assumptions, I seek the values of covariance  $\Sigma_{\theta|y}$  that satisfy (5.12) and I define the demand  $\bar{\Sigma}_{\theta|y}$  as the value for which the ENGS is zero:

$$\bar{\Sigma}_{\theta|y} = \Sigma_{\theta|y} : \int_{\Omega_y} \left[ \max_{a^{(3)} \in \Omega_a^{(3)}} \int_{\Omega_0} u(z + z_{\text{SHM}}(\Sigma_{\theta|y}) | \theta, a^{(3)}, a_{\text{SHM}}^{(1)}) p^{(1)}(\theta, \Sigma_{\theta|y} | y) d\theta \right] \cdot p^{(1)}(y, \Sigma_{\theta|y}) dy - \max_{a^{(2)} \in \Omega_a^{(2)}} \int_{\Omega_0} u(z | \theta, a^{(2)}, a_0^{(1)}) \cdot p^{(1)}(\theta) d\theta = 0. \tag{5.13}$$

**Table 5.1. Analogy between structural design and monitoring system design**

	<b>Semi-probabilistic structural design</b>	<b>Performance-based monitoring system design</b>
Objective	Structural stability with appropriate safety	Knowledge of structural state with appropriate confidence
Demand	Effects of design loads (e.g. bending moments, axial forces)	Required precision of knowledge about the structural state
Capacity	Structural capacity	Precision of the SHM solution
Model	Relationship between material properties and structural capacity	Relationship between sensor measurements and precision of knowledge
Limit state	Effect of design loads vs. structural capacity	Required precision of knowledge of the structural state vs. precision of knowledge provided by the SHM solution

Equation (5.13) enables us to calculate the demand as the limit to the covariance for which the corresponding monitoring system is financially convenient. We can also improve our design by seeking the monitoring system corresponding to the value of covariance that maximizes the ENGS:

$$\begin{aligned} & \Sigma_{\theta|y,\text{opt}} = \\ & = \arg \max_{\Sigma_{\theta y}} \int_{\Omega_y} \left[ \max_{a^{(3)} \in \Omega_a^{(3)}} \int_{\Omega_{\theta}} u(z + z_{\text{SHM}}(\Sigma_{\theta y}) | \theta, a^{(3)}, a_{\text{SHM}}^{(1)}) p^{(1)}(\theta, \Sigma_{\theta y} | y) d\theta \right] \cdot \\ & \quad \cdot p^{(1)}(y, \Sigma_{\theta y}) dy. \end{aligned} \quad (5.14)$$

In (5.14), I left out the second term of (5.11) because it does not depend on  $\Sigma_{\theta y}$ . The second term of (5.11) would be the expected utility of the choice not to install the SHM system, and it does not depend on the monitoring effectiveness. The utility  $u(z + z_{\text{SHM}}(\Sigma_{\theta y}) | \theta, a^{(3)}, a_{\text{SHM}}^{(1)})$  depends on the structural state  $\theta$  and on the action  $a^{(3)}$  that will be taken once that the observations  $y$  are available. After a cursory glance, it may appear that the solution of (5.14) is  $\Sigma_{\theta y,\text{opt}} = \mathbf{0}$  because  $p^{(1)}(\theta, \Sigma_{\theta y} | y) \xrightarrow{\Sigma_{\theta y} \rightarrow \mathbf{0}} +\infty$  for any  $\theta$  and  $y$ . However, this is not the case, because extreme monitoring precisions result in extreme monitoring costs, i.e.  $z_{\text{SHM}}(\Sigma_{\theta y}) \xrightarrow{\Sigma_{\theta y} \rightarrow \mathbf{0}} +\infty$ . Therefore, the solution is usually a balance between the monitoring precision and the monitoring cost, and satisfies

$$\begin{aligned} & \frac{\partial}{\partial \Sigma_{\theta y}} \int_{\Omega_y} \left[ \max_{a^{(3)} \in \Omega_a^{(3)}} \int_{\Omega_{\theta}} u(z + z_{\text{SHM}}(\Sigma_{\theta y}) | \theta, a^{(3)}, a_{\text{SHM}}^{(1)}) p^{(1)}(\theta, \Sigma_{\theta y} | y) d\theta \right] \cdot \\ & \quad \cdot p^{(1)}(y, \Sigma_{\theta y}) dy \Big|_{\bar{\Sigma}_{\theta y}} = \mathbf{0}. \end{aligned} \quad (5.15)$$

The solution is a stationary point of the ENGS function with respect to the covariance matrix of the posterior distribution, which is assumed a multivariate normal. In (5.15) we have the derivative of a scalar function with respect to the matrix  $\Sigma_{\theta y}$ . The result is a matrix in which each element is the derivative of the function with respect to the corresponding element in matrix  $\Sigma_{\theta y}$ .

The demand  $\bar{\Sigma}_{\theta y}$  depends on the costs that may follow each possible structural state  $\theta$ . These costs usually include direct and indirect costs, which may be difficult to assess. Nevertheless, (5.13) does not need to be solved for every case study. In analogy with performance-based structural design, (5.13) can be solved once for

families of monitoring problems and the results can be posted in a design code. The great advantage of using the demand  $\bar{\Sigma}_{\theta|y}$  as defined in (5.13) is that the elements of the matrix are quantities of engineering units (or of a combination of engineering units), which can be easily handled and interpreted by structural engineers.

### 5.3.2 Capacity

The capacity of a monitoring system needs to be calculated using Bayesian pre-posterior analysis [50] [10]. In simple words, pre-posterior analysis is a simulation of Bayesian inference *a posteriori* that occurs before the acquisition of the true measurements. Thus, in pre-posterior analysis, the observations  $\mathbf{y}$  are an unknown variable but the posterior distribution reads like in (3.3):

$$p(\boldsymbol{\theta} | \mathbf{y}, \mathbf{x}) = \frac{p(\mathbf{y} | \boldsymbol{\theta}, \mathbf{x}) \cdot p(\boldsymbol{\theta} | \mathbf{x})}{p(\mathbf{y} | \mathbf{x})}, \quad \boldsymbol{\theta} \in \Omega_{\boldsymbol{\theta}}.$$

The evidence  $p(\mathbf{y} | \mathbf{x})$  and the posterior distribution  $p(\boldsymbol{\theta} | \mathbf{y}, \mathbf{x})$  become functions of the observations  $\mathbf{y}$ . This means that, in the pre-posterior analysis, the mean  $\boldsymbol{\mu}_{\theta|y}(\mathbf{y})$  and the covariance matrix  $\Sigma_{\theta|y}(\mathbf{y})$  of the posterior distribution are also functions of  $\mathbf{y}$ .

We are interested in the value of the covariance matrix  $\Sigma_{\theta|y}$ , *a posteriori*, which must be compared with the demand  $\bar{\Sigma}_{\theta|y}$ . However, in pre-posterior analysis, we cannot calculate the exact value of  $\Sigma_{\theta|y}$  because the observations  $\mathbf{y}$  are still missing. Indeed, the measurements  $\mathbf{y}$  are provided by the monitoring system, which is chosen at the end of the design stage. Therefore, I define the capacity as the expected value of  $\Sigma_{\theta|y}$ , calculated in the pre-posterior analysis. The calculation of capacity requires a distribution of the observations,  $p(\mathbf{y})$ . The distribution  $p(\mathbf{y})$  is usually available in the design stage, because we know: (1) the model  $g(\mathbf{x}, \boldsymbol{\theta})$  that correlates the state parameters  $\boldsymbol{\theta}$  to the observed quantities,  $\hat{\mathbf{y}} = g(\mathbf{x}, \boldsymbol{\theta})$ ; (2) the distribution of the residuals  $\boldsymbol{\varepsilon} = \hat{\mathbf{y}} - \mathbf{y}$ , which include sensor noise, sensor bias and model uncertainties; (3) the prior distribution  $p(\boldsymbol{\theta})$  of the state parameters  $\boldsymbol{\theta}$ . In the worst case, we can always carry out a Monte Carlo simulation in which we draw values of  $\boldsymbol{\theta}$  from  $p(\boldsymbol{\theta})$  in order to get samples of  $\hat{\mathbf{y}}$  using the model  $g(\mathbf{x}, \boldsymbol{\theta})$ , and then draw values of  $\boldsymbol{\varepsilon}$  to obtain  $p(\mathbf{y})$ . Once that we have  $p(\mathbf{y})$ , the capacity can be calculated as

$$\Sigma_{\theta(y)} = E_{p(y)} [\Sigma_{\theta|y}(\mathbf{y})], \quad (5.16)$$

where the expected value of the covariance matrix is the matrix of the expected value of the elements.

The capacity, as defined in (5.16), depends on the monitoring strategy that is evaluated. The elements of  $\Sigma_{\theta(y)}$  usually decrease if: (1) the number of uncorrelated measurements increases; (2) the correlation among the measurements decreases; (3) the magnitude of the noise that affects the measurements decreases; (4) the measured quantities are more sensitive to the state parameters  $\theta$ .

### 5.3.3 Capacity of the monitoring system concept versus prior information

There are two checks that must be carried out after the calculation of the monitoring capacity using (5.16). First, we need to check that the monitoring system concept is actually expected to provide information about all the state parameters  $\theta$ . In order to do so, we can align the principal directions of the expected posterior distribution, which has the covariance matrix of (5.16), to the principal directions of the prior distribution and see if the prior distribution dominates the posterior in every direction. After we rotate and scale the posterior distribution with respect to the prior distribution, we can check if the resulting matrix has the first eigenvalue less than one. The matrix used to rotate and scale the posterior distribution is the inverse of the Cholesky decomposition of the covariance matrix  $\Sigma_{\theta}$ ,

$$\Phi = [\text{Cholesky}(\Sigma_{\theta})]^{-1}. \quad (5.17)$$

We can rotate and scale the posterior distribution using  $\Phi$ , and get the following dimensionless matrix:

$$\Sigma'_{\theta(y)} = \Phi^T \cdot \Sigma_{\theta(y)} \cdot \Phi. \quad (5.18)$$

The monitoring system concept provides information about all the state parameters  $\theta$  if

$$\max_i \lambda'_{\theta(y),i} < 1, \quad \Sigma'_{\theta(y)} \mathbf{v}'_{\theta(y)} = \lambda'_{\theta(y)} \mathbf{v}'_{\theta(y)}, \quad (5.19)$$

where  $\lambda'_{\theta(y)}$ ,  $\mathbf{v}'_{\theta(y)}$  are eigenvalues and eigenvectors of  $\Sigma'_{\theta(y)}$ .

### 5.3.4 Capacity of the monitoring system concept versus demand

The preceding section showed how to evaluate whether a monitoring system concept is expected to provide information on all the state parameters  $\theta$ . In this section, I propose the same approach to evaluate if the capacity of the tentative monitoring solution is greater than demand. In this case, the posterior probability distribution, with covariance matrix  $\Sigma_{\theta(y)}$ , must be rotated and scaled with respect to the distribution of covariance matrix  $\bar{\Sigma}_{\theta(y)}$ , and then again we can check if the resulting matrix has the first eigenvalue less than one.

In formulae, the matrix used to rotate and scale the posterior distribution is

$$\bar{\Phi} = \left[ \text{Cholesky}(\bar{\Sigma}_{\theta(y)}) \right]^{-1}. \quad (5.20)$$

Now, we can rotate a scale the posterior distribution using  $\bar{\Phi}$ , and get the following dimensionless matrix:

$$\bar{\Sigma}'_{\theta(y)} = \bar{\Phi}^T \cdot \Sigma_{\theta(y)} \cdot \bar{\Phi}. \quad (5.21)$$

The monitoring system concept provides a capacity greater than the demand, if

$$\max_i \bar{\lambda}'_{\theta(y),i} < 1, \quad \bar{\Sigma}'_{\theta(y)} \bar{\mathbf{v}}'_{\theta(y)} = \bar{\lambda}'_{\theta(y)} \bar{\mathbf{v}}'_{\theta(y)}, \quad (5.22)$$

where  $\bar{\lambda}'_{\theta(y)}$ ,  $\bar{\mathbf{v}}'_{\theta(y)}$  are eigenvalues and eigenvectors of  $\bar{\Sigma}'_{\theta(y)}$ .

### 5.3.5 Calculation of the expected covariance using uncertainty propagation

There are some cases in which performance-based monitoring system design can be carried out using the analytical expressions of the propagation of uncertainty – without numerical algorithms. This can be done if we can write an expression that provides the state parameters as a function of the model output:

$$\boldsymbol{\theta} = f(\hat{\mathbf{y}}, \mathbf{x}). \quad (5.23)$$

This circumstance enables us to calculate by propagation of uncertainty a covariance matrix  $\tilde{\boldsymbol{\Sigma}}_{\boldsymbol{\theta}, \text{LF}}$ , which is an approximation of the covariance matrix of the likelihood function expressed in terms of state parameters. Then, we can calculate the covariance matrix of the posterior distribution using the formulas for the product of two multivariate normal distributions. The expected covariance matrix of the posterior distribution calculated using uncertainty propagation is an exact estimate when the function  $f(\hat{\mathbf{y}}, \mathbf{x})$  is linear with respect to  $\hat{\mathbf{y}}$ , and both the posterior distribution and the likelihood function are multivariate normal distributions. The formal procedure for the calculation of the expected covariance matrix of the posterior distribution through uncertainty propagation is the following.

Calculate the approximate mean value  $\tilde{\boldsymbol{\mu}}_{\mathbf{y}}$  of the observations  $\mathbf{y}$  using the model function and the mean value  $\boldsymbol{\mu}_{\boldsymbol{\theta}}$  of the prior distribution  $p(\boldsymbol{\theta})$  of the state parameters:

$$\tilde{\boldsymbol{\mu}}_{\mathbf{y}} = g(\boldsymbol{\mu}_{\boldsymbol{\theta}}, \mathbf{x}). \quad (5.24)$$

Calculate the Jacobian matrix  $\mathbf{J}_f|_{\tilde{\boldsymbol{\mu}}_{\mathbf{y}}}$  of  $f(\hat{\mathbf{y}}, \mathbf{x})$ , with respect to the observations  $\hat{\mathbf{y}}$ , near the approximate mean value  $\tilde{\boldsymbol{\mu}}_{\mathbf{y}}$  of the observations.

Calculate the covariance matrix  $\tilde{\boldsymbol{\Sigma}}_{\boldsymbol{\theta}, \text{LF}}$  expressed in terms of state parameters:

$$\tilde{\boldsymbol{\Sigma}}_{\boldsymbol{\theta}, \text{LF}} = \mathbf{J}_f|_{\tilde{\boldsymbol{\mu}}_{\mathbf{y}}} \cdot \boldsymbol{\Sigma}_{\mathbf{y}|\boldsymbol{\theta}} \cdot \left[ \mathbf{J}_f|_{\tilde{\boldsymbol{\mu}}_{\mathbf{y}}} \right]^T. \quad (5.25)$$

Calculate the approximation of the covariance matrix:

$$\tilde{\boldsymbol{\Sigma}}_{\boldsymbol{\theta}(\mathbf{y})} = \left[ \tilde{\boldsymbol{\Sigma}}_{\boldsymbol{\theta}, \text{LF}}^{-1} + \boldsymbol{\Sigma}_{\boldsymbol{\theta}}^{-1} \right]^{-1}. \quad (5.26)$$

This procedure does not take into account the uncertainty of the prior distribution of the state parameters. Therefore, we can conclude that the expected

covariance matrix obtained using uncertainty propagation is unreliable if one of the following is true:

- the function  $f(\hat{\mathbf{y}}, \mathbf{x})$  is severely non-linear in the range where  $p(\mathbf{y})$  is high;
- the prior probability distribution is severely asymmetric;
- the likelihood function is severely asymmetric.

### 5.3.6 Monte Carlo algorithm for the expected covariance matrix

The posterior distribution of state parameters depends on the observations. In performance-based monitoring system design, we use the prior distribution of the observations in order to calculate the expected covariance matrix that characterizes the posterior distribution. In some cases, discussed in the preceding section, we can calculate the expected variance of the posterior distribution by uncertainty propagation. However, the model is often a complex numerical function of multiple state parameters and we cannot find an analytical function that provides each state parameter based on the model output. Therefore, often we need to use a numerical algorithm like the one presented below. With that algorithm: (1) we draw samples from the prior distribution of the state parameters; (2) from some of these samples, we obtain samples of the observations considering the sensor noise, which must be assumed; (3) for each observation, we calculate a value of the covariance matrix using the remaining samples of the state parameters; (4) we calculate the expected value of the covariance matrix. A formal presentation of the algorithm follows.

Draw  $N$  values,  $\boldsymbol{\theta}_{(n)}$ , of the state parameter vector  $\boldsymbol{\theta}$ , from the prior distribution  $p(\boldsymbol{\theta})$ , where  $1 \leq n \leq N$ .

Use the last  $M$  values calculated in the above step to draw  $M$  samples  $\mathbf{y}_{(m)}$  of the observations from  $p(\mathbf{y}|\boldsymbol{\theta}_{(w+m)})$ , where  $1 \leq m \leq M$ .

For each  $m$ th observation  $\mathbf{y}_{(m)}$ :

calculate a set of  $W$  weights  $q_{(m,w)} = p(\mathbf{y}_{(m)} | \boldsymbol{\theta}_{(w)})$ ;

calculate the mean vector

$$\tilde{\boldsymbol{\mu}}_{\boldsymbol{\theta}|Y(m)} = \frac{\sum_{w=1}^W \boldsymbol{\theta}_{(w)} q_{(m,w)}}{\sum_{w=1}^W q_{(m,w)}} ; \quad (5.27)$$

calculate the variance of each  $i$ th parameter,

$$\tilde{\sigma}_{\theta_i|Y(m)}^2 = \frac{\sum_{w=1}^W (\theta_{i,(w)} - \tilde{\mu}_{\theta_i|Y(m)})^2 q_{(m,w)}}{\sum_{w=1}^W q_{(m,w)}} ; \quad (5.28)$$

calculate the off-diagonal elements of the covariance matrix,

$$\tilde{\sigma}_{\theta_i,j|Y(m)} = \frac{\sum_{w=1}^W (\theta_{i,(w)} - \tilde{\mu}_{\theta_i|Y(m)}) (\theta_{j,(w)} - \tilde{\mu}_{\theta_j|Y(m)}) q_{(m,w)}}{\sum_{w=1}^W q_{(m,w)}}, \quad j > i. \quad (5.29)$$

Calculate the expected covariance matrix by solving

$$\tilde{\boldsymbol{\Sigma}}_{\boldsymbol{\theta}(y)} = \frac{1}{M} \sum_{m=1}^M \begin{bmatrix} \tilde{\sigma}_{\theta_1|Y(m)}^2 & \tilde{\sigma}_{\theta_1,2|Y(m)} & \cdots & \tilde{\sigma}_{\theta_1,j|Y(m)} & \cdots \\ & \tilde{\sigma}_{\theta_2|Y(m)}^2 & \cdots & \tilde{\sigma}_{\theta_2,j|Y(m)} & \cdots \\ & & \cdots & \cdots & \cdots \\ & \text{Sym} & & \tilde{\sigma}_{\theta_j|Y(m)}^2 & \cdots \\ & & & & \cdots \end{bmatrix}. \quad (5.30)$$

In case we need to design a monitoring solution for the estimation of a single state parameter, the above algorithm can be easily adapted. Each sample of state parameters  $\boldsymbol{\theta}_{(n)}$  will be a scalar, we will not need to calculate the off-diagonal elements with (5.29), and the matrix of (5.30) will be a scalar instead.

## 5.4 Summary of the chapter

In this chapter, I formalized a performance-based monitoring system design method that is the counterpart of semi-probabilistic structural design. This method was developed based on the formulation that Raiffa and Schlaifer [10] proposed for the design of experiments, which implements EUT. The proposed approach, maintains the formalism of the Raiffa and Schlaifer's, but does not require the designer to assume a utility function nor the calculation of the outcomes – direct and indirect costs. In the performance-based monitoring system design method, capacity and demand can be calculated separately. The calculation of demand does require a utility function and the outcomes, but the demand can be prescribed by design codes similar to the codes that prescribe the requirements for semi-probabilistic structural design. The calculation of capacity is only based on the uncertainties that are expected to affect the analysis of monitoring data *a posteriori*. Like in the scheme of structural design, the calculation of the monitoring capacity is the only task that is left to practitioners. The chapter presented the formulation of capacity, demand, and also the algorithms that can be used to calculate and compare capacity and demand in real-life applications.

# 6 Decision support system for Colle Isarco Viaduct

In this chapter, I show how the management of a strategic structure – Colle Isarco Viaduct – can be optimized by implementing the SHM-based DSS formalized in §3 of this dissertation. Colle Isarco Viaduct, introduced in the first section below, suffered from a high deflection trend, which required a retrofit intervention and extensive SHM. Measurements of displacement and temperature are acquired and stored thanks to a multi-technology monitoring system. The system also includes FOSs, which will start acquiring measurements of strain in 2017. In the chapter, I present the monitoring system and the data acquired so far. Then, I show how the framework of §3 can be implemented in this real-life case study to develop a SHM-based DSS that suggests the optimal action the bridge manager should take. In §6.6.2 of this chapter, I show how the DSS can identify the optimal action among “do nothing”, “send inspector” and “close the bridge”, based on the measurements of displacement acquired in the 14 days preceding the decision.

## 6.1 Colle Isarco Viaduct

I had the pleasure to work with Colle Isarco Viaduct since the design of the first part of the monitoring system, installed in 2014. Colle Isarco Viaduct, built in 1971 and managed by Autostrada del Brennero SpA, is one of the longest bridges in northern Italy and is a strategic highway link between Italy and Austria. The bridge is made of two independent decks, each one supporting a carriageway 10.30 m wide. The description of the viaduct, of the construction process and of the problems occurred during the last decades is taken from [104]. The total length of the bridge is 1,028 m and the structure consists of 13 spans. The longest span, presented in Figure 6.1, is 163 m long and is made of two balanced segmental reinforced concrete cantilevers, which support a simply supported span.

Figure 6.2 and Figure 6.3 show the geometry of the structure. Each cantilever arm that belongs to the longest span juts 59 m out of the piers, which are in common between the two parallel decks, and is balanced by a back arm 91 m long. Each cantilever (four overall) is made of 33 box-girder segments, which were casted in place. Each segment has a depth varying from 10.80 m, near the piers, to 2.55 m, at the edge. The thickness of the top slab, after the intervention completed in 2015, is 285 mm. Instead, the bottom slab has a variable thickness: from 980 mm to 150 mm. The thickness of the two webs is 400 mm and constant along the cantilevers [105]. The suspended spans, made with two prefabricated beams, have not shown any anomaly. A concrete class corresponding to the modern Eurocode C35/45 was used for all the structural elements of the girders. The original prestressing force was applied by 266 32 mm Dywidag ST 85/105 tendons, with an initial jacking tension of 720 MPa (70% of the nominal tensile strength, 1,030 MPa). For each cantilever, the total prestressing force at the piers was about 120 MN.

The structure was built between 1968 and 1971. Figure 6.4a shows the erection of the piers. After the piers were completed, the box girders were casted in segments from each side of the piers. These segments were long between 3 and 4 m and were casted into their formworks, which were fixed to the preceding segments. Figure 6.4b was taken in 1969 and shows the construction of the two northernmost cantilevers, by pier #8. Since the two cantilever arms had different lengths (59 m and 91 m), the balanced construction required the erection of temporary supports, which were built 50 m away from the piers and removed after the completion of the girders. These temporary supports are presented in Figure 6.4c. Finally, Figure 6.4d shows one of the last phases of the construction: the launch of the simply-supported prefabricated beams. After the construction, the deflection of the central span was periodically monitored using a dumpy level. Two years from the opening of the viaduct, the measurements showed an excessive deflection trend. Figure 6.5 shows the deflection of the edge of the northernmost cantilever-southbound carriageway. Although during the design the deflection was expected to be less than 20 mm, the actual deflection exceeded 100 mm in 1976, and 200 mm in 1984. In this year, the velocity was about 8 mm/year. This behavior was observed for all the four cantilevers [106].



(a) Map with the position of Colle Isarco Viaduct



(b) Central span of Colle Isarco Viaduct; left pier is #8, right pier is #9

Figure 6.1. Position and view of Colle Isarco Viaduct.

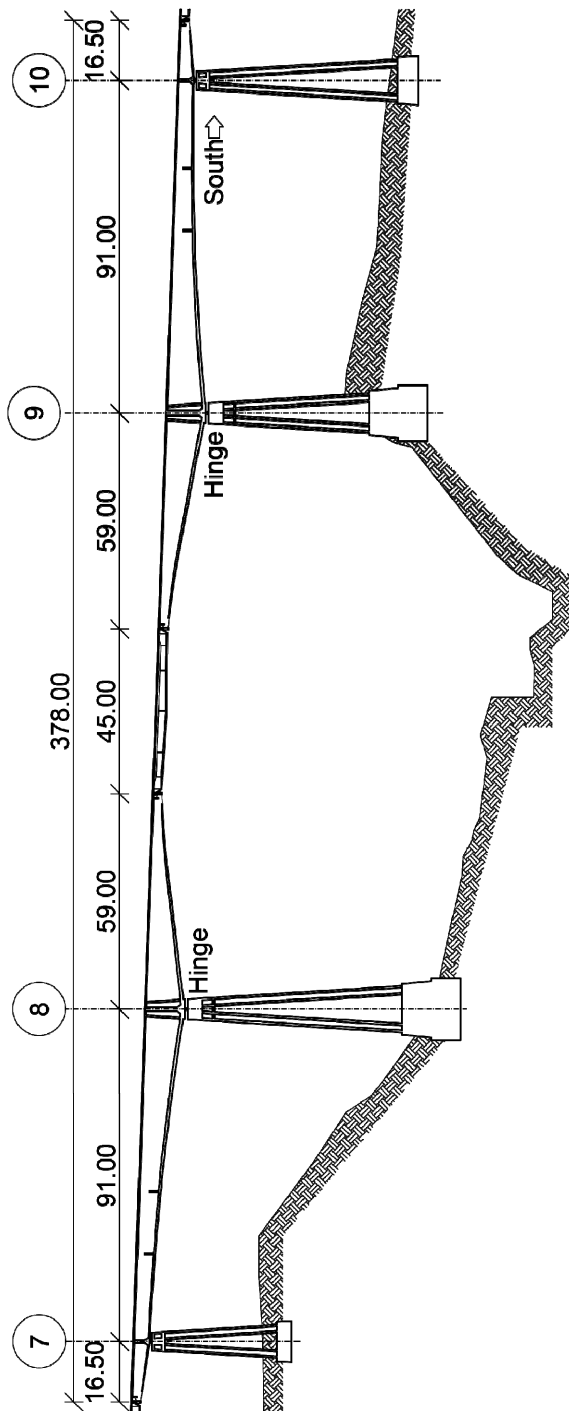


Figure 6.2. Lateral view of Colle Isarco central span; dimensions in [m].

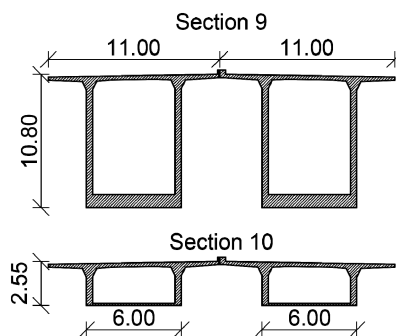


Figure 6.3. Cross-sections of Colle Isarco at piers #9 and #10; dimensions in [m].

Between 1988 and 1989, these inconveniences pushed Autostrada del Brennero SpA to perform a retrofit intervention regarding the main span. As a result, the load on the central span was reduced by removing the original pavement from the cantilever arms and the prefabricated beams. The old pavement was replaced by thin lightweight asphalt. After this work, the edge of the cantilevers immediately recovered 70 mm of displacement and the deflection trend apparently stopped, as showed by Figure 6.5. The second intervention occurred between 1998 and 1999, and was aimed at a repair of the top slab, which was severely deteriorated by the use of salt for de-icing. The repair consisted in: (1) scarification of the damaged concrete; (2) replacement of the corroded reinforcement bars; (3) casting of new concrete. Since 1999, the measurements provided by dumpy level showed a new deflection trend, with an apparent velocity of 2 mm/year. Between 2007 and 2008, the state of the prestressed tendons in the box girders was investigated by removing a layer of concrete from the upper slab, inspection of the tendons and restoration of the concrete layer. Thanks to the inspection, some bars were found broken and others damaged due to surface corrosion. The deterioration was not judged critical for the safety of the structure, but it was clear that the bridge required a major retrofit strengthening to extend its lifespan and comply with the new structural codes. The retrofit, carried out between 2014 and 2015, was designed by Autostrada del Brennero SpA and SEICO SRL [107], an engineering consulting company. During the intervention the thickness of the top slab was increased from 260 mm to 285 mm, the torsional stiffness was enhanced by construction of internal steel truss diaphragms and external cables applied additional post-tensioning. The additional prestress was provided by 212 strands of diameter 0.6", tensioned with a design jacking load of 213 kN. At the end, the total force applied by these cables above the piers was about 45 MN – almost

40% of the original prestress. The strands were grouped in sets of 19 and 15 strands and each group was covered by a polyethylene sheath in order to allow inspection and replacement. All the blocks required to anchor the new post-tensioning system were made of concrete and were connected to the web of the box girders using chemical-grout connectors of diameter 20 mm.

After this intervention, Autostrada del Brennero SpA decided to apply SHM to the structure in order to assess the effectiveness of the work, provide information about possible changes in the structural behavior, predict the future structural performance and support bridge management decisions.



(a) Erection of piers



(b) Erection of northernmost cantilevers



(c) Northernmost cantilevers leaning on temporary support



(d) Erection of the suspended spans

Figure 6.4. Construction phases of the main span of Colle Isarco Viaduct [108].

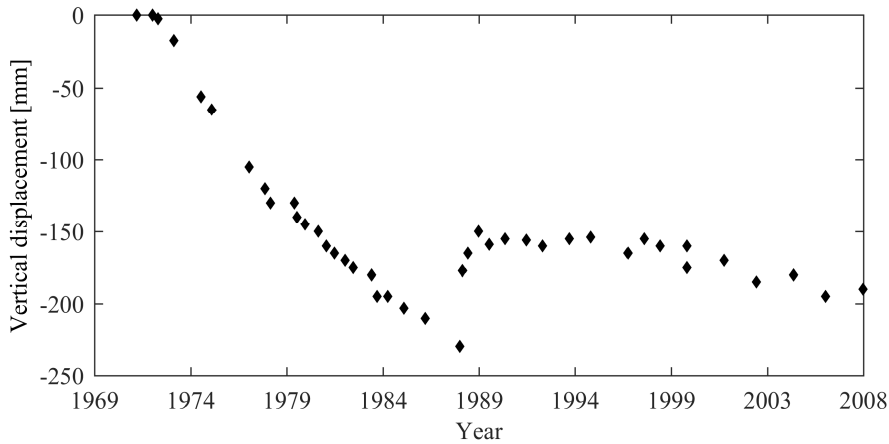


Figure 6.5. Deflection observed at the edge of the northernmost cantilever of the southbound carriageway.

## 6.2 Monitoring system

The monitoring system was designed in 2014 by Intelligent Infrastructure Group of the University of Trento – my research group. We decided to implement three technologies for a comprehensive monitoring of the viaduct behavior and to investigate the causes of possible anomalies. The first part of the monitoring system was installed and activated in 2014, before the retrofit intervention, and is made of two topographic total stations and a set of prisms for the measurement of displacements. The second part of the system was installed in late 2016 and is a network of RTDs. The third part of the system, installed together with the RTDs, is based on FOSs for the measurement of strain. Strain and temperature measurements that are read over long periods are among the most useful data for anomaly detection in concrete box-girder bridges [109] [110] [111] [112].

### 6.2.1 Topographic network

The topographic network was designed to monitor the displacements of the decks between pier #7 and pier #10 during the intervention of 2014–2015 and in the following years. The total stations are two Leica Nova TM50 [113], depicted in Figure 6.6. Unlike the stations Leica Nova TS50, which are for topographic surveys, these topographic stations provide the precision required for SHM. For topographic

total stations, producers indicate an estimate of the measurement precision that can be reached in ideal conditions. However, on site, the noise of the measurements is severely affected by the:

1. number of benchmarks;
2. stability of the stations;
3. temperature of air;
4. pressure of air;
5. rays of sunlight that may hit the stations;
6. vibrations of the prisms.

Therefore, before the installation of topographic total stations, the actual magnitude of the noise that will affect the measurements is usually predicted based on experience. Moreover, producers do not always provide indications on how to design the support and the protection of the stations, which is a task that must be carried out by the customer. In our case, we designed a 1.50 m-high concrete pile for the support of the two total stations. After the installation, the stations were protected by low-iron glass, which minimizes the measurement error due to refraction.



Figure 6.6. The south station, Leica Nova TM50.

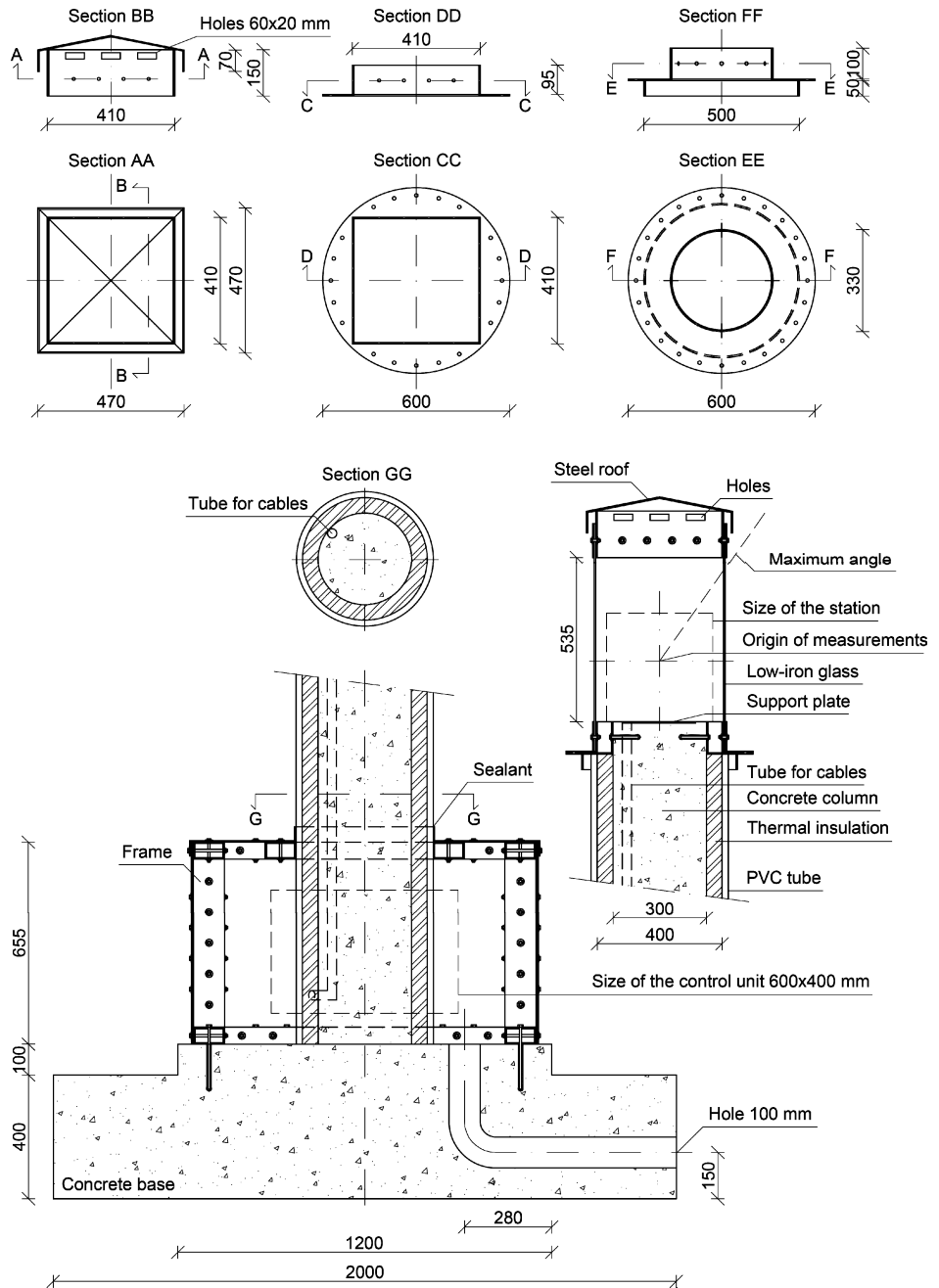


Figure 6.7. Support of the Leica Nova TM50 total stations; dimensions in [mm].

The things that should be considered in the design of the support and protection of topographic total stations for SHM are:

1. the protection box must be big enough to allow the automatic movement of the station;
2. the glass of the protection box must be low-iron glass, to minimize the bias due to refraction;
3. the corner of the protection box and the roof of the protection box must not interfere with the measurements;
4. the air inside of the protection box must remain at about the same temperature of the external air, to reduce the uncertainty of the measurements;
5. the humidity inside the protection box must be able to flow out of the box, throughout holes, but rain and snow must not penetrate the box;
6. a permanent mark must identify the position of the protection box because a rotation of the box could produce an offset of the measurements<sup>1</sup>;
7. the protection box may be very heavy;
8. the protection box should be locked for safety reasons;
9. the pile that supports the station should be insulated to minimize sudden elongations due to hourly temperature variations;
10. a box must be placed by the base of the support pile, in order to contain the devices that control the station;
11. the devices that are inside the box must be placed 10–20 cm above the floor, in case the box is flooded;
12. the box that contains the devices and the protection box must be able to be accessed for maintenance;

---

<sup>1</sup> The same could happen if a glass of the protection box is replaced. The optical properties of each glass may be different and may even change differently in time.

13. one person must be enough to open the box that contains the devices and the protection box.

The choice of the location of the two stations and of the benchmarks also requires experience. In order to reduce the uncertainty:

1. the distance between the prism used for the measurements and the total stations should be the same as the distance between the benchmarks and the stations;
2. the same type of prism should be used for both measurements and benchmarks;
3. the prisms used for the measurements, the benchmarks and the stations should be at about the same altitude.

For the monitoring system of Colle Isarco Viaduct, we chose GPR112 prisms for all the 60 measurement points, as shown in Figure 6.9 and Figure 6.8, and for the 12 benchmarks. The approximate position of the benchmarks was chosen based on the criteria above and optimized by analyzing the propagation of uncertainty [114]. Six benchmarks in sparse locations around the Isarco Valley were used for each total station.

Figure 6.10 shows the final moments of the setup of the north station Leica Nova TM50. The total stations, placed in the protection box on the top of the pile, are connected through a (serial) RS-232 interface to the devices located in the white waterproof box underneath. These devices include:

1. RS-232-TCP/IP converter;
2. Ethernet switch;
3. RJ45-optical fiber media converter;
4. 100AH battery;
5. Smart Protector for the battery;
6. circuit breaker and fuses.

Thanks to the media converter, the total stations are connected to the personal computer *PCI-C* that controls the stations, located in a control cabin about 500 m away from the central span of the viaduct. From this cabin, the data coming from all

the sensors of the monitoring system is continuously sent to the headquarters of Autostrada del Brennero SpA.

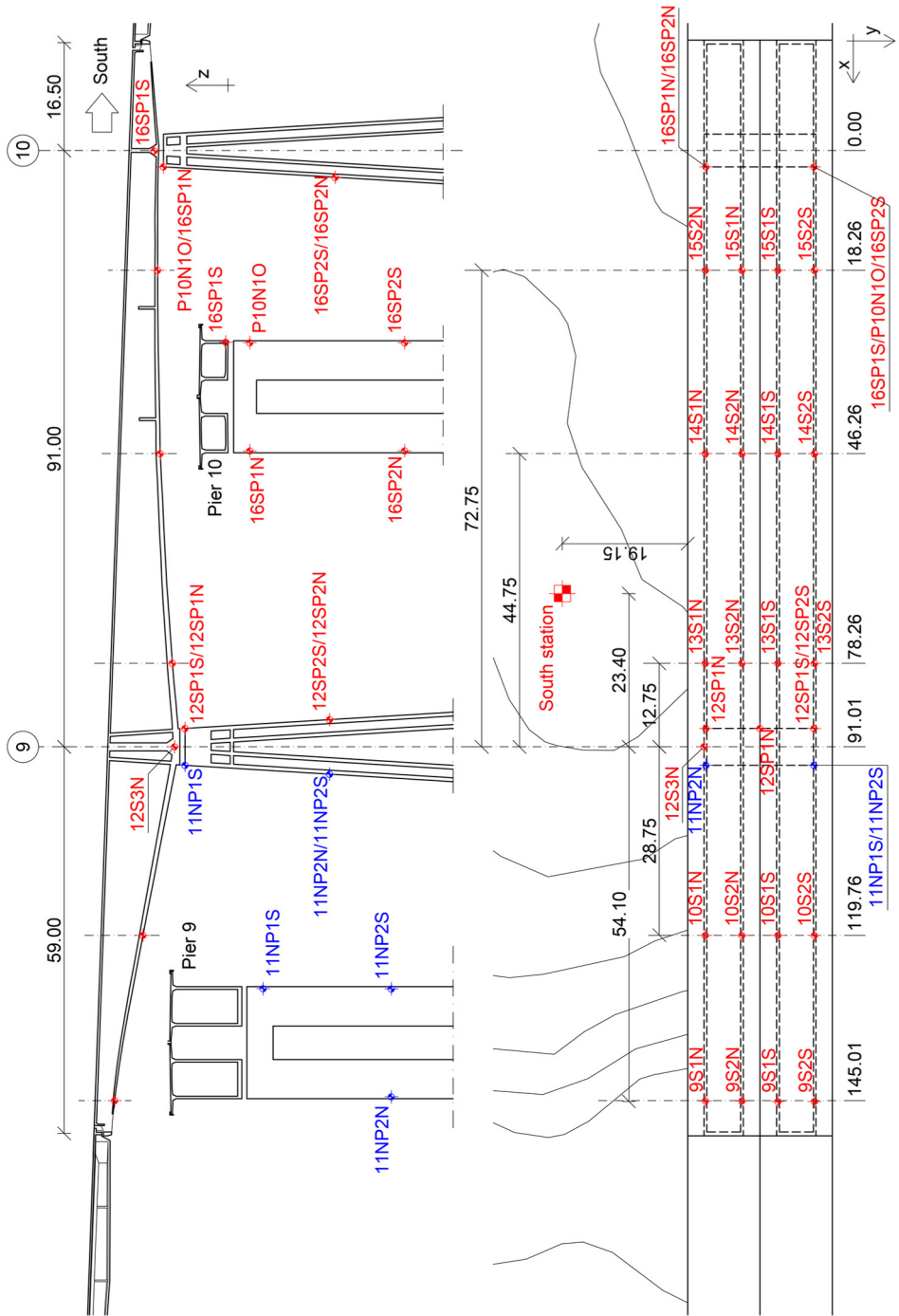


Figure 6.8. Prisms on piles 9 and 10, and on the southernmost girders.





Figure 6.10. Setup of the north station Leica Nova TM50.

## 6.2.2 Resistance thermometers

The RTDs of choice are the *TH-PT100* provided by Nova Metrix [115]. With these sensors, we can detect the absolute value of temperature from the changes in the electrical resistance of the sensors, which should be  $100\ \Omega$  at  $0\ ^\circ\text{C}$ . These sensors are implemented with four-wire bridge mounting. The specifications, taken from the datasheet, are presented here in Table 6.1.

For each RTD that had to be installed in the concrete, a hole of diameter 8 mm or more was drilled in the concrete. Then, the RTD was placed inside the hole, which was finally filled. It is important that the material used to fill the holes be:

1. of low viscosity, because air should be completely removed from inside the hole;
2. of the same thermal conductivity of concrete, so that the installation of the RTD does not change the nearby temperature pattern.

In our case, we employed concrete prepared with a high content of water. The RTD that were designed to measure the air temperature were simply covered by steel plates, to protect them.

A total number of 82 RTDs was connected to 24 4-channel NI 9217 modules [116], provided by National Instruments, whose specifications are presented in Table 6.2. According to the datasheet of NI 9217, for  $100\ \Omega$  RTDs in four-wire mode, the typical precision at  $25\ ^\circ\text{C}$  is  $0.15\ ^\circ\text{C}$ , with a limit of  $0.35\ ^\circ\text{C}$ . The NI 9217 modules are installed on NI cDAQ-9188XT 8-slot Ethernet chassis [117], provided by National Instruments, as depicted in Figure 6.12. The operating temperature of these devices is from  $-40\ ^\circ\text{C}$  to  $70\ ^\circ\text{C}$ . Each chassis is then connected through FTP CAT5e Ethernet cables to one of the two switches installed in each girder. The connection between the switches that are inside the girders and the switch inside the control cabin is made with optical fibers.

Figure 6.11 shows a RTD installed on the bottom slab of southbound southernmost girder of Colle Isarco Viaduct. Figure 6.14, Figure 6.13 and Figure 6.15 show the position of the RTDs. Table 6.3 presents the installation depths. In the design, we adopted the following strategy. The temperature pattern of the tallest (C5) and shortest (C7) section of the north girders is completely identified by 8 RTDs for each section. For the other instrumented sections, 3 RTDs measures the temperatures

that are used as boundary conditions, with the assumption that the temperature pattern of these sections is similar to that of the sections instrumented with 8 RTDs.

**Table 6.1. Specifications of Nova Metrix TH-PT100 resistance thermometers**

Characteristic	Value
Range	-50 °C to +300 °C
Precision	0.1 °C at 0 °C
Thermal drift	0.385 $\Omega$ /°C

**Table 6.2. Specifications of National Instruments NI 9217 input units**

Characteristic	Value
Sampling rate	400 Hz
ADC resolution	24 bit
Range	0 $\Omega$ to 400 $\Omega$
Excitation current	1 mA per channel
Maximum humidity	90%
Operating temperature	-40 °C to 70 °C



Figure 6.11. A RTD installed on the bottom slab of southbound southernmost girder of Colle Isarco Viaduct.

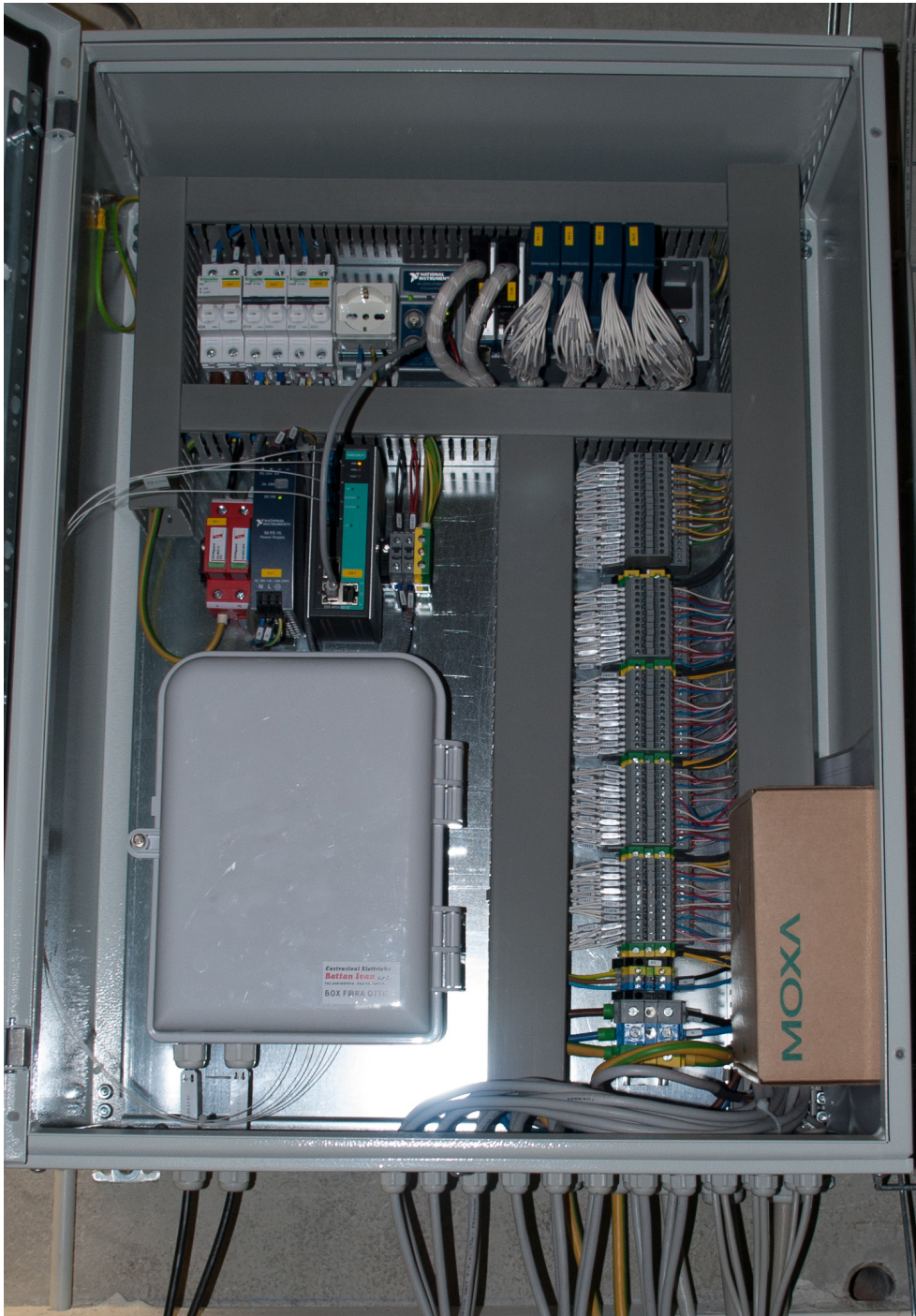


Figure 6.12. Box containing NI 9217 modules and a NI cDAQ-9188XT 8-slot Ethernet chassis used for the acquisition of data from the RTDs.

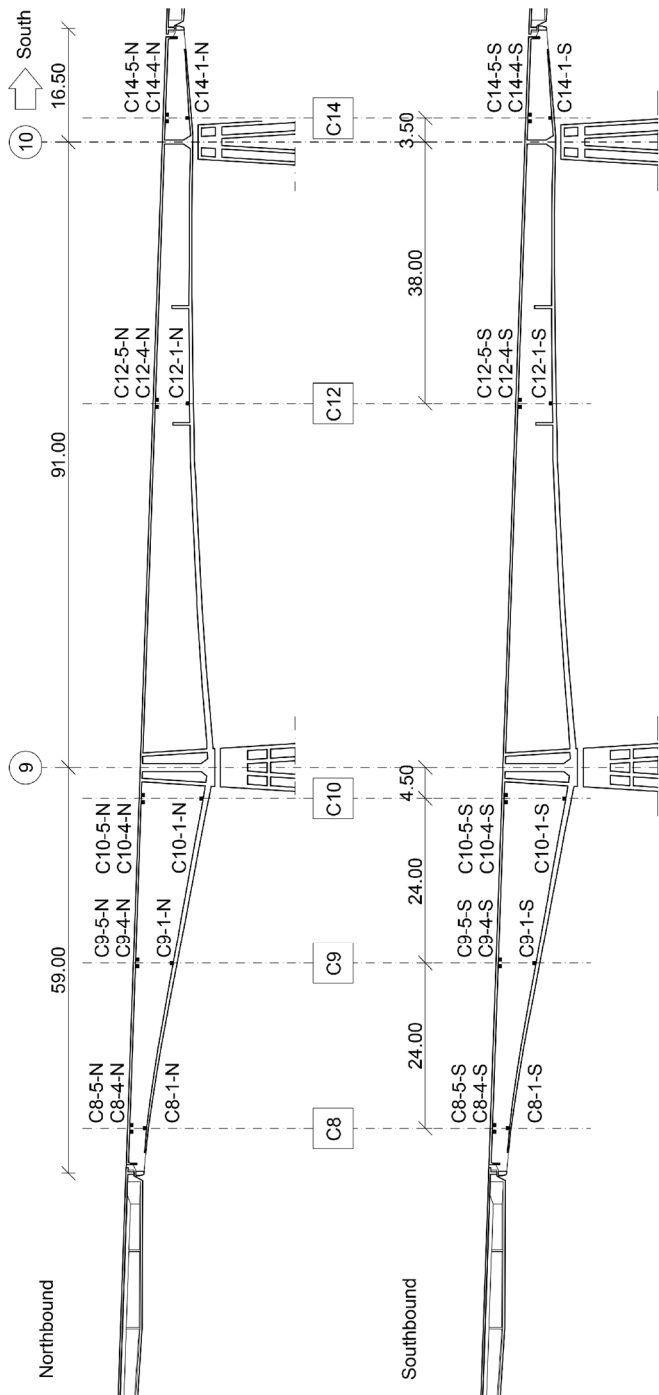


Figure 6.13. Position of the RTDs on the southernmost girders.

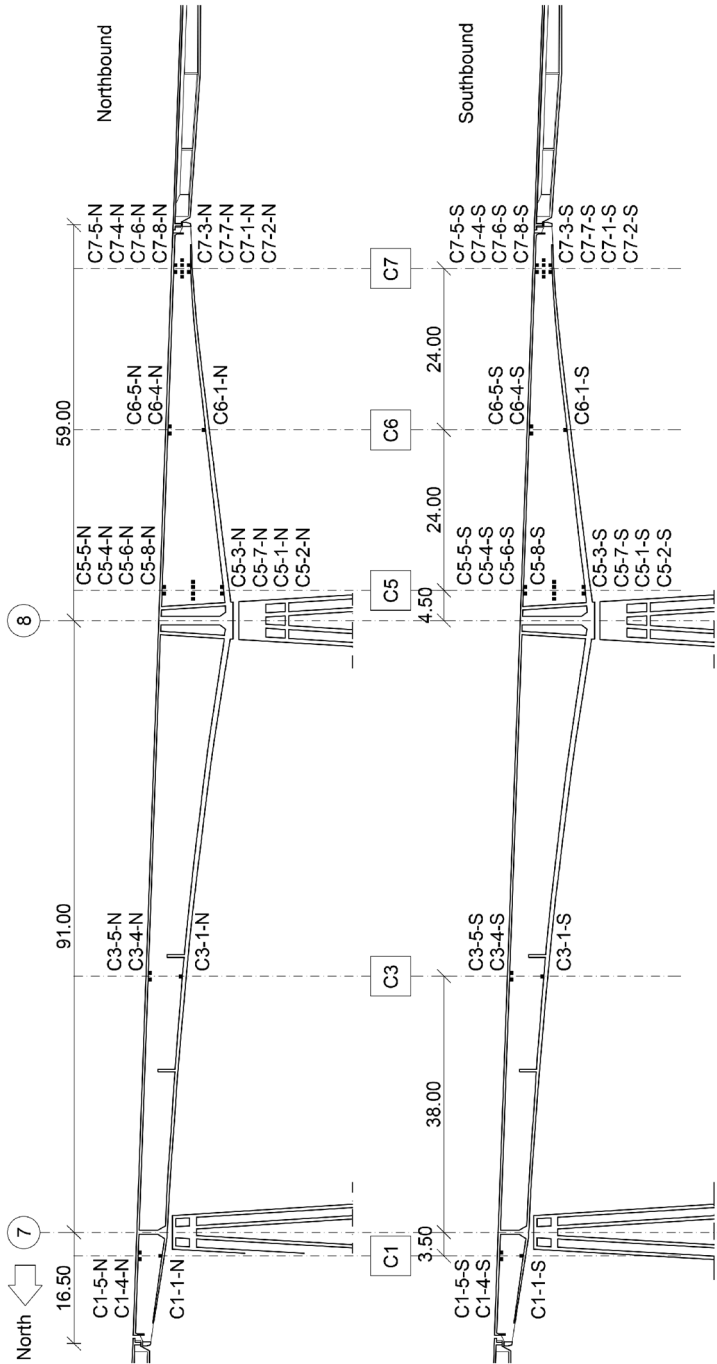


Figure 6.14. Position of the RTDs on the northernmost girders.

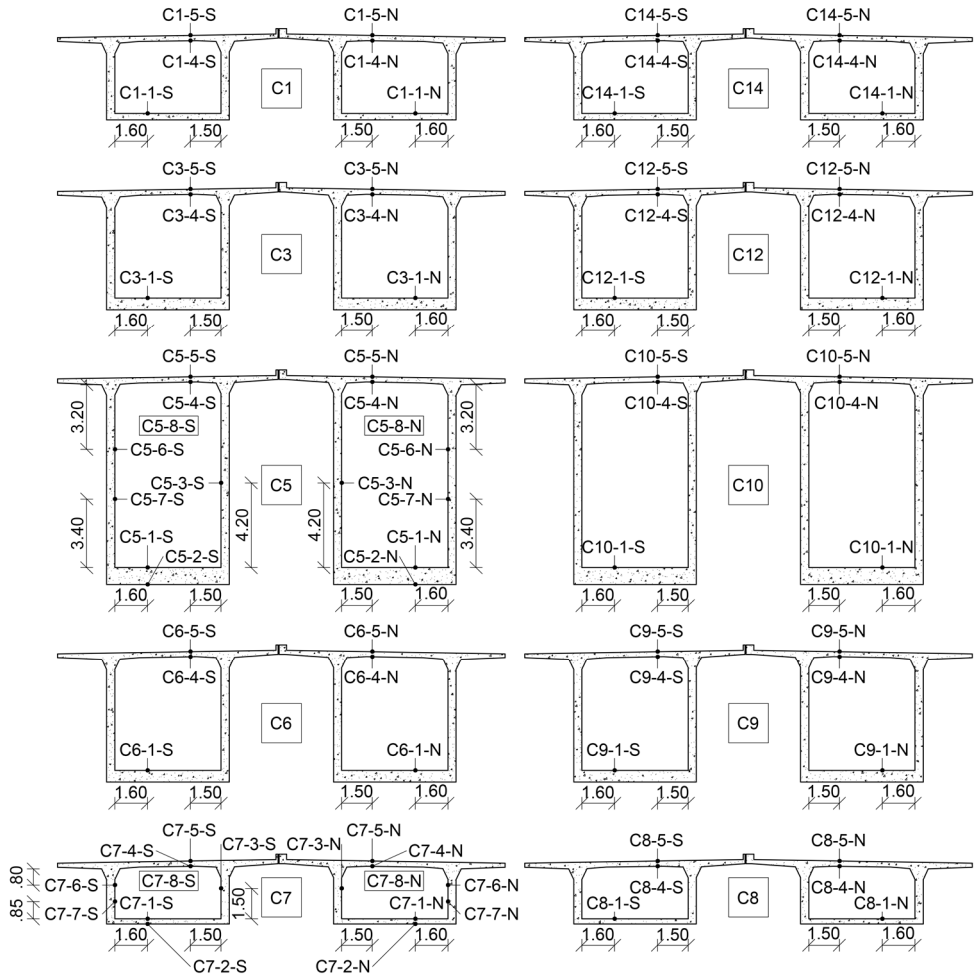


Figure 6.15. Position of the RTDs on the cross sections.

Table 6.3. Installation depths of the RTDs by position

Position	Element	Distance from inside [mm]	Distance from outside [mm]	Concrete thickness [mm]
1	Bottom slab	80	–	Variable
2	Bottom slab	270	–	Variable
3	Inner web	175	175	400
4	Top slab	40	170	260
5	Top slab	170	40	260
6	Outer web	175	175	400
7	Outer web	175	175	400
8	Air, inside	–	–	–

### 6.2.3 Fiber-optic sensors

The system based on FOSs was designed to monitor the long-term effects of the recent post-tensioning intervention. We chose long-gauge FOSs based on fiber Bragg grating (FBG) [118] that provide measurements of strain. These sensors were installed in the middle of the top and bottom slab, in order to effectively calculate the curvature of the girders and therefore investigate the causes of possible excessive long-term deformation trends. In fact, because of the propagation of uncertainty, the curvature calculated from displacements provided by topographic systems would be affected by severe error. Likewise, the displacements calculated by integration of a curvature obtained from strains would be very uncertain.

We installed 56 FOSs overall: 7 FOSs in series were installed in the middle of each slab (two slabs for each of the four girders). At the beginning, all the 56 sensors were designed to be 2 m-long. However, because of the irregular geometry of the slab surface, 8 out of the 56 sensors had to be 1 m-long, as depicted by Figure 6.17 and Figure 6.18. The sensor of choice were the *12.1010 MuST deformation sensor* [119], provided by Smartec SA [120] [15]. These sensors have an active zone that can be long between 0.20 m and 2 m, and an optional passive zone for temperature compensation that can be long between 1 m to 200 m. Before installation, the active zone must be pre-tensioned of 0.5% of its length before installation, in order to measure shortening. Instead, the passive zone, which is used to remove the effects of the temperature on the measurements (not on the structural behavior), must be left free to deform. Each FOS had to be installed using the installation kit. The sensors were pre-tensioned and anchored on two L brackets, which had been fixed to the concrete surface using four M6 bolts 50 mm long. Table 6.4 shows the characteristics of the FOSs of choice, which are taken from the Smartec SA datasheet. Figure 6.16 shows a moment of the installation of a FOS on the bottom slab of southbound southernmost girder of Colle Isarco Viaduct and a detail of the sensor.

In each chain, the sensors were joined without connectors. However, 10 m of additional optical fiber were left near each sensor, in case of maintenance. Each chain ends with an E-2000 APC (8°) connector and all the chain are connected to a single 8-channel reading unit<sup>2</sup>, located in the control cabin. We chose a *SOFO VII reading unit* [121], which was also provided by Smartec SA. This reading unit has an Ethernet

---

<sup>2</sup> In order to improve the robustness of the monitoring system based on FOSs, both ends of the sensor chains reach the control cabin.

interface and is controlled by the industrial computer *PC2-C*, which is located in the control cabin along with the reading unit. The features of the reading unit, taken from the Smartec SA datasheet, are presented in Table 6.5.

**Table 6.4. Technical characteristics of Smartec SA 12.1010 MuST deformation sensor**

Characteristic	Value
Strain range	-2500 $\mu\epsilon$ to +3000 $\mu\epsilon$
Temperature range	-40 °C to +80 °C
Resolution	0.2 $\mu\epsilon$
Precision	2 $\mu\epsilon$

**Table 6.5. Technical characteristics of Smartec SA SOFO VII reading unit**

Characteristic	Value
Measurement resolution	1 pm
Precision	2 pm
Sample rate	1 Hz
Range	1500 to 1600 nm
Measurement time	< 2 s per channel
Operating temperature	10 °C to 40 °C
Maximum humidity	90%



(a) Installation of a FBG FOS



(b) Label on a FBG FOS showing an active length of 2.00 m, a passive length of 39.0 m and a nominal wavelength of 1582.972 nm

Figure 6.16. Installation of a FBG FOS on the bottom slab of southbound southernmost girder of Colle Isarco Viaduct and a detail of the sensor.

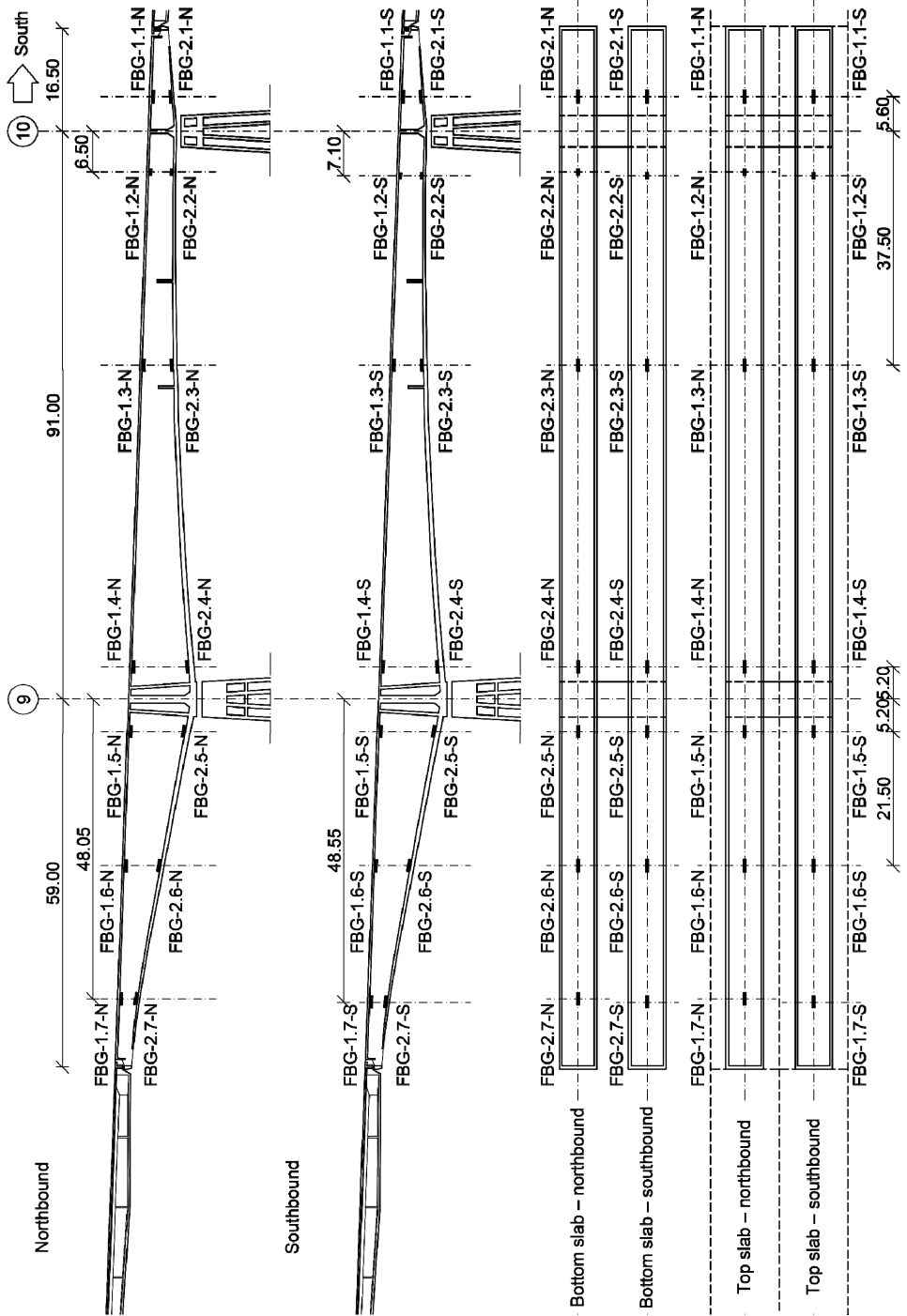


Figure 6.17. Configuration of the FOSs on the southernmost girders.

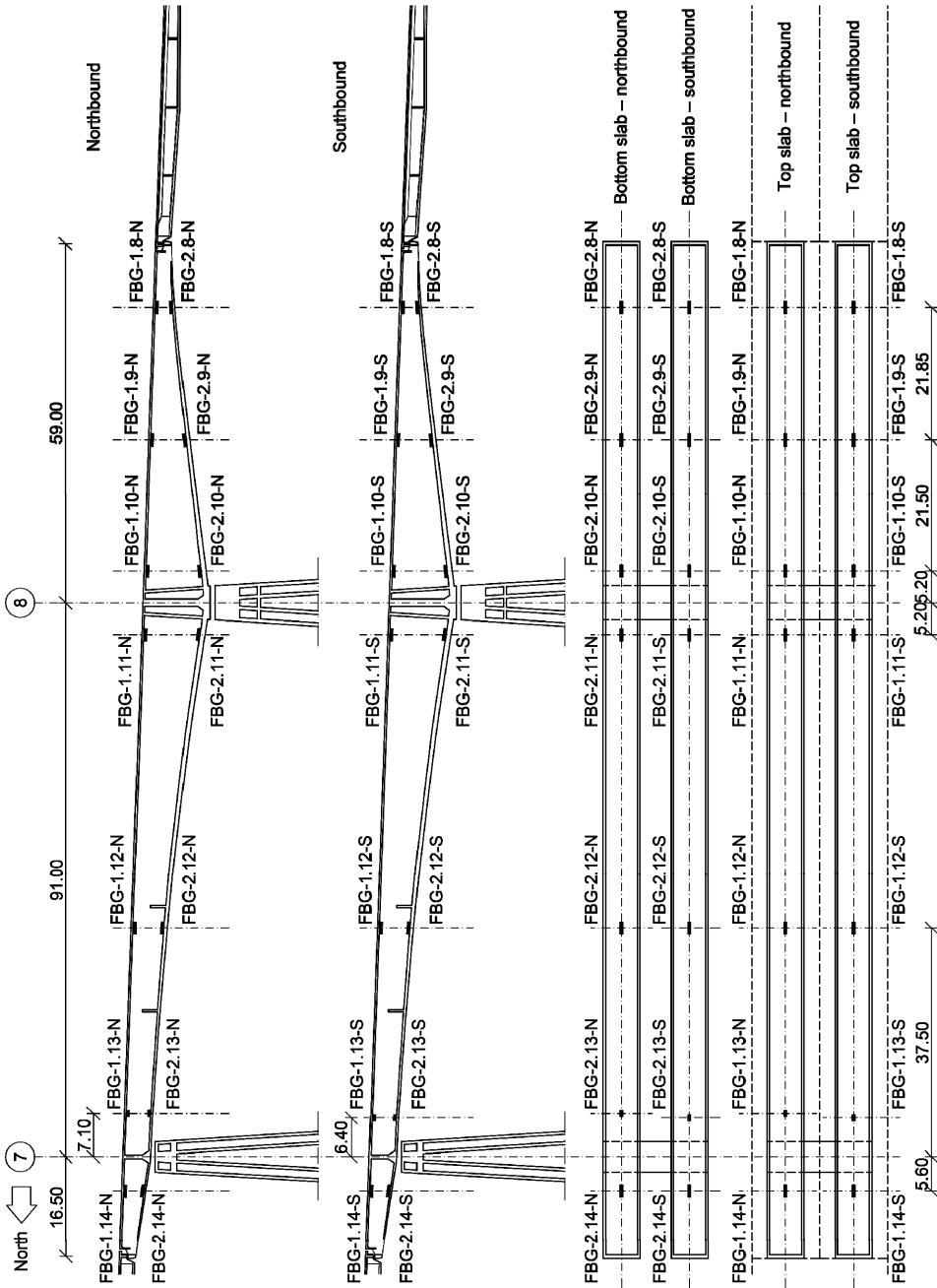


Figure 6.18. Configuration of the FOSs on the northernmost girders.

## 6.2.4 Networking

Figure 6.19 shows a scheme of the network that is used to acquire data from the sensors installed on Colle Isarco Viaduct. Above I explained how the sensors are physically connected to their reading units and how the data reach the control cabin located about 500 m away from the bridge central span. To sum up, each reading unit is in the control cabin or is connected to a computer in the control cabin through a TCP/IP interface. In the control cabin, two PCs control the topographic total stations for the measurement of the viaduct displacements (*PCI-C*), read the wavelength provided by the FBG FOSs (*PC2-C*) and acquire the resistance of the RTDs (*PC2-C*). All this data is saved locally in a PostgreSQL database, which is also replicated in computer *PC3-H*, located in the headquarters of Autostrada del Brennero SpA. All the devices that are located inside the bridge girders and in the control cabin are connected to a Mastersys BC UPS of 8 kVA [122], provided by Socomec, to avoid loss of data.

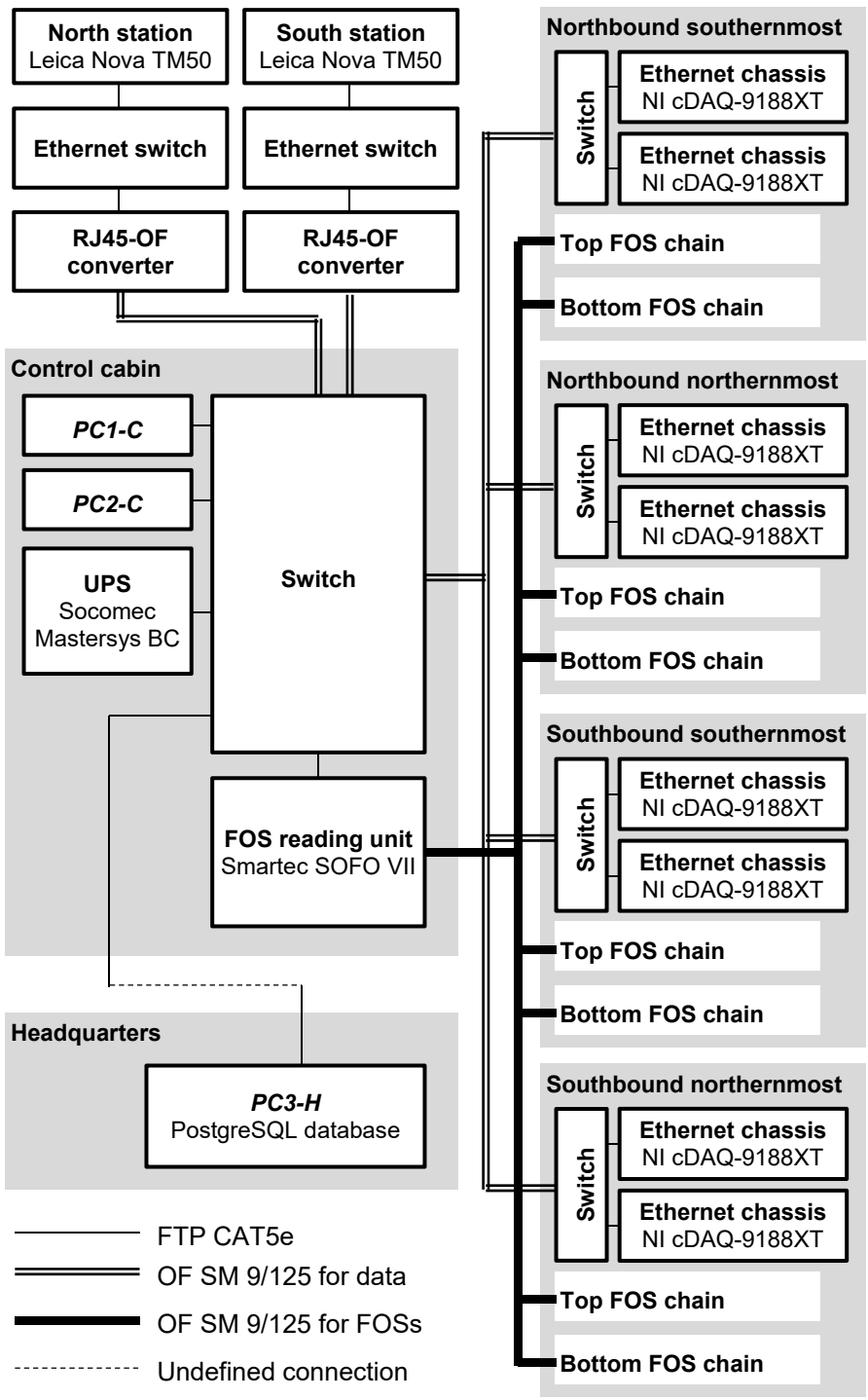


Figure 6.19. Scheme of the network for the acquisition of data.

## 6.3 Temperature data

The acquisition of data from the topographic network started on June 9, 2014, from the RTDs, it started on February 15, 2017. The acquisition of data from the FOSs has not started yet. We already know that we need to compensate the displacements measured by the topographic total stations in order to remove the effects of temperature. Figure 6.20 shows two days of temperature data from sections C5 and C7 of the southbound and northbound girders. The two days are February 25 and 26, 2017. The figures show that temperature variations in time up to 2.0 °C can be expected. The temperature variations during summertime may be even greater. The temperature measured by the RTDs in position 8 changes very rapidly because is the temperature of the air inside the girders. However, this temperature is of little interest. The variation of the hourly temperature measured by the other RTDs is worth some comments.

1. The temperatures from position 1 and 2 come from the bottom slab. The bottom slab of section C5 is the thickest and is close to pile 8. This explains that the temperature in the bottom slab of section C5 is approximately constant along the slab height and in time. In section C7, the temperature variations in time of the bottom slab are greater – about 1.5 °C – than those measured in section C5. Curiously, in the bottom slab of the southbound girder the temperature also changes up to 1.0 °C along the height, whereas in the northbound girder the temperature of position 1 is the same as position 2.
2. The temperatures coming from the RTDs installed in position 3 are those of the web that faces the parallel girder. These webs are not exposed to sunlight and, as shown by Figure 6.20, their temperature does not change much in time.
3. The temperatures of position 4 and 5 are those of the top slabs. These are those that change the most because the top slab is the most exposed to the sunlight and to the night sky. The temperature variations in time of the top slab are in the order of 2.0°C. Figure 6.20b, Figure 6.20c and Figure 6.20d also show that the temperature variations in position 5 is similar to that of position 4, but the latter heats up with a delay of about 2 hours. This phenomenon is easily explained by the fact that

the RTDs of position 4 are installed only 40 mm in the concrete slab, from the inside, whereas the RTDs of position 5 are installed 170 mm in the slab 40 mm from the surface.

4. The temperatures of the RTDs installed in position 6 and 7 are those of the outer webs. The temperature variations in time are up to 2.0 °C. The temperatures of position 6 are about the same as those of position 7 and this is reasonable because both the RTDs are installed 175 mm in the web. The temperature of the webs of the northbound girders increases before that of the southbound girders. This is also reasonable because the former are exposed to the sunlight in the morning, the latter in the afternoon.

Figure 6.21 shows the daily temperature measurements coming from section C5 and C7, from February 15, 2017. The hourly temperature variations, shown in Figure 6.20, have different phases, which depend on the part of the section that is measured. Nevertheless, the daily temperatures shown in Figure 6.21 have variations of similar phase. The reason for this is that the temperatures of Figure 6.21 are taken every day at 6 AM, when the temperature of each location is close to a daily average value. This phenomenon is more evident for section C7, whose bottom slab is the smallest. The bottom slab of section C5 is very thick (1,000 mm); thus, the temperature of this slab at 6 AM is probably closer to a weekly average value than a daily one. As a result, the phase of the daily temperature variations for position 1 and 2 are different from those of the other locations.

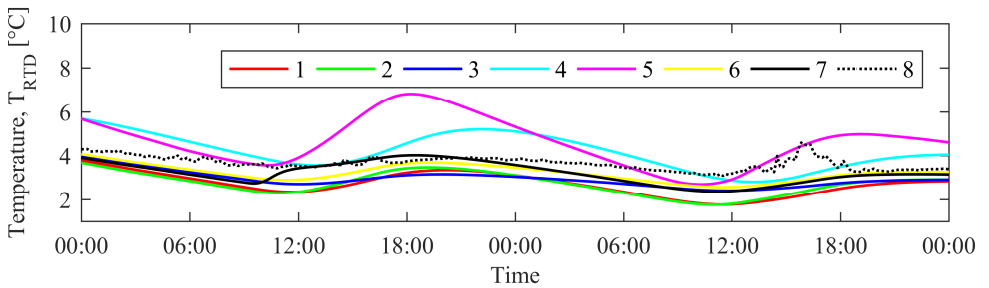
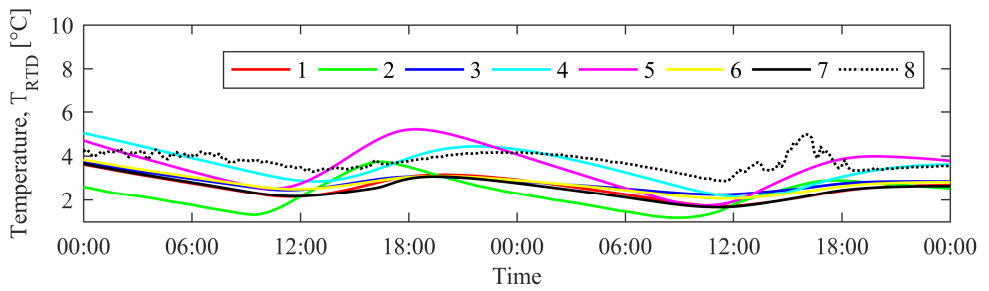
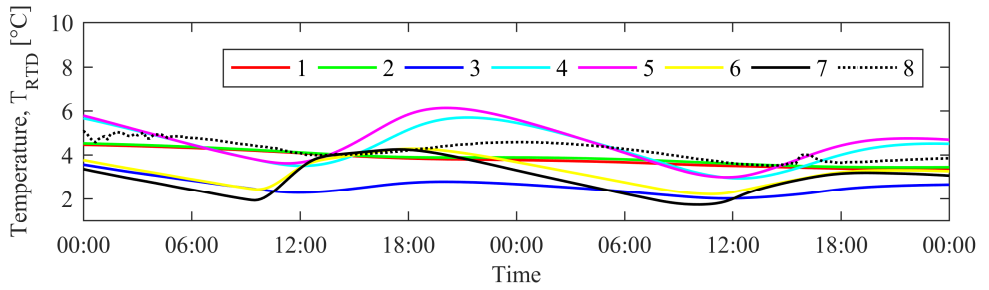
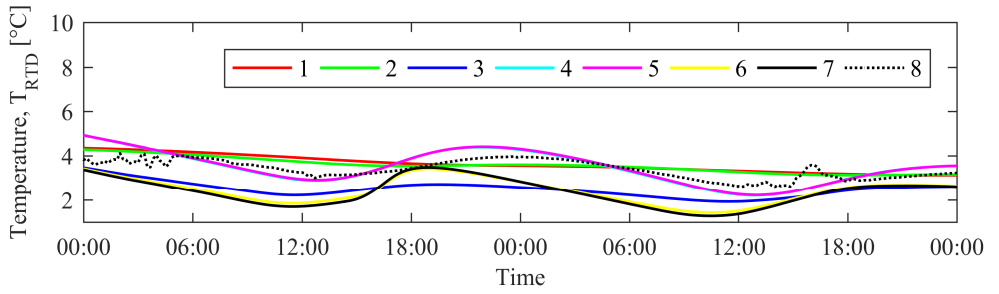
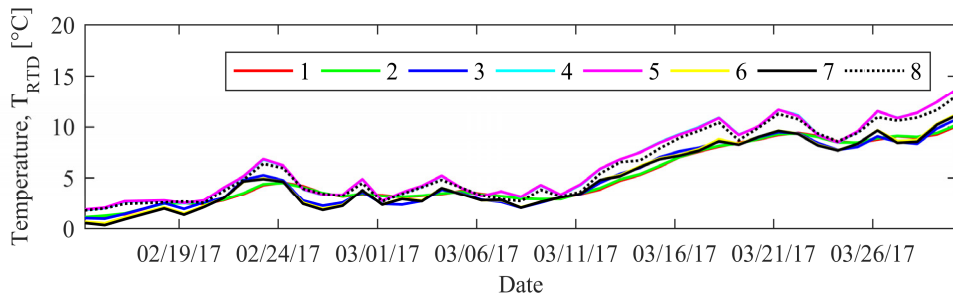
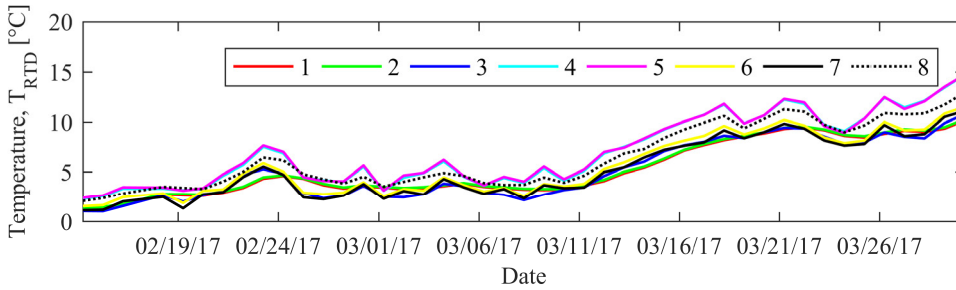


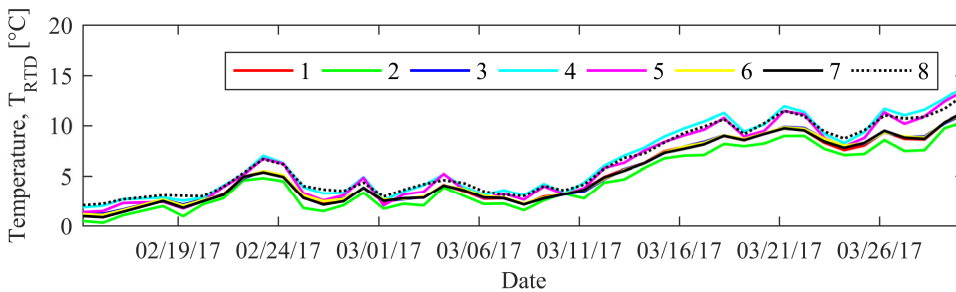
Figure 6.20. Two days (February 25 and 26, 2017) of temperature data.



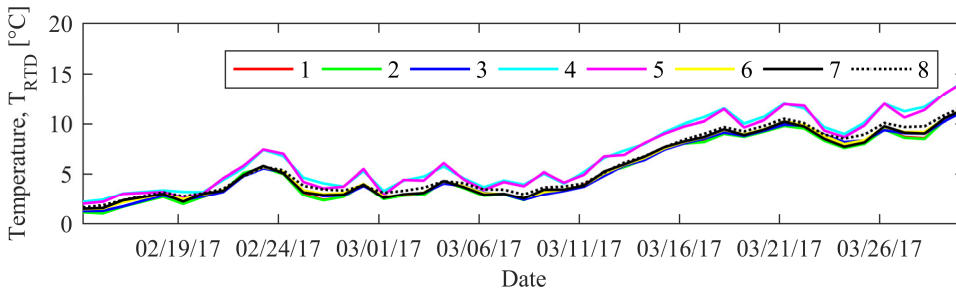
(a) Section C5, southbound girder



(b) Section C5, northbound girder



(c) Section C7, southbound girder



(d) Section C7, northbound girder

Figure 6.21. All temperature data.

## 6.4 Temperature compensation

Now that we understood the temperature variations that have been measured from the RTDs, we can analyze their effects on the displacements measured by the total stations. The direction of the displacements  $x$ ,  $y$  and  $z$  is defined in Figure 6.9 and Figure 6.8:  $x$  is parallel to the viaduct axis,  $y$  is orthogonal and  $z$  is vertical. Based on our engineering judgement, I assume that the displacements  $x$ ,  $y$  and  $z$  of the girders are influenced by the temperature differences defined below. The temperature that mostly affects the vertical displacements measured at the end of the cantilevers (by prism 9S1N, 9S2N, 9S1S, 9S2S, 8N1N, 8N2N, 8N1S and 8N2S) is assumed to be that of section C5. Figure 6.22a shows the displacement measured using prism 8N2S. Below, in Figure 6.22b, there are the temperature differences that affect the longitudinal displacements,  $\Delta T_{C5,x}$ , the orthogonal displacements,  $\Delta T_{C5,y}$ , and the vertical displacements,  $\Delta T_{C5,z}$ . All the temperatures come from section C5, southbound. Assuming that  $T_{RTD}(\mathbf{t})$  indicates the temperatures corresponding to times  $\mathbf{t}$ , measured by the RTD named *RTD*, the temperature differences of section C5 are then calculated as

$$\Delta T_{C5,x}(\mathbf{t}) = \frac{T_{C5-1-S}(\mathbf{t}) + T_{C5-2-S}(\mathbf{t}) + T_{C5-4-S}(\mathbf{t}) + T_{C5-5-S}(\mathbf{t})}{4}, \quad (6.1)$$

$$\Delta T_{C5,y}(\mathbf{t}) = \frac{T_{C5-6-S}(\mathbf{t}) + T_{C5-7-S}(\mathbf{t})}{2} - T_{C5-3-S}(\mathbf{t}), \quad (6.2)$$

$$\Delta T_{C5,z}(\mathbf{t}) = \frac{T_{C5-1-S}(\mathbf{t}) + T_{C5-2-S}(\mathbf{t})}{2} - \frac{T_{C5-4-S}(\mathbf{t}) + T_{C5-5-S}(\mathbf{t})}{2}. \quad (6.3)$$

Figure 6.22c shows the temperature of each RTD. From Figure 6.22, we can say that hourly measurements show a phase difference between the displacements of a section and the temperatures that affect the structural behavior of that section. This makes difficult to compensate hourly measurements. However, we are interested in monitoring the long-term behavior of the bridge.

Figure 6.23 shows the daily displacement measured using prism 8N2S and the daily temperature differences of section C5. Fortunately, the variations of the two series of data have the same phase. In order to study the effectiveness of RTD-based

temperature compensation of displacement data, I had to define a model in the form of (4.2). I chose a heuristic model that is linear with respect to the temperature differences  $\Delta T_{C5}$  and quadratic with respect to time  $\mathbf{t}$ :

$$\hat{\mathbf{x}}_{prism}(\mathbf{t}, \boldsymbol{\theta}_{prism}) = x_{0,prism} [1 \quad \dots \quad 1] + \alpha_{prism,x} \Delta T_{C5,x}(\mathbf{t}) + \beta_{prism,x} \mathbf{t} + \frac{\gamma_{prism,x}}{2} \mathbf{t} \cdot \mathbf{t}^T, \quad (6.4)$$

$$\hat{\mathbf{y}}_{prism}(\mathbf{t}, \boldsymbol{\theta}_{prism}) = y_{0,prism} [1 \quad \dots \quad 1] + \alpha_{prism,y} \Delta T_{C5,y}(\mathbf{t}) + \beta_{prism,y} \mathbf{t} + \frac{\gamma_{prism,y}}{2} \mathbf{t} \cdot \mathbf{t}^T, \quad (6.5)$$

$$\hat{\mathbf{z}}_{prism}(\mathbf{t}, \boldsymbol{\theta}_{prism}) = z_{0,prism} [1 \quad \dots \quad 1] + \alpha_{prism,z} \Delta T_{C5,z}(\mathbf{t}) + \beta_{prism,z} \mathbf{t} + \frac{\gamma_{prism,z}}{2} \mathbf{t} \cdot \mathbf{t}^T, \quad (6.6)$$

where the state parameters are

$$\boldsymbol{\theta}_{prism} = \left\{ \begin{array}{l} x_{0,prism}, y_{0,prism}, z_{0,prism}, \\ \alpha_{prism,x}, \alpha_{prism,y}, \alpha_{prism,z}, \\ \beta_{prism,x}, \beta_{prism,y}, \beta_{prism,z}, \\ \gamma_{prism,x}, \gamma_{prism,y}, \gamma_{prism,z} \end{array} \right\}. \quad (6.7)$$

Since we are interested in the long-term acceleration of prisms at the time of the analysis, it is important that  $\mathbf{t}$  has the origin – its zero – at the time of the analysis, rather than at the time of the first measurement.

Before using the model of (6.4) on the data, I had to remove the effects of the pier displacements from the data, because the behavior of the piers is not considered by the model. The equations used to remove the effects of the piers are

$$\mathbf{x}_{prism} = \mathbf{x}'_{prism} - \begin{cases} \mathbf{x}_{5NP1S} & \text{north girders,} \\ \mathbf{x}_{12SP1S} & \text{south girders,} \end{cases} \quad (6.8)$$

$$\mathbf{y}_{prism} = \mathbf{y}'_{prism} - \begin{cases} (\mathbf{y}_{1NP1S} - \mathbf{y}_{5NP1S}) \cdot \frac{\xi_{prism} - 2.54 \cdot 10^5 \text{ mm}}{9.1 \cdot 10^4 \text{ mm}} + \mathbf{y}_{5NP1S}, & \text{north g.,} \\ (\mathbf{y}_{12SP1S} - \mathbf{y}_{16SP1S}) \cdot \frac{\xi_{prism}}{9.1 \cdot 10^4 \text{ mm}} + \mathbf{y}_{16SP1S}, & \text{south g.,} \end{cases} \quad (6.9)$$

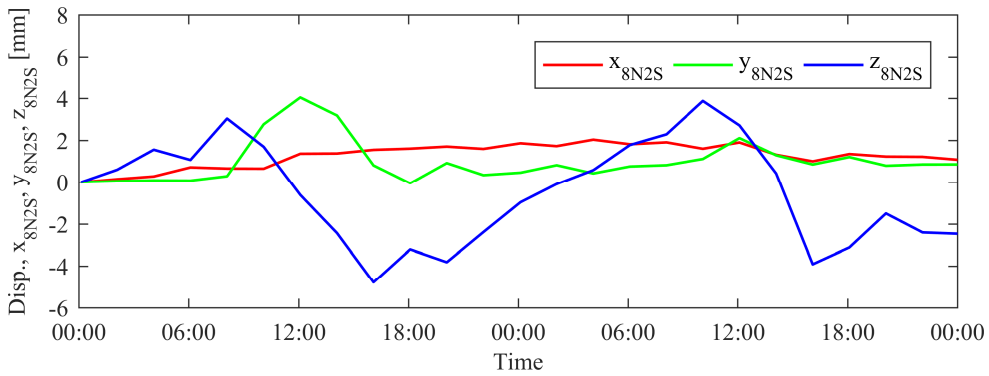
$$\mathbf{z}_{prism} = \mathbf{z}'_{prism} - \begin{cases} (\mathbf{z}_{1NP1S} - \mathbf{z}_{5NP1S}) \cdot \frac{\xi_{prism} - 2.54 \cdot 10^5 \text{ mm}}{9.1 \cdot 10^4 \text{ mm}} + \mathbf{z}_{5NP1S}, & \text{north g.,} \\ (\mathbf{z}_{12SP1S} - \mathbf{z}_{16SP1S}) \cdot \frac{\xi_{prism}}{9.1 \cdot 10^4 \text{ mm}} + \mathbf{z}_{16SP1S}, & \text{south g.,} \end{cases} \quad (6.10)$$

where  $\xi_{prism}$  is the distance of the prism from Pier 10, which is shown in Figure 6.9 and Figure 6.8. Figure 6.24 shows the displacements of prism 8N2S before and after the compensation with the pier displacements.

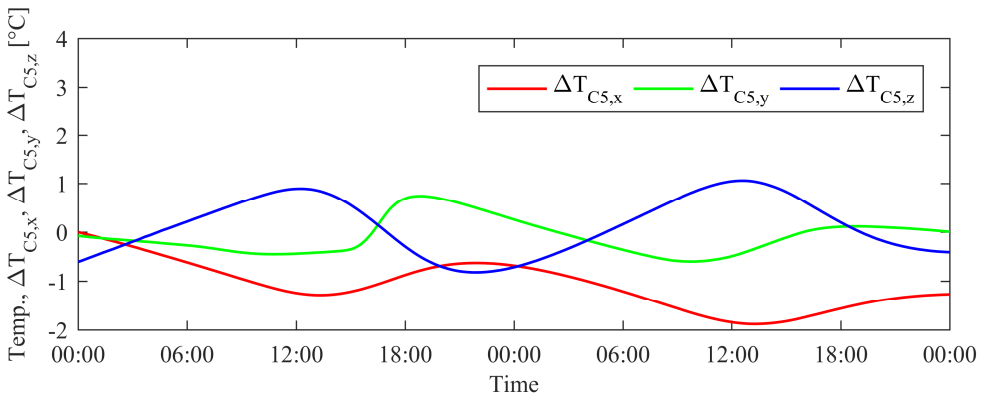
I corrected the data with the displacement of the piers using (6.8). Afterwards, the data were ready to be fitted using the model of (6.4). For this preliminary analysis, I performed parameter identification using non-linear least squares regression [73]. The results are summarized in Table 6.6 and Figure 6.25 shows the interpolation of data using the model of (6.4). Then, I used the state parameters of (6.7) to remove the effects of temperature from the data obtained from (6.8):

$$\begin{aligned} \mathbf{x}''_{prism} &= \mathbf{x}_{prism} - \alpha_{prism,x} \cdot \Delta \mathbf{T}_{C5,x}(\mathbf{t}), \\ \mathbf{y}''_{prism} &= \mathbf{y}_{prism} - \alpha_{prism,y} \cdot \Delta \mathbf{T}_{C5,y}(\mathbf{t}), \\ \mathbf{z}''_{prism} &= \mathbf{z}_{prism} - \alpha_{prism,z} \cdot \Delta \mathbf{T}_{C5,z}(\mathbf{t}). \end{aligned} \quad (6.11)$$

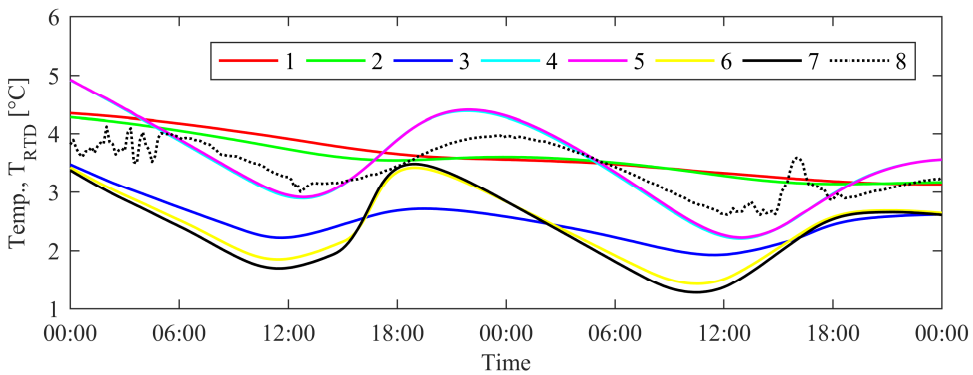
The results are shown in Figure 6.24c. The temperature compensation appeared to be satisfactory because it significantly reduced the temperature-induced displacements. As shown by Table 6.6, this preliminary analysis also evidenced the sensitivity of the vertical displacements to temperature. Prism 8N2S is expected to rise of 4.8 mm if the temperature difference between the two slabs of section C5 increases by 1 °C.



(a) Displacements of prism 8N2S, southbound girder

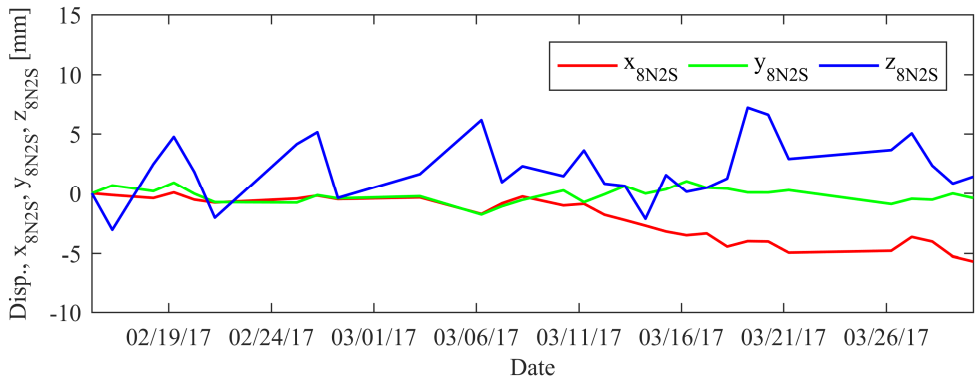


(b) Temperature difference between the top and bottom slab of section C5, southbound girder

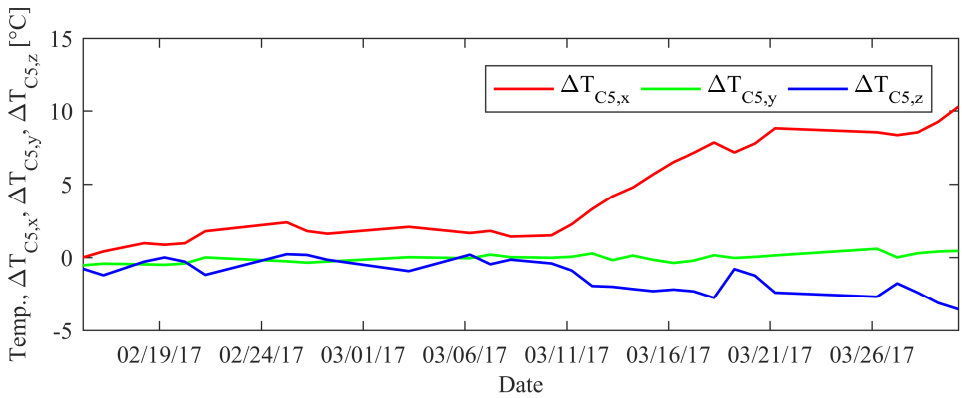


(c) Temperatures of section C5, southbound girder

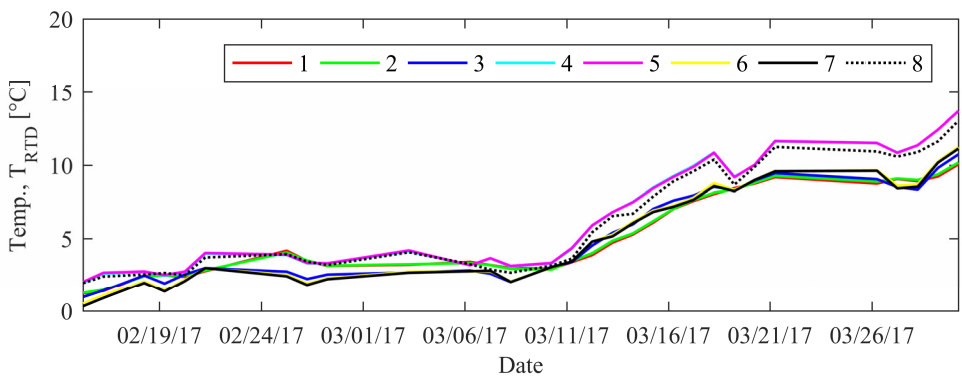
Figure 6.22. Two days (February 25 and 26, 2017) of data.



(a) Displacements of prism 8N2S, southbound girder

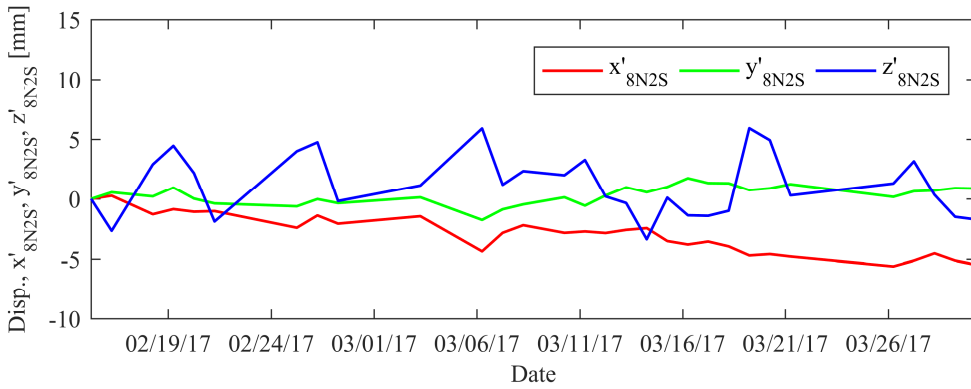


(b) Temperature difference between the top and bottom slab of section C5, southbound girder

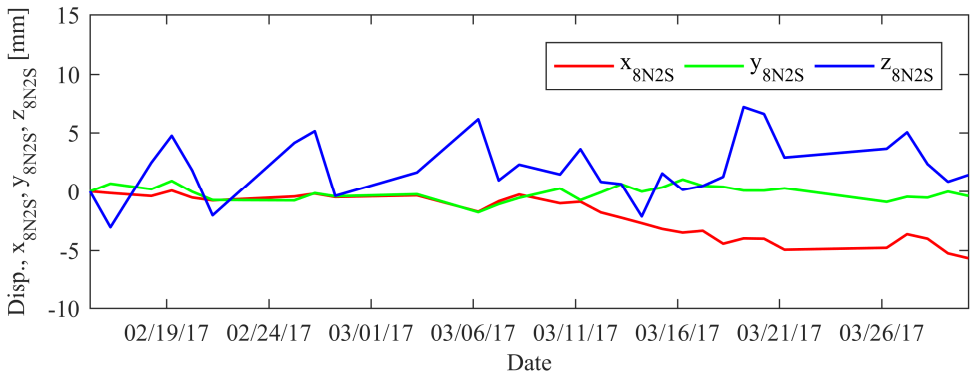


(c) Temperatures of section C5, southbound girder

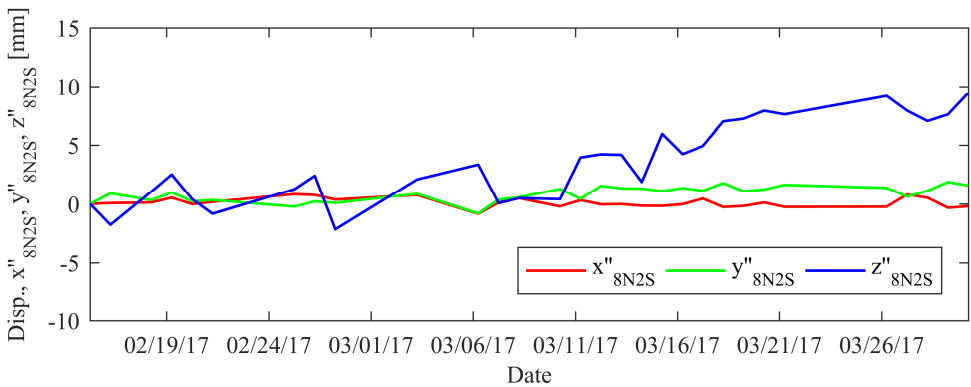
Figure 6.23. All data concerning the displacements of prism 8N2S.



(a) Raw data



(b) Compensated with the displacements of piers



(c) After temperature compensation

Figure 6.24. Compensated data of prism 8N2S.

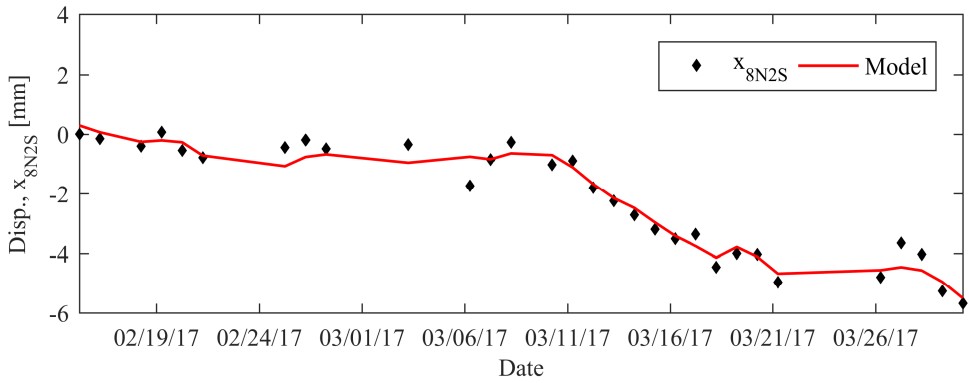
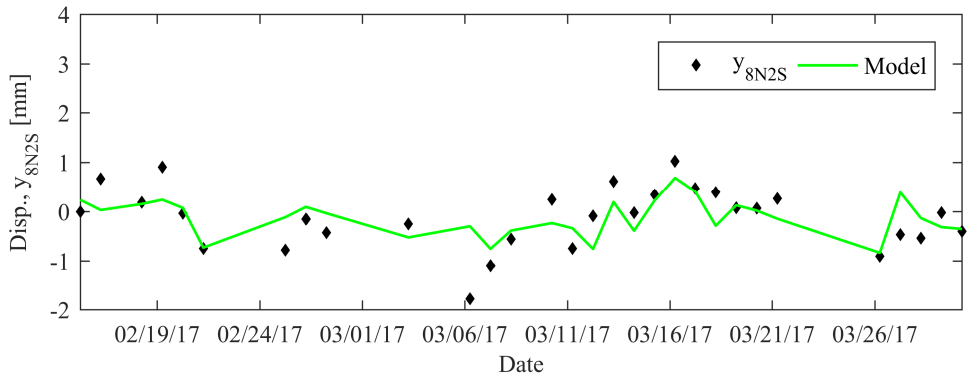
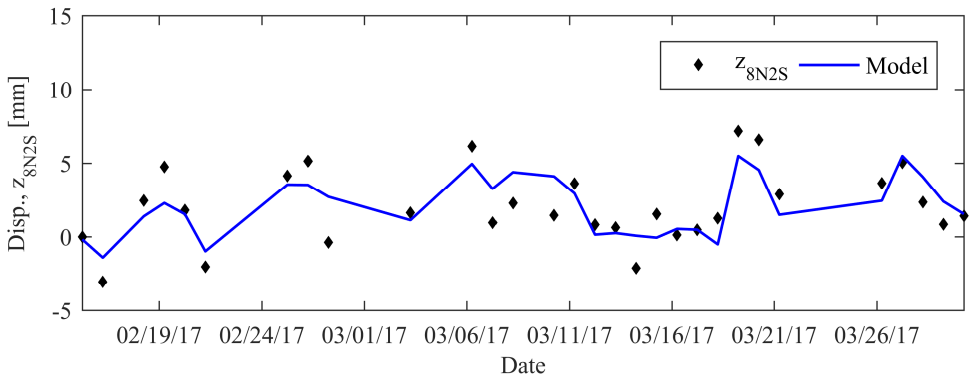
(a) Displacement  $x$ (b) Displacement  $y$ (c) Displacement  $z$ 

Figure 6.25. Model and data from prism 8N2S.

**Table 6.6. Results of preliminary parameter identification obtained by performing non-linear least squares regression**

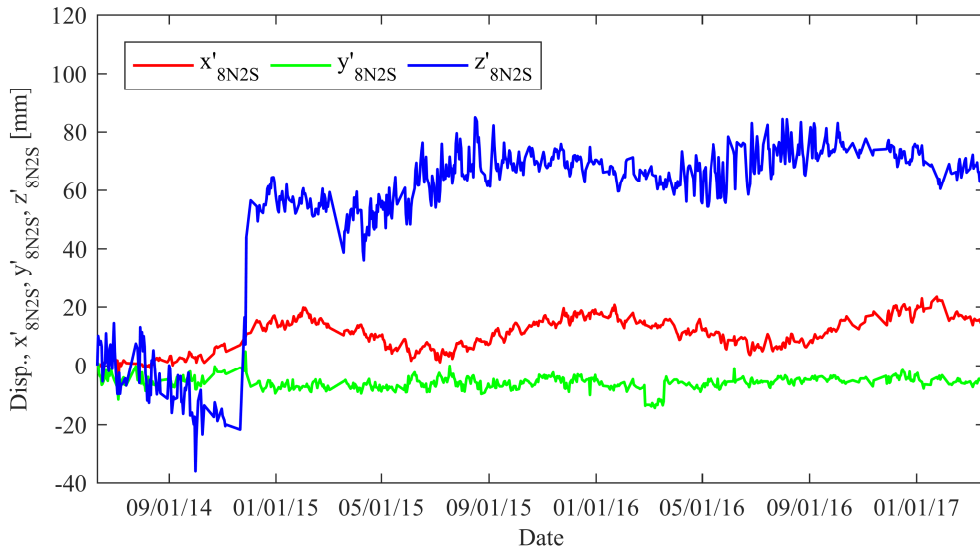
Axis	Parameter	Unit	Mean	SD	COV [%]
$X_{8N2S}$	$x_{0,8N2S}$	[mm]	0.0	0.8	–
	$\alpha_{8N2S,x}$	[mm/°C]	–0.5	0.1	13
	$\beta_{8N2S,x}$	[mm/year]	–2.0	13.8	687
	$\gamma_{8N2S,x}$	[mm/year/day]	0.0	0.4	–
	$\sigma_{8N2S,x}$	[mm]	0.4	–	–
$Y_{8N2S}$	$y_{0,8N2S}$	[mm]	0.5	0.3	56
	$\alpha_{8N2S,y}$	[mm/°C]	–2.0	0.5	26
	$\beta_{8N2S,y}$	[mm/year]	17.9	10.5	59
	$\gamma_{8N2S,y}$	[mm/year/day]	0.3	0.4	154
	$\sigma_{8N2S,y}$	[mm]	0.5	–	–
$Z_{8N2S}$	$z_{0,8N2S}$	[mm]	11.8	1.7	14
	$\alpha_{8N2S,z}$	[mm/°C]	2.9	0.5	16
	$\beta_{8N2S,z}$	[mm/year]	150.9	40.4	27
	$\gamma_{8N2S,z}$	[mm/year/day]	3.2	1.5	49
	$\sigma_{8N2S,z}$	[mm]	1.6	–	–

## 6.5 Displacement data

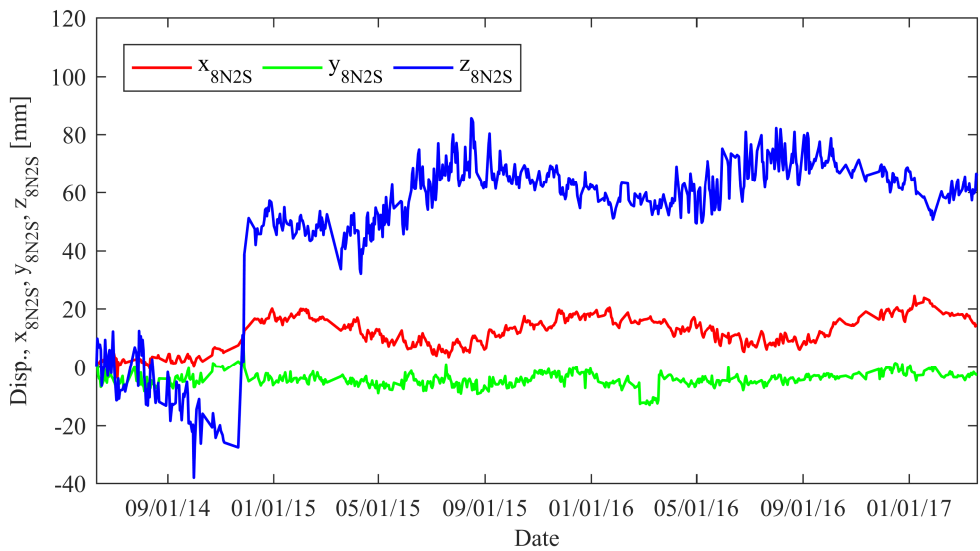
Figure 6.26 to Figure 6.29 show the daily displacement of the prisms that are installed at the end of each cantilever, since June 9, 2014, without temperature compensation. By observing these data, we can understand that the general behavior of the decks as well as the effects due to post-tensioning. Three things can be pointed out.

1. From July 31 to August 11, 2014, part of the top slab of the southbound girders was removed and new concrete was cast to the required thickness. This operation reduced the effective prestress of the two southbound decks, which started to lower very quickly until the post-tensioning of the new external cables. The same phenomenon can be observed for the northbound girders.
2. The new external cables of the southbound girders were tensioned on November 22, 2014; the new external cables of the northbound girders were tensioned on October 1, 2015. The figures show the tensioning process very clearly and evidenced that the end of the cantilevers raised by about 70 mm.

3. The effects of temperature on the bridge behavior throughout the years mainly affected the vertical and longitudinal displacements. Temperature induced variations of about 40 mm in the vertical displacement of the cantilever edges, and variations of about 15 mm in the longitudinal displacements of the same points.
4. Data recorded by the north station between February 25 to March 19, 2016, is shifted. This phenomenon is particularly severe for the orthogonal displacements,  $y$ , but it is not due to an actual structural displacement. This shift in the data occurred because the box that protects the north station was opened for maintenance and rotated by mistake. This caused a rotation of the protection glass that resulted in the anomaly. The data shifted back to the original trend on March 19, 2016, when the protection box was rotated to the original position.

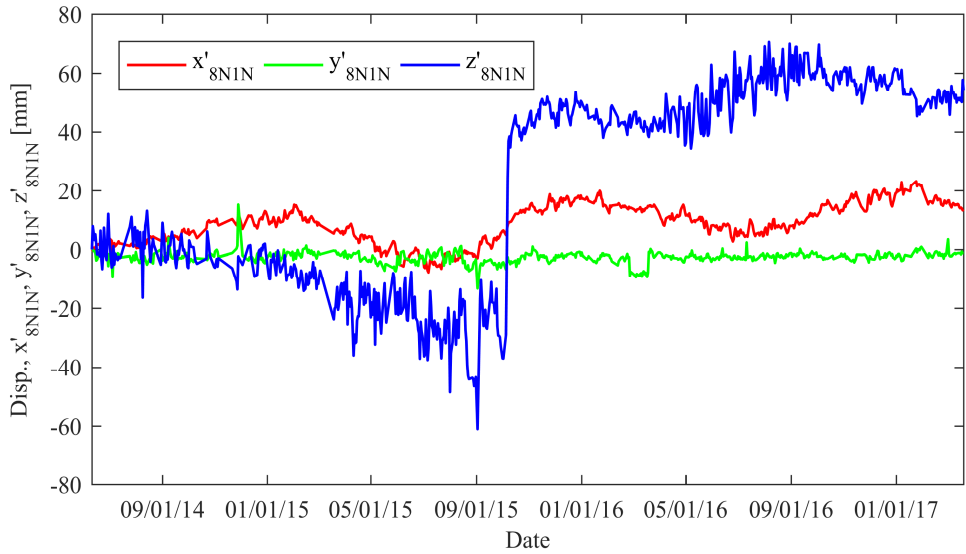


(a) Raw data

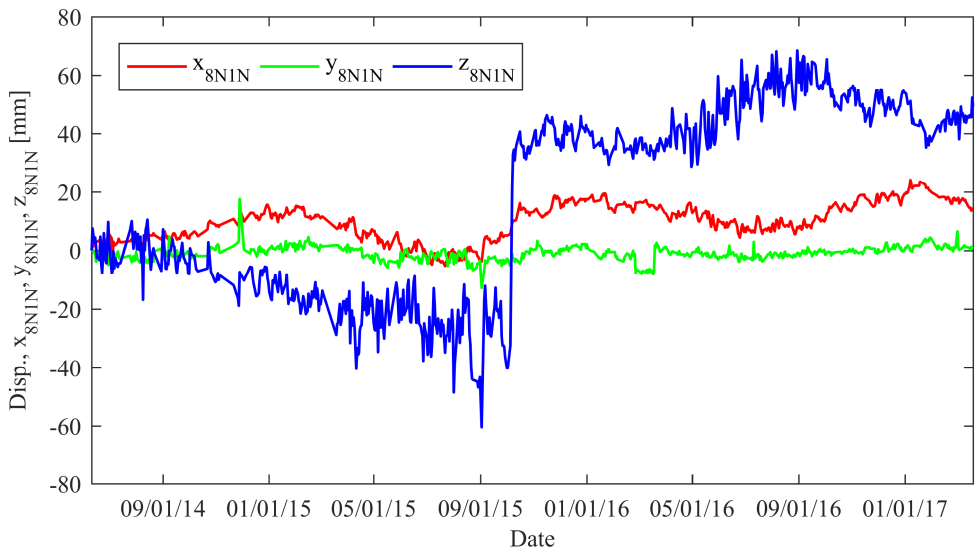


(b) Compensated with the displacements of piers

Figure 6.26. Displacements of prism 8N2S, since 2014.

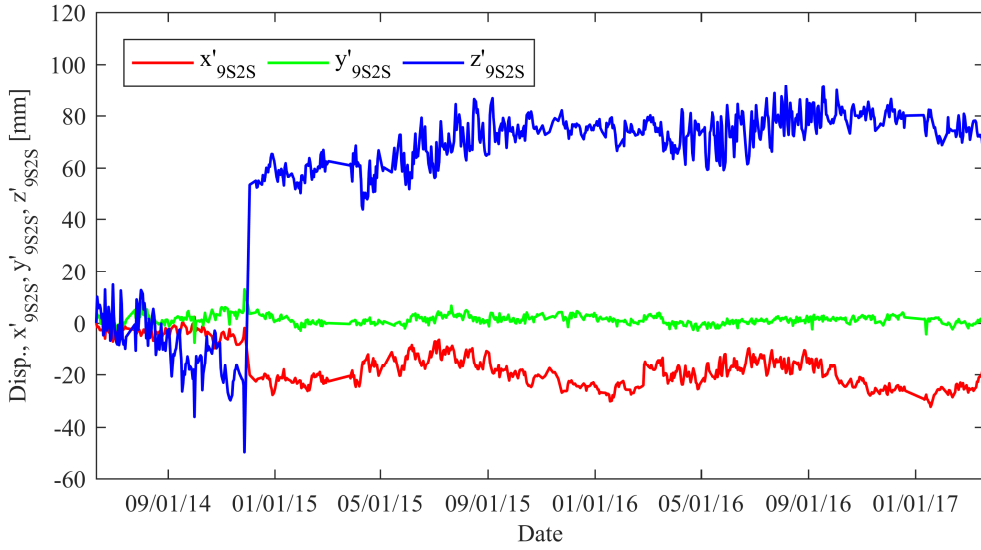


(a) Raw data

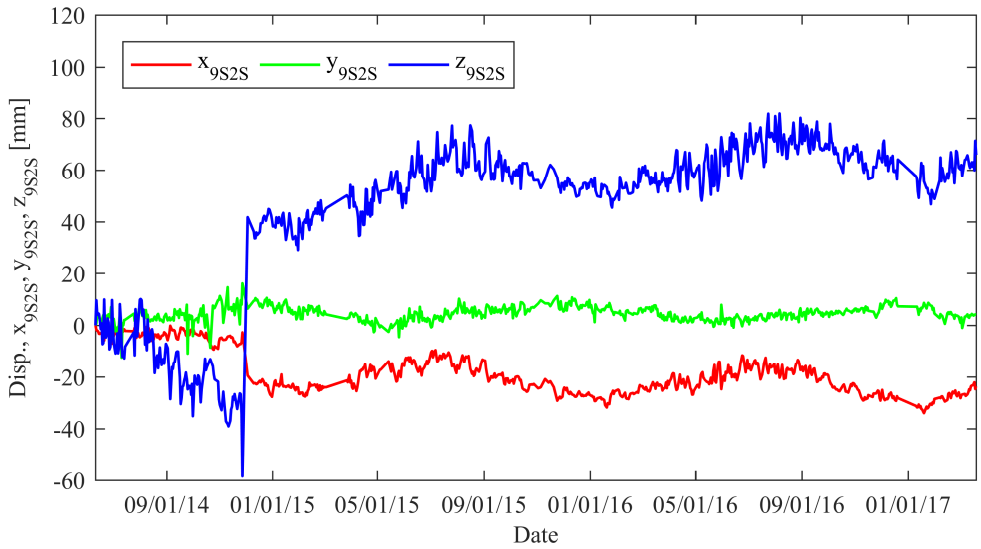


(b) Compensated with the displacements of piers

Figure 6.27. Displacements of prism 8N1N, since 2014.

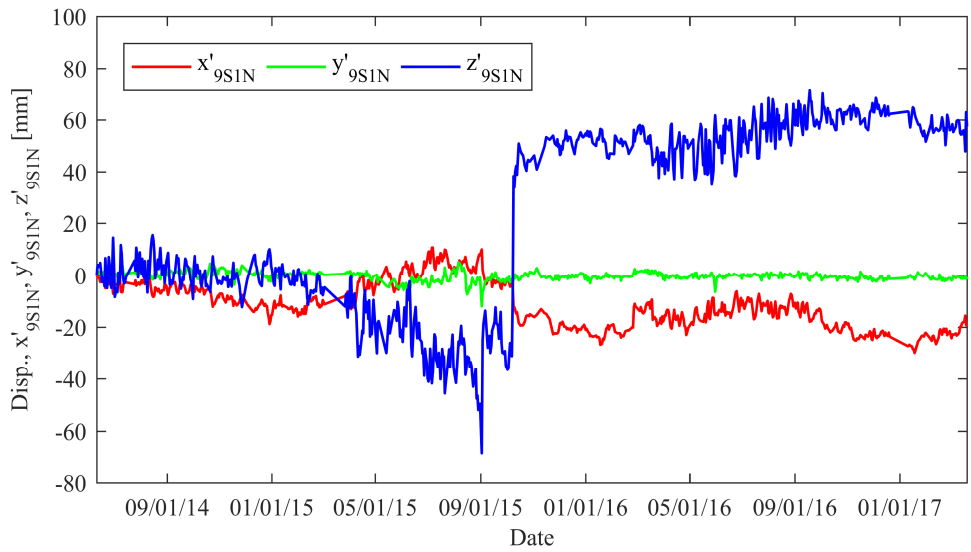


(a) Raw data

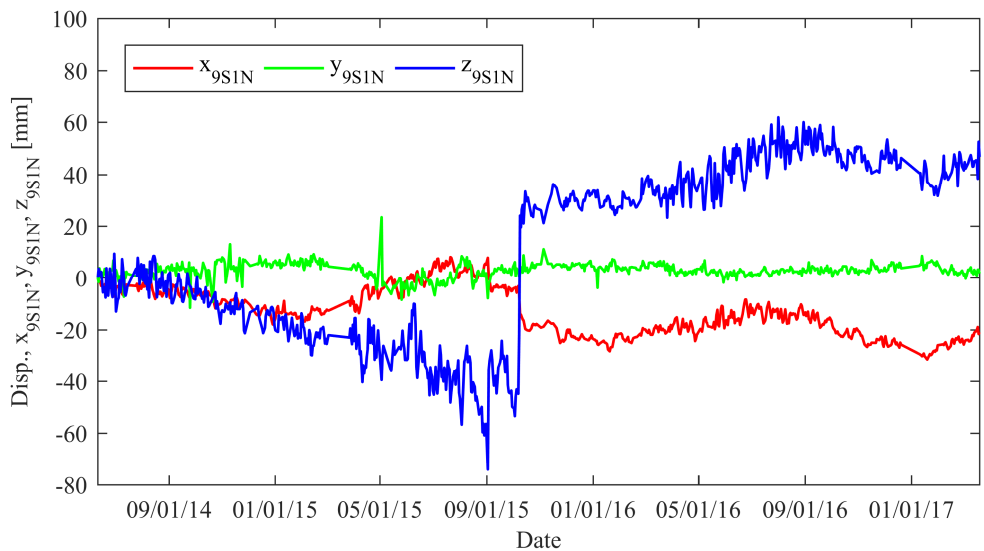


(b) Compensated with the displacements of piers

Figure 6.28. Displacements of prism 9S2S, since 2014.



(a) Raw data



(b) Compensated with the displacements of piers

Figure 6.29. Displacements of prism 9S1N, since 2014.

## 6.6 Decision support system

The measurements of displacement and temperature provided by the total stations and the RTDs are available and shall be used to assist the management policies of the viaduct operator. The classifiers developed in this section were used to define the DSS that was provided to Autostrada del Brennero SpA. Herein, I calculate two classifiers. Both the classifiers take the temperature-compensated displacements of the 14 days preceding the analysis as an input and provide financially optimal actions as an output. In the first example, I considered a single-stage decision problem in which each action is a terminal action. The actions considered for this example are: “do nothing” and “close the bridge”. In the second example, one non-terminal action is added: the agent can choose action “send inspector”, and an inspector is sent to the bridge before, again, the agent has to choose between “do nothing” and “close the bridge”. In this section, I focus on SHM-based decision-making while the probability distributions are provided. The classifiers are defined by one (for the first example) and two (for the second example) thresholds. Throughout the entire section, the measurements used to calculate the thresholds and to show the results are the displacements taken from the end of the southbound northernmost cantilever – prism 8N2S.

### 6.6.1 Single-stage decisions

Concisely, the SHM-based decision problem is to identify the financially optimal action  $a_{\text{opt}}(\mathbf{y})$ , based on a set of observations  $\mathbf{y}$  provided by a monitoring system. Therefore, we are looking for a map that defines a relationship between the domain of the observations  $\Omega_{\mathbf{y}}$  and the set of possible actions  $\Omega_a$ . In this section, I consider a single-stage decision tree (which consists in only one decision node) and I implement EUT to obtain the aforementioned map.

In a single-stage decision problem, the agent in charge of the decision has to choose a terminal action  $a$  that may affect the state of the structure  $S$ . I also assume that a unique monetary outcome  $z$  follows a realization of  $S$  and  $a$ . Using EUT, the optimal choice depends on the observations  $\mathbf{y}$ , and may be affected also by prior knowledge. Equation (3.13) is used to calculate the expected utility of each action  $a$ . The maximum expected utility for the decision is

$$u_{\max}^*(\mathbf{y}) = \max_{a \in \Omega_a} u^*(a, \mathbf{y}), \quad (6.12)$$

and the optimal action is

$$a_{\text{opt}}^*(\mathbf{y}) = \arg \max_{a \in \Omega_a} u^*(a, \mathbf{y}). \quad (6.13)$$

Equation (6.13) is a function of the observations  $\mathbf{y}$  and maps each possible  $\mathbf{y}$  to an optimal action  $a_{\text{opt}}$ . Given an observation set  $\mathbf{y}$  from the monitoring system, (6.13) automatically provides the optimal action  $a_{\text{opt}}$  to the agent in charge of the decision.

Now, we want to solve the SHM-based decision problem for Colle Isarco Viaduct. Given the observations from the monitoring system, the agent wonders whether the structural state is unsafe and the bridge should be closed to traffic. Here, I assume that the structural state  $S$  can be one of two mutually exclusive and exhaustive realizations: “undamaged”  $U$  and “damaged”  $D$ , defined as follows.

- *Undamaged,  $U$ .* The viaduct is “undamaged” if it is undamaged at all or has negligible damage, which does not affect the structural capacity.
- *Damaged,  $D$ .* The structure is “damaged” if it has been subjected to major damage and there is a significant probability of collapse under a live load.

Formally,  $S$  is a discrete variable, defined in the domain  $\Omega_S = \{U, D\}$ .

The observation used to identify the optimal action are the last 14 daily vertical displacements of a selected prism (two weeks of data). The information contained in these data are condensed into a single variable, by *feature extraction* [123]. In practice, every morning the DSS performs non-linear least squares regression as presented in §6.4 to calculate the value of long-term acceleration  $\gamma_{prism,z}$ , which is then treated as a unique observation by the DSS. The vertical displacements used in the feature extraction are assumed to be temperature-compensated.

After the definition of the mutually exclusive and exhaustive structural states  $S$ , we always need to define the likelihood functions of the decision problem, which in this case provide the probability of observing a value of long-term acceleration  $\gamma_{prism,z}$ , given each structural state  $S$ . Zonta *et al.* [104] developed a FEM of Colle Isarco Viaduct that was used to study the structural behaviour of the bridge and the

uncertainty in the future deflection trends. This structural model has been analysed by another research group at the University of Trento, and its presentation is out of the scope of this dissertation. However, here I use the information resulted from the analysis of the structural behaviour to define the likelihood functions of the decision problem.

In a 14 day interval, the analysis of the structural behaviour showed that for the prism installed at the end of the cantilevers (9S1N, 9S2N, 9S1S, 9S2, 8N1N, 8N2N, 8N1S and 9N2S) the long-term acceleration  $\gamma_{prism,z}$  in the “undamaged” state  $U$  can be assumed distributed according to a Gaussian probability density function  $p(\gamma_{prism,z}|U)$  with mean  $\mu_{\gamma|U} = 0$  mm/year/day (mm/year per day) and standard deviation  $\sigma_{\gamma|U} = 0.731$  mm/year/day. Instead, in the “damaged” state  $D$ ,  $p(\gamma_{prism,z}|D)$  is a Gaussian distribution with mean  $\mu_{\gamma|D} = -1.826$  mm/year/day and standard deviation  $\sigma_{\gamma|D} = 1.096$  mm/year/day.

The next step is to define the prior probability distributions. Based on the literature [124] [31] and heuristics, I assume that for Colle Isarco Viaduct the prior probability of structural failure in a 100 year period is  $10^{-6}$  and that the structural reliability is constant day by day<sup>3</sup>. The DSS checks the structural condition every day, therefore, using the binomial distribution, I can indirectly calculate the daily probability of structural failure, which is the prior probability  $p(D)$  to be used in the DSS. Formally, I solved

$$10^{-6} = \binom{36525 \text{ day}}{1 \text{ day}} p(D) [1 - p(D)]^{36524}, \quad (6.14)$$

which resulted in about  $p(D) = 3 \cdot 10^{-11}$  (for 1 day).

The evidence of a realization of  $\gamma_{prism,z}$  is

$$p(\gamma_{prism,z}) = p(\gamma_{prism,z} | D) \cdot P(D) + p(\gamma_{prism,z} | U) \cdot P(U). \quad (6.15)$$

Each day, the monitoring observations are available to the manager, who can update the estimate of the state probability using Bayes’ theorem:

---

<sup>3</sup> In reality, the probability of failure of a structure is high immediately after construction, then it drops during the first year of service and slowly increases in time.

$$P(S|\gamma_{prism,z}) = \frac{P(\gamma_{prism,z}|S) \cdot P(S)}{P(\gamma_{prism,z})}, \quad (6.16)$$

where  $S$  is either  $U$  or  $D$ . The two posterior probabilities, which are functions of  $\gamma_{prism,z}$ , are depicted in Figure 6.31a. There is a threshold of long-term acceleration  $\bar{\gamma}_p = -5.78$  mm/year/day whereby  $P(U|\gamma_{prism,z}) = P(D|\gamma_{prism,z})$ . When  $\gamma_{prism,z} > \bar{\gamma}_p$ , the bridge is more likely to be damaged than undamaged.

Each day, given a value of long-term acceleration  $\gamma_{prism,z}$ , the agent has to choose one of the following actions, which, in this example, are restrained to two.

- *Do nothing, DN*. No restriction is enforced to the traffic over and under the viaduct.
- *Close the bridge, CB*. Both the highway and the road under the viaduct are closed to traffic, for the time required by structural rehabilitation, which is estimated in 3 months.

This defines the domain of actions,  $\Omega_a = \{DN, CB\}$ . Of course, choosing to close the viaduct would prevent any effect of a possible collapse of the structure. The loss incurred from this action is mainly due to RUC. This cost was estimated by Tonelli [125] to be  $z_{CB} = \text{€}2,300,000$  for the three-month period. However, the agent can decide to do nothing ( $DN$ ) and allow the traffic on the viaduct as usual. If the agent decides to do nothing and the state  $S$  is undamaged  $U$ , the monetary outcome is  $z_U = \text{€}0$ . Instead, if the state  $S$  is damaged  $D$ , the structure may collapse resulting in an overall cost of  $z_D = \text{€}9,340,000$ , including direct and indirect costs. The decision problem that is modeled herein is represented with the single-stage decision tree of Figure 6.30.

The costs and the probabilities introduced above are both necessary and sufficient to solve the SHM-based decision problem. Now, I want to calculate two domains in the space of  $\gamma_{prism,z}$  where the two possible actions – “do nothing” ( $DN$ ) and “close the bridge” ( $CB$ ) – are optimal. For simplicity, I assume that the agent is risk neutral and therefore I define the utility function  $u(z) = -z$ . Then, the expected utilities of actions  $DN$  and  $CB$  are:

$$\begin{aligned} u^*(DN, \gamma_{prism,z}) &= -z_U \cdot P(U | \gamma_{prism,z}) - z_D \cdot P(D | \gamma_{prism,z}), \\ u^*(CB, \gamma_{prism,z}) &= -z_{CB}. \end{aligned} \quad (6.17)$$

Assuming that the agent follows the suggestions of the DSS and takes the least expensive option, the maximum expected utility, in the condition *a posteriori*, is:

$$u_{\max}^*(\gamma_{prism,z}) = \max\{u^*(DN, \gamma_{prism,z}), u^*(CB, \gamma_{prism,z})\}. \quad (6.18)$$

The expected utility functions calculated for each action as in (6.17) are represented in Figure 6.31b. In this case,  $u^*(CB, \gamma_{prism,z})$  is constant, while  $u^*(DN, \gamma_{prism,z})$  decreases with the value of  $\gamma_{prism,z}$ . The two expected utilities are equal for the threshold  $\bar{\gamma}_u = -5.59$  mm/year/day. Closing the viaduct is the most convenient option when  $\gamma_{prism,z} > \bar{\gamma}_u$ . This defines two mutually exclusive and exhaustive regions in the domain of the long-term acceleration:

$$a_{\text{opt}}(\gamma_{prism,z}) = \begin{cases} DN & \gamma_{prism,z} \leq \bar{\gamma}_u, \\ CB & \gamma_{prism,z} > \bar{\gamma}_u. \end{cases} \quad (6.19)$$

Note that the threshold  $\bar{\gamma}_u$  does not coincide with the threshold  $\bar{\gamma}_p$ . The manager should decide to close the bridge not when the long-term acceleration  $\gamma_{prism,z}$  shows that the bridge is more likely to be damaged  $D$  than undamaged  $U$ , but when the expected utility for doing nothing,  $u^*(DN, \gamma_{prism,z})$ , is lower than the expected utility of closing the bridge,  $u^*(CB, \gamma_{prism,z})$ .

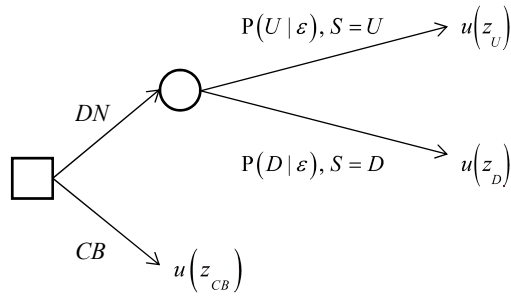
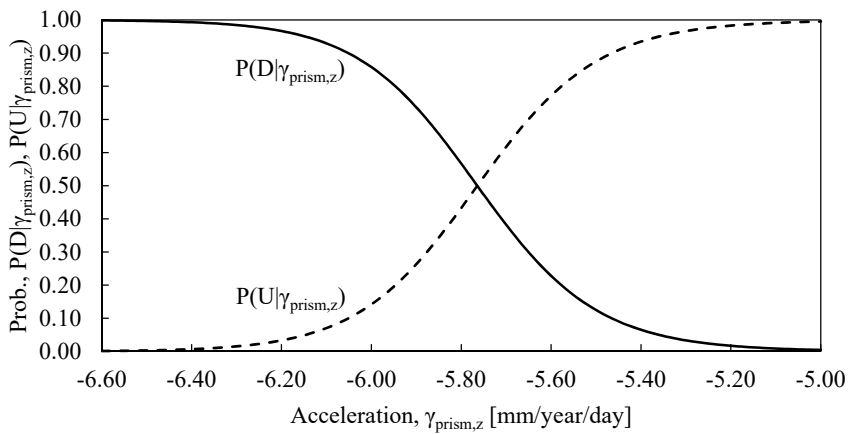


Figure 6.30. Decision tree of the SHM-based single-stage decision problem.



(a) Posterior distributions of the two possible states

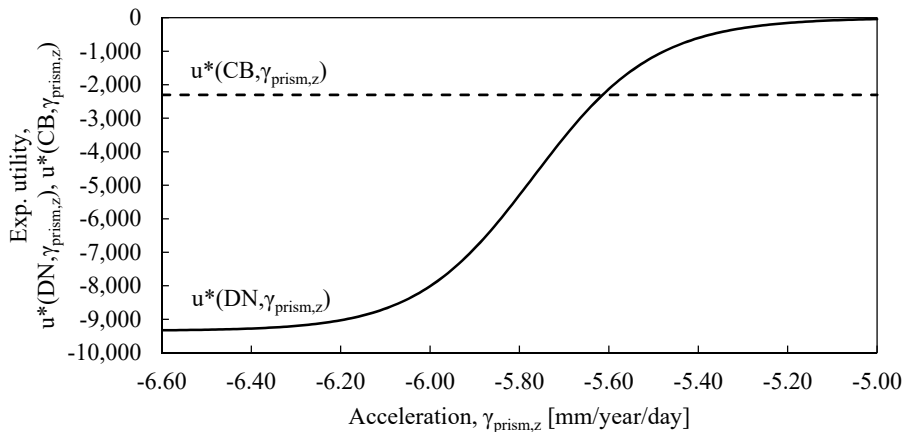

 (b) Expected utilities of the two actions (“do nothing” *DN* and “close the bridge” *CB*)

Figure 6.31. Probabilities and expected utilities of the SHM-based single-stage decision problem.

## 6.6.2 Multi-stage decisions

The SHM-based decision problem of the preceding section is relatively simple. In real life, agents choose among multiple available actions, some of which may become available after others, in a different decision stage. In this section, I present another solution of the SHM-based decision problem of Colle Isarco Viaduct in which the problem is expanded with one additional decision stage.

In multi-stage decision problems, the agent may have to take multiple actions, i.e. the action  $a^{(1)}$  in the first stage may not be a terminal action. In reality, the agent may not know *a priori* the actions that will be available in the stages after the first one. However, when we develop a DSS with EUT, we need to define the decision tree and the probabilities of the states  $S$ . In this formulation, I denote the predicted probabilities using a superscript “ $(n)$ ”, where  $n$  is the stage in which the prediction occurs. I use the same superscript “ $(n)$ ” with the expected value operator  $E[\dots]$  in order to indicate the stage  $n$  in which we calculate the expected value. In order to provide a DSS for multi-stage decision problems, we also have to define a *decision rule* [10], which is an assumption on how the decision-maker will act after the first stage. Here, I assume that the agent will always follow the suggestions of the SHM-based DSS and choose actions corresponding to the highest expected utility

When the decision tree has multiple stages, the optimal decision in stage  $n$  satisfies

$$a_{\text{opt}}^{(n)} \left( \gamma_{prism,z} \right) = \arg \max_{a^{(n)} \in \Omega_a^{(n)}} u^* \left( a^{(n)}, \gamma_{prism,z} \right). \quad (6.20)$$

However, calculating  $u^* \left( a^{(n)}, \gamma_{prism,z} \right)$  is not straightforward because other decision nodes may be nested in each branch of the decision tree. In order to solve this problem, we need to apply the principle of *backward induction* [62]. First, for each  $t$ th decision node connected to a terminal action, we calculate the expected utility using the probabilities  $p^{(n)}(S|a^{(t)}, \dots, \gamma_{prism,z})$  expected in stage  $n$ . Then, we assign to each  $t$ th decision node a utility  $u_{\text{node}}^{(t)} \left( \gamma_{prism,z} \right)$  equal to the maximum expected utility:

$$u_{\text{node}}^{(t)} = \max_{a^{(t)} \in \Omega_a^{(t)}} E_{S|a^{(t)}, \dots}^{(n)} \left[ u \left( z^{(t)} | S, a^{(t)}, \dots \right) \right]. \quad (6.21)$$

By doing this, I had to use the assumption that the agent always chooses the option that corresponds to the highest expected utility. If we assume that each decision node

connected to a terminal action has a virtual outcome that leads to a utility  $u_{\text{node}}^{(t)}(\gamma_{\text{prism},z})$ , we can solve the decision nodes that are connected to the left of the  $t$ th node in the same way and repeat this process until we can calculate the expected value of  $a^{(n)}$ , required to solve (6.20).

In the single-stage decision problem presented in the preceding section, the agent must take a decision between only two actions (“do nothing” or “close the bridge”). In real life, the agent would probably consider the option of acquiring more information about the state  $S$  of the viaduct. Therefore, in the multi-stage decision problem the agent can choose to send to the viaduct an inspector in charge of giving an expert judgment based on his experience. In this case, the following option must be added to the actions “do nothing”  $DN$  and “close the bridge”  $CB$ .

- *Send inspector, SI.* The viaduct is temporarily closed while an expert inspection, expected to last 10 days, is done.

Before the actual inspection, in order to reach the bottom of the deck, an *under bridge inspection unit*<sup>4</sup> has to be hired. Then, one lane at a time needs to be closed to traffic while the unit operates on the viaduct in safe conditions. Visual inspection of the deck is performed and material samples may be taken from the structure. The inspection concludes by testing the material samples and by analyzing the collected data.

The domain of the actions  $a^{(1)}$  available in the first stage must be redefined in  $\Omega_a^{(1)} = \{DN, SI, CB\}$ . If the action “send inspector”  $SI$  is chosen, the inspector provides a judgment  $\tilde{S}$  on the state of the viaduct, which can be either “undamaged”  $U$  or “damaged”  $D$ . The judgment of the inspector is represented by the variable  $\tilde{S} \in \{U, D\}$ , which is defined in the same domain as the states,  $\Omega_S$ . After the inspector’s judgement, the agent can eventually choose again between the two remaining actions,  $a^{(2)} \in \Omega_a^{(2)} = \{DN^{(2)}, CB^{(2)}\}$ . The decision tree of this multi-stage decision problem is represented in Figure 6.32.

Unfortunately, the inspector’s judgment  $\tilde{S}$  is not the true state  $S$  of the viaduct but is just an uncertain estimation of  $S$ . The chances to identify correctly the actual state  $S$  mostly depend on the inspector’s experience and skills. The inspector’s judgement is like an observation – a piece of information related to the state  $S$  through a probabilistic model. The relationship between the inspector’s judgment  $\tilde{S}$  and the actual state  $S$  is defined through the probability  $P(\tilde{S} | S)$ , which is a *confusion matrix*

<sup>4</sup> An *under bridge inspection unit* is a large truck equipped with a mechanical arm and a basket that can be used to reach the bottom of a bridge deck.

[126] that plays the role of the likelihood function in the acquisition of the inspector’s judgement. In this case, the probability  $P(\tilde{S} | S)$  is a two-by-two matrix. The element in column  $i$  and row  $j$  is the probability that the inspector classifies the viaduct in the  $j$ th state whereas the viaduct is actually in the  $i$ th state:

$$P(\tilde{S} | S) = \begin{bmatrix} P(\tilde{U} | U) & P(\tilde{U} | D) \\ P(\tilde{D} | U) & P(\tilde{D} | D) \end{bmatrix}, \quad (6.22)$$

where here I use “~” on the states  $U$  and  $D$  to indicate that they are the estimation of  $S$  provided by the inspector.

The components of the confusion matrix represent the agent’s judgment about the capacity of the inspector to identify correctly the viaduct state. I assume that, when the true structural state is “undamaged”  $U$ , the inspector correctly identifies the condition in 80% of cases and misclassifies the condition in 20% of cases. When the structural condition is “damaged”  $D$ , the inspector correctly identifies the state in 99% of cases and misclassifies the state in 1% of cases. As a result, the values of the confusion matrix are:

$$P(\tilde{S} | S) = \begin{bmatrix} 0.80 & 0.01 \\ 0.20 & 0.99 \end{bmatrix}. \quad (6.23)$$

Now we have to follow the principle of backward induction in order to solve the multi-stage decision problem and obtain a map of the optimal actions in the first stage (“do nothing”  $DN^{(1)}$ , “close the bridge”  $CB^{(1)}$  and “send inspector”  $SI^{(1)}$ ). I start from the second and last stage of the tree, i.e. I assume that the agent has already decided to send the inspector to the viaduct and the inspector has already provided a judgement  $\tilde{S}$ . The updated posterior probability  $P(S | \gamma_{prism,z}, \tilde{S})$  of “damaged”  $D$  or “undamaged”  $U$  state perceived by the agent will be also affected by the inspector’s judgment  $\tilde{S}$ . Formally, I can update the posterior probability obtained by considering the monitoring data using again Bayes’ rule:

$$P(S | \tilde{S}, \gamma_{prism,z}) = \frac{P(\gamma_{prism,z} | S) \cdot P(\tilde{S} | S) \cdot P(S)}{P(\tilde{S}, \gamma_{prism,z})}, \quad (6.24)$$

where the evidence is

$$\begin{aligned}
p(\tilde{S}, \gamma_{prism,z}) &= p(\gamma_{prism,z} | U) \cdot P(\tilde{S} | U) \cdot P(U) + \\
& p(\gamma_{prism,z} | D) \cdot P(\tilde{S} | D) \cdot P(D).
\end{aligned} \tag{6.25}$$

The posterior probabilities on the left-hand side are shown in Figure 6.34a and Figure 6.35a, for  $\tilde{S} = U$  and  $\tilde{S} = D$ , respectively.

After that the inspector has reported, the agent's decision problem is the same as that discussed in §6.6.1 for the single-stage, but with two differences: the posterior probabilities are now given by (6.24), and the utilities must include the cost  $z_{SI}$  of sending the inspector to the viaduct. I assume that  $z_{SI}$  includes both the fee for the inspector's work and the RUC stemming from a temporary downtime that is necessary to perform the inspection, for a total monetary loss of  $z_{SI} = \text{€}250,000$ . The expected utilities of stage 2 can be calculated as

$$\begin{aligned}
u^*(DN^{(2)}, \tilde{S}, \gamma_{prism,z}) &= -(z_U + z_{SI}) \cdot P(U | \tilde{S}, \gamma_{prism,z}) + \\
& +(z_D + z_{SI}) \cdot P(D | \tilde{S}, \gamma_{prism,z}), \\
u^*(CB^{(2)}, \tilde{S}, \gamma_{prism,z}) &= -(z_{CB} + z_{SI}),
\end{aligned} \tag{6.26}$$

and the maximum expected utility is

$$u_{\max}^{*(2)}(\tilde{S}, \gamma_{prism,z}) = \max \left\{ u^*(DN^{(2)} | \tilde{S}, \gamma_{prism,z}), u^*(CB^{(2)} | \tilde{S}, \gamma_{prism,z}) \right\}. \tag{6.27}$$

The utilities of (6.26) and (6.27) are shown in Figure 6.34b and Figure 6.35b, for  $\tilde{S} = U$  and  $\tilde{S} = D$ , respectively. The two thresholds that suggest to the agent when it is more convenient to close the bridge are:  $\bar{\gamma}_u^{(2)}(\tilde{U}) = -6.18$  mm/year/day if  $\tilde{S} = U$ , and  $\bar{\gamma}_u^{(2)}(\tilde{D}) = -5.38$  mm/year/day if  $\tilde{S} = D$ . Therefore, the optimal classifier at stage 2 is

$$a_{\text{opt}}^{(2)}(\tilde{S}, \gamma_{prism,z}) = \begin{cases} DN^{(2)} & \gamma_{prism,z} \leq \bar{\gamma}_u^{(2)}(\tilde{S}), \\ CB^{(2)} & \gamma_{prism,z} > \bar{\gamma}_u^{(2)}(\tilde{S}). \end{cases} \tag{6.28}$$

This is the solution of the second stage of Colle Isarco Viaduct multi-stage decision problem, and is a function of the observation  $\gamma_{prism,z}$  and of the inspector's judgment  $\tilde{S}$ .

Once I solved the second stage of the decision problem, I can move to the first stage. The expected utility of actions “do nothing” and “close the bridge” for this stage are the same as those of the single-stage decision problem, so I just need to calculate the expected utility of the action “send inspector”. For this purpose, I have to calculate the probability that the inspector's judgement is  $\tilde{S} = U$  or  $\tilde{S} = D$ . The inspector's judgment will depend on the structural state, which is related to the SHM observation  $\gamma_{prism,z}$ . In formulae:

$$P(\tilde{S} | \gamma_{prism,z}) = P(\tilde{S} | U) \cdot P(U | \gamma_{prism,z}) + P(\tilde{S} | D) \cdot P(D | \gamma_{prism,z}). \quad (6.29)$$

For example, the inspector will provide  $\tilde{S} = U$  either if he correctly identifies the state when the state is “undamaged”  $U$  or if he makes a mistake when the state is “damaged”  $D$ . Equation (6.29) is presented in Figure 6.33.

Now, I can calculate the expected utility of action “send inspector”, while the other expected utilities were calculated in §6.6.1 of this dissertation. All the three expected utilities of stage 1 are

$$\begin{aligned} u^*(DN^{(1)}, \gamma_{prism,z}) &= -z_U \cdot P(U | \gamma_{prism,z}) - z_D \cdot P(D | \gamma_{prism,z}), \\ u^*(CB^{(1)}, \gamma_{prism,z}) &= -z_{CB}, \\ u^*(SI^{(1)}, \gamma_{prism,z}) &= u_{\max}^{*(2)}(\tilde{U}, \gamma_{prism,z}) \cdot P(\tilde{U} | \gamma_{prism,z}) + \\ &+ u_{\max}^{*(2)}(\tilde{D}, \gamma_{prism,z}) \cdot P(\tilde{D} | \gamma_{prism,z}). \end{aligned} \quad (6.30)$$

Figure 6.36 shows the three expected utilities of stage 1 as a function of the monitoring observation – the long-term acceleration  $\gamma_{prism,z}$ . In Figure 6.36, we can recognize two thresholds:  $\bar{\gamma}_u^{(1)} = -5.46$  mm/year/day separates  $DN^{(1)}$  from  $SI^{(1)}$ ;  $\bar{\gamma}_u^{(1)} = 5.98$  mm/year/day separates  $SI^{(1)}$  from  $CB^{(1)}$ . Notice that the optimal action depends on the long-term acceleration  $\gamma_{prism,z}$  provided by the monitoring system:

$$a_{\text{opt}}^{(1)}(\gamma_{prism,z}) = \begin{cases} DN^{(1)} & \gamma_{prism,z} \leq \bar{\gamma}_u^{(1)}, \\ SI^{(1)} & \bar{\gamma}_u^{(1)} < \gamma_{prism,z} \leq \bar{\bar{\gamma}}_u^{(1)}, \\ CB^{(1)} & \gamma_{prism,z} > \bar{\bar{\gamma}}_u^{(1)}. \end{cases} \quad (6.31)$$

The expected utilities of the three actions in stage 1 (“do nothing”  $DN^{(1)}$ , “send inspector”  $SI^{(1)}$  and “close the bridge”  $CB^{(1)}$ ) are shown in Figure 6.36. In the first stage, when the long-term acceleration  $\gamma_{prism,z}$  is lower than  $\bar{\gamma}_u^{(1)}$ , the SHM-based DSS suggests  $DN^{(1)}$  to the agent because it is the financially optimal choice given the agent’s risk profile. When the long-term acceleration  $\gamma_{prism,z}$  is higher than  $\bar{\bar{\gamma}}_u^{(1)}$ , the DSS suggests  $CB^{(1)}$  to the agent. When the long-term acceleration  $\gamma_{prism,z}$  is between  $\bar{\gamma}_u^{(1)}$  and  $\bar{\bar{\gamma}}_u^{(1)}$  the DSS suggests  $SI^{(1)}$  to the agent and the agent should send the inspector to the viaduct to minimize the expected loss. Actions  $DN^{(1)}$  and  $CB^{(1)}$  are in the first stage but are terminal actions. Therefore, they do not depend on the confusion matrix  $P(\tilde{S}|S)$  because the inspector’s judgement is considered only if action  $SI^{(1)}$  is taken. However, both  $\bar{\gamma}_u^{(1)}$  and  $\bar{\bar{\gamma}}_u^{(1)}$  depend on the expected utility of action  $SI^{(1)}$ , which is affected by  $P(\tilde{S}|S)$ .

## 6.7 Discussion of results and conclusions

In this chapter, I showed how to develop a SHM-based DSS for a real-life bridge management problem. Colle Isarco Viaduct is instrumented with a monitoring system including topographic prisms for the measurement of displacements. From the displacements recorded in the 14 days before the analysis, we can calculate the long-term acceleration of the viaduct decks, which is sensitive to the structural health. The DSS of Colle Isarco Viaduct is a map that provides the optimal bridge management action to take, given the latest value of long-term acceleration. The structural state can be “damaged” or “undamaged”; the available actions are “do nothing”, “send inspector” and “close the bridge”. If the inspector is sent to the viaduct, the inspector provides information on the actual state of the structure and then the DSS suggests an action between the remaining two. The suggested actions depend on the probability of the structural states, which is updated using the latest estimate of long-term acceleration, and on the costs (direct and indirect) that may result from each combination of action and structural state. In the development of the DSS map, I

calculated two thresholds for the first stage of the decision problem: if the long-term acceleration is below the first threshold, the most convenient action is “do nothing”; if the long-term acceleration is above the second threshold, the most convenient action is “close the bridge”; if the long-term acceleration is between the thresholds, the most convenient action is “send inspector”. For the second stage of the decision problem (i.e. after the bridge manager decides to send the inspector to the viaduct), I calculated one threshold that depends on the inspector response: if the long-term acceleration is below the threshold, the most convenient action is “do nothing”; otherwise, the most convenient action is “close the bridge”. The calculation of the thresholds enables the DSS to suggest the optimal action immediately after a new value of long-term acceleration is available.

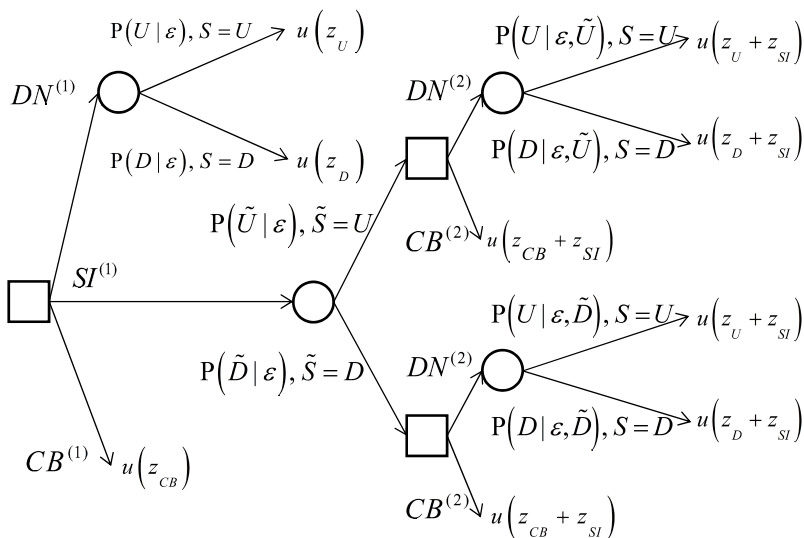


Figure 6.32. Decision tree of Colle Isarco multi-stage decision problem.

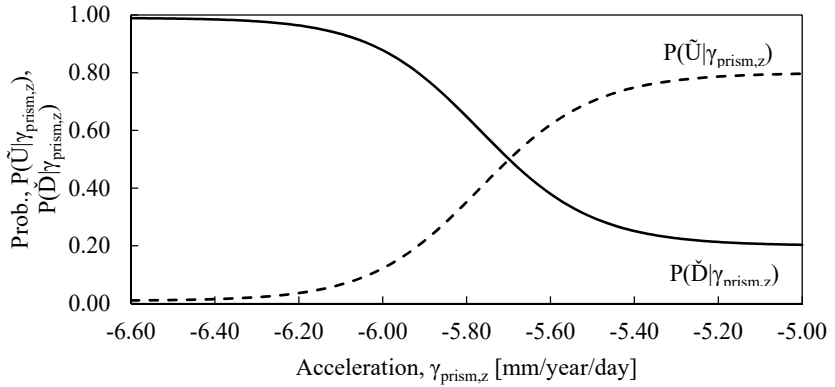
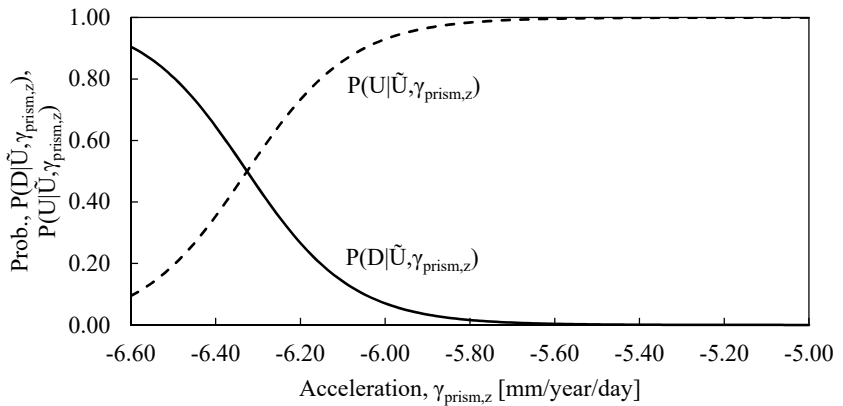
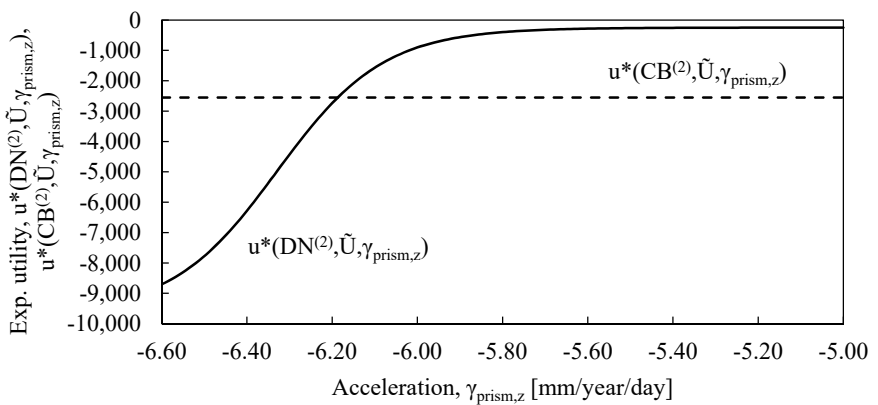


Figure 6.33. Probabilities of the inspector's judgement, given a value of long-term acceleration, for Colle Isarco multi-stage decision problem.

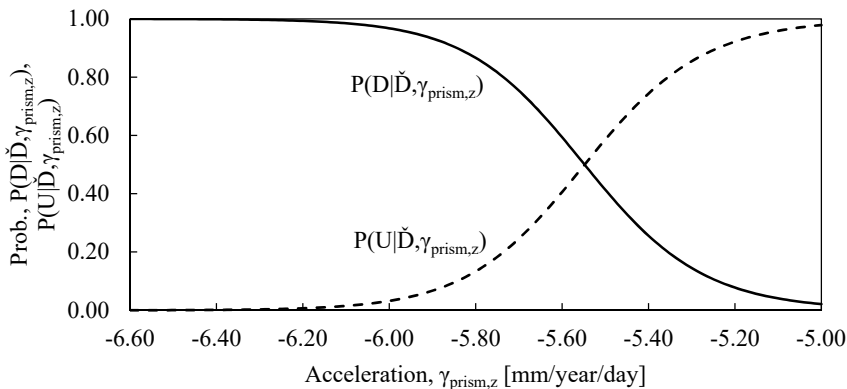


(a) Posterior probabilities

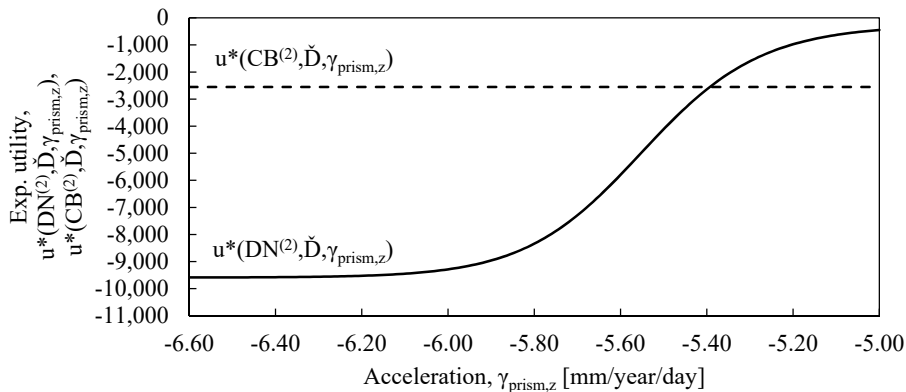


(b) Expected utilities

Figure 6.34. Posterior probabilities and expected utilities for inspector's decision  $\tilde{S} = U$ .



(a) Posterior probabilities



(b) Expected utilities

Figure 6.35. Posterior probabilities and expected utilities for inspector’s decision  $\tilde{S} = D$ .

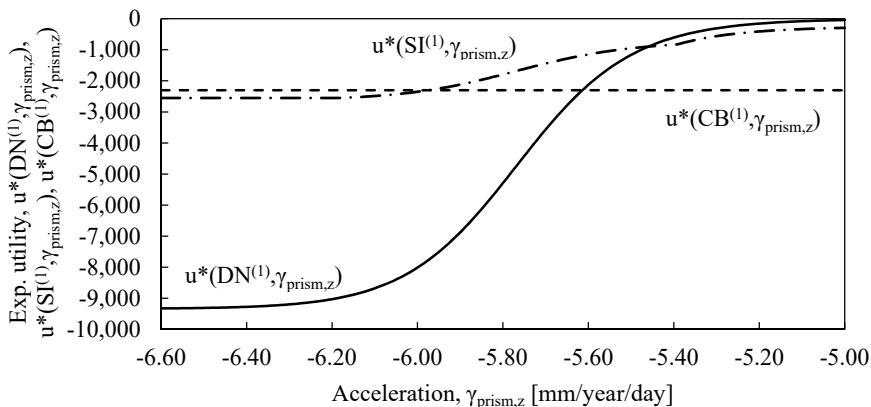


Figure 6.36. Expected utilities of the actions in stage 1 of Colle Isarco multi-stage decision problem.

# 7 Single-parameter monitoring system design: the case study of Adige Bridge

In this chapter, I apply the performance-based monitoring system design method that was described in §5.3 to a real-life case study. In this monitoring problem, we need to acquire a single observation  $y$  to estimate a single state parameter  $\theta$ , which must be calculated with a required precision. The monitored structure is Adige Bridge, a cable-stayed bridge located near Trento, Italy. The construction of this bridge, depicted in Figure 7.1, was completed in 2008 [127]. The stay cables were tensioned during the last stages of the construction. However, the bridge is a statically indeterminate structure and the force in the cables was expected to change in time due to steel relaxation, settlement of the foundations and creep of the concrete slab, which is in composite action with four weathering steel girders. In the monitoring system design, we need to estimate the effectiveness with which the monitoring solution identifies the force in the cables. The monitoring system concept is a single accelerometer installed on the stay cables for the measurement of the first natural frequency, which is the observation, and the consequent estimation of the cable tension force, which is the state parameter. Below, I describe Adige Bridge and the monitoring system concept. Then, I formalize the model used for the interpretation of data and I present the statistical distributions that are used in the design. The results of the pre-posterior analysis are finally presented and discussed at the end of the chapter.

## 7.1 Adige Bridge

Adige Bridge is a cable-stayed bridge completed in 2008 near Trento, Italy. As depicted in Figure 7.2a and Figure 7.2b, the bridge has two spans and is 260 m long overall. The deck, shown in Figure 7.2c, is made of a 25 cm-thick concrete slab in

composite action with four weathering steel girders, which are 2 m high with flanges of variable dimensions. The deck is also supported by 12 stay cables, which are anchored to a central tower. The properties of the cables are summarized in Table 7.1. Figure 7.3a and Figure 7.3b show the top and the bottom anchorage of the cables.

Since the deck has a considerable bearing capacity and it is supported by six stay cables for each side, it is a statically indeterminate structure. For this reason, immediately after the construction, the bridge was instrumented with strain and temperature sensors. The strain of each stay cable is continuously monitored by a 1 m-long FBG FOS [120] [15]. These sensors measure the strain of the cables and the temperature variations for temperature compensation. The FOSs have continuously provided reliable data of elongation. Since we know the tensioning force of the cables and the cables were instrumented immediately after tensioning, we may think that we can calculate the tension to which the cables are currently subjected by adding to the initial tensioning force the force that corresponds to the elastic elongations. However, this approach is not accurate because: (1) the initial tensioning force of the stay cables is very uncertain; (2) the axial stiffness is affected by significant uncertainty; (3) even with zero elongation, the tensioning force may decrease because of steel relaxation. The initial tensioning force is uncertain because it was measured, as usual, by reading the pressure of the oil in the hydraulic circuit of the jack used to apply the force to the cables. We assume that now, in 2017, the transportation department of the Autonomous Province of Trento, who manages the bridge, wants to obtain a reliable estimate of the force to which the cables are currently subjected.



(a) Map with the position of Adige Bridge



(b) View of Adige Bridge

Figure 7.1. Position and view of Adige Bridge.

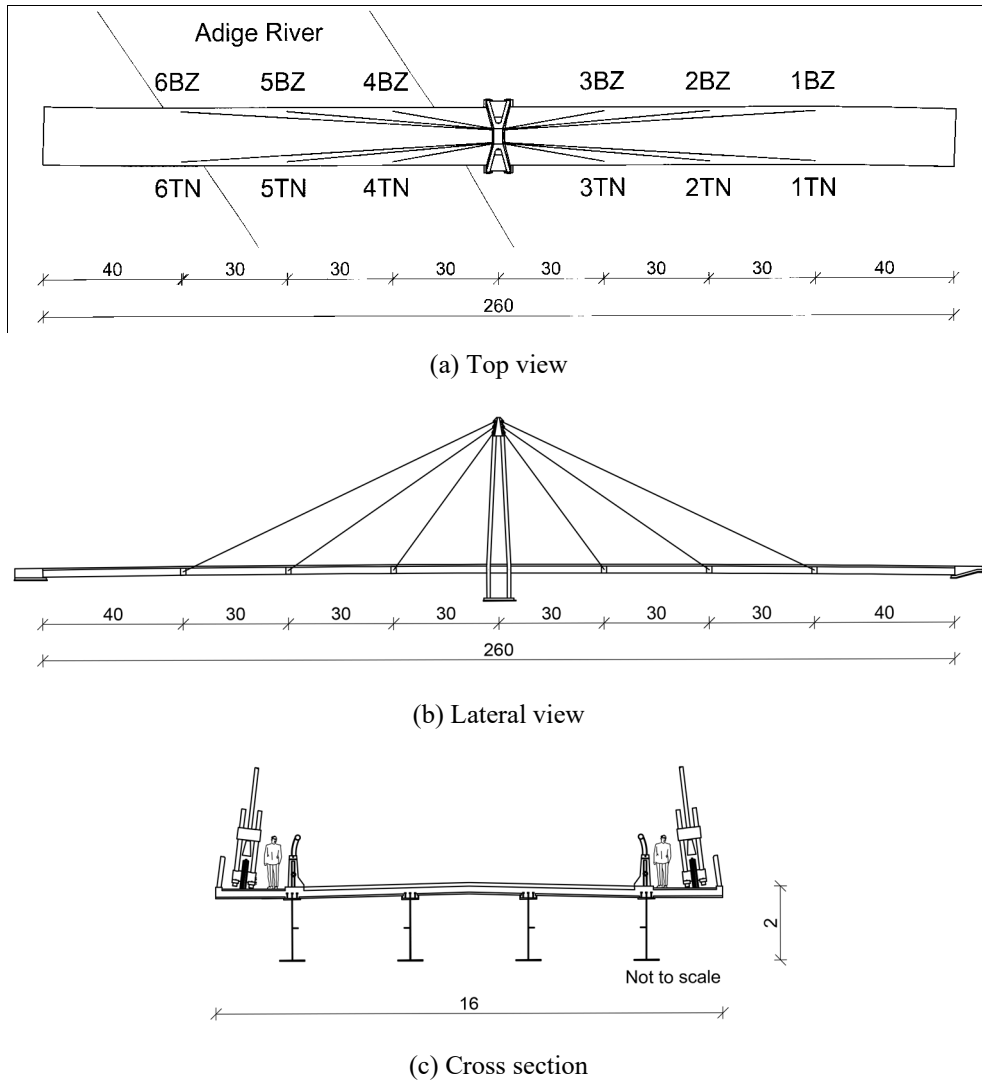


Figure 7.2. Geometry of Adige Bridge [127]; dimensions in [m].

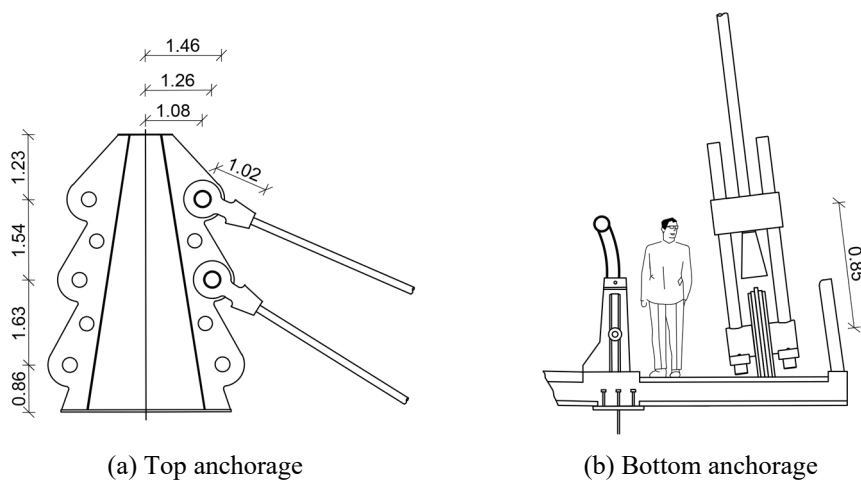


Figure 7.3. Anchorages of the stay cables that support the deck of Adige Bridge; dimensions in [m].

Table 7.1. Characteristics of the stay cables of Adige Bridge

Cable	Diameter	Linear mass	Length	Axial stiffness	Design load	Load capacity
–	$d$ [mm]	$m$ [kg/m]	$L$ [m]	$EA$ [MN]	[kN]	[kN]
1BZ	128	88.62	95.06	1840	7818	16385
1TN	128	88.62	95.06	1840	7818	16385
2BZ	128	88.62	68.88	1840	7818	16385
2TN	128	88.62	68.88	1840	7818	16385
3BZ	116	72.78	46.51	1511	4975	13480
3TN	116	72.78	46.51	1511	4975	13480
4BZ	116	72.78	46.51	1511	4975	13480
4TN	116	72.78	46.51	1511	4975	13480
5BZ	128	88.62	68.88	1840	7818	16385
5TN	128	88.62	68.88	1840	7818	16385
6BZ	128	88.62	95.06	1840	7818	16385
6TN	128	88.62	95.06	1840	7818	16385

## 7.2 Monitoring system concept

We need a monitoring solution that enables us to calculate the tensioning force with the required precision, defined by a value of standard deviation of  $\bar{\sigma}_{\theta(y)} = 200$  kN. The threshold of 0.2 MN is a reasonable value if the expected value of the force *a posteriori* has to be compared with the nominal capacity of the cables in order to evaluate the global structural reliability.

Based on our experience, we decide to proceed with a concept in which we observe the first natural frequency of the cables and use the analytical models available in the literature [128] to calculate the tensioning forces. The capacity of the monitoring system in the design process is the precision of the tension force  $\theta$  that will be calculated based on the cable first natural frequency  $y$ . The capacity will be compared with the threshold of  $\bar{\sigma}_{\theta(y)}^2 = 0.04$  MN<sup>2</sup> – the demand of monitoring effectiveness. In this example, I do not present the results for all the cables, but I focus on cable 1BZ. The same approach can be followed for the other cables, with similar results.

In order to measure the first natural frequency of the cables, I assume the monitoring system concept of Figure 7.4. A metallic shell is placed around the cables; then, two different accelerometers are fixed to an L-shape metallic plate using glue; finally, the plate is screwed to the shell to ensure the transmission of vibrations. In the analysis of data, I assume that the connection between the accelerometers and the cables is perfectly rigid. After the installation of the accelerometers, the cables are struck using a special hammer and the free vibrations are recorded by piezoelectric accelerometers (e.g. PCB 393B12 accelerometers) with a sampling rate of 500 Hz. Then, the first natural frequency of the cables is calculated by performing a fast Fourier transform (FFT) on the accelerations recorded by either one of the accelerometers [129] while the data collected by the other accelerometer are used to heuristically check that the accelerations are consistent. Based on previous tests carried out with this SHM methodology, we expect to obtain an observation of the first natural frequency that is affected by an uncertainty of standard deviation  $\sigma_{y|\theta} = 0.01$  Hz.



Figure 7.4. The monitoring system concept: the first natural frequency of cable 1BZ is observed using two accelerometers.

### 7.3 Structural model and distributions

In the analysis of data, I assume that: (1) the effects of the bending stiffness on the first natural frequency are negligible; (2) the combined effects of the sag and extensibility of the cables are negligible; (3) the ends of the cables are perfectly pinned – the rotation of the ends is not restrained. With these hypotheses, I can use the following model [130] in order to calculate the theoretical value of the first natural frequency  $\hat{y}$ , given the tension force  $\theta$ :

$$\hat{y}(\theta) = \sqrt{\frac{\theta}{4\rho \cdot L^2}}, \quad (7.1)$$

where  $\rho = 88.62$  kg/m is the linear mass and  $L = 95.06$  m the cable length of cable 1BZ.

The prior distribution of the state parameter  $\theta$  for cable 1BZ is assumed to be a log-normal probability density, with mean value set equal to the design service load of the cable,  $\mu_\theta = 7,818$  kN, and coefficient of variation 0.20:

$$p(\theta) = \ln\mathcal{N}(7818 \text{ kN}, 0.20), \quad (7.2)$$

where the generic notation  $\ln\mathcal{N}(\mu, V)$  denotes a log-normal probability density with mean  $\mu$  and coefficient of variation  $V$ .

If the natural frequency is calculated using (7.1) the result is the theoretical value of frequency  $\hat{y}(\theta)$  that corresponds to the state parameter  $\theta$ . Instead, if the natural frequency is provided by the FFT based on the actual accelerations, it is an observation, i.e. a value that may be different from  $\hat{y}$  because it is affected by a random residual  $\varepsilon(\sigma_{y|\theta}^2)$  that I assume to be normally distributed with mean zero and standard deviation  $\sigma_{y|\theta}$ . In mathematical terms:

$$y = \hat{y} + \varepsilon(\sigma_{y|\theta}^2). \quad (7.3)$$

Based on (7.3), we can define the likelihood function  $p(y|\theta)$  of our Bayesian inference problem, which gives the probability of observing  $y$  given a value of tension force  $\theta$ , as a normal distribution:

$$p(y|\theta) = \frac{1}{\sqrt{2\pi \cdot \sigma_{y|\theta}^2}} \exp \left[ -\frac{\left( y - \sqrt{\frac{\theta}{4\rho \cdot L^2}} \right)^2}{2\sigma_{y|\theta}^2} \right]. \quad (7.4)$$

In the pre-posterior analysis, the distribution of (7.4) is a function of both the observation  $y$  and the state parameter  $\theta$ . The pre-posterior distribution, which is also a function of  $y$  and  $\theta$ , is calculated with the Bayes theorem:

$$p(\theta|y) = \frac{p(y|\theta) \cdot p(\theta)}{p(y)}. \quad (7.5)$$

Figure 7.5 depicts the prior distribution, the likelihood function and the pre-posterior distribution, which are worth a discussion. First, we should notice that the prior distribution (Figure 7.5a) does not depend on the observation and therefore the position of its mode in the domain of  $\theta$  is constant, regardless the value of  $y$ . The likelihood function (Figure 7.5b) depends both on  $y$  and  $\theta$ . However, although we showed  $p(y|\theta)$  for constant values of  $y$ , we should notice that  $p(y|\theta)$  is a probability distribution with respect to  $y$ , not to  $\theta$ , and the mode of  $p(y|\theta)$  in the domain of  $y$  is proportional to  $\sqrt{\theta}$ . On the contrary, the pre-posterior distribution (Figure 7.5c) is a

function of both  $y$  and  $\theta$  but provides the probability density only of the state parameter  $\theta$ . As we can notice in Figure 7.5c, for different values of  $y$ , the peak of the posterior distribution changes in magnitude with  $y$ . The reason for that is the variance of the posterior distribution, defined in the domain of  $\theta$ , changes with the value of the observation  $y$  because the model is non-linear.

## 7.4 Pre-posterior analysis and results

Using the Monte Carlo simulation, I obtained  $N = 1.1 \cdot 10^5$  values  $\theta_{(n)}$  of the state parameter from its prior distribution: the last  $M = 1.0 \cdot 10^4$  of them were used to calculate a sample of observations, affected by an additional uncertainty of  $\sigma_{y|\theta} = 0.01$  Hz. The algorithm successfully provided a sample of variances  $\tilde{\sigma}_{\theta|y_{(m)}}^2$  of the state parameter. I applied kernel density estimation (KDE) [126] to the sample of observations and variances *a posteriori*, in order to obtain the probability density functions depicted in Figure 7.6. In Figure 7.7a, I show a series of points whose coordinates are the values of variance  $\tilde{\sigma}_{\theta|y_{(m)}}^2$  and the values  $\theta_{(m)}$  of tension force used to generate the sample of observation. In this figure, we can observe the relationship between the state parameter and the variance of the posterior distribution in the domain of interest defined by the prior distribution of the state parameter. Finally, in Figure 7.7b, I compare the values of variance  $\tilde{\sigma}_{\theta|y_{(m)}}^2$  with the samples  $y_{(m)}$  of observation.

Now, I want to compare the results above with the expected variance of the posterior distribution obtained through the uncertainty propagation approach. Using (7.1), we can calculate the expected value of the observation based on the mean of the prior distribution:

$$\tilde{\mu}_y = \sqrt{\frac{\mu_\theta}{4\rho \cdot L^2}} = 1.56 \text{ Hz} . \quad (7.6)$$

Then, we need a function that provides the parameter based on the observation. In order to obtain this function, we can rewrite (5.23):

$$f(\hat{y}) = \hat{y}^2 \cdot 4\rho \cdot L^2 . \quad (7.7)$$

The derivative of  $f(\hat{y})$  with respect to  $\hat{y}$  is:

$$\frac{\partial f}{\partial \hat{y}} = 8\hat{y} \cdot \rho \cdot L^2 . \tag{7.8}$$

At this point, we can use (5.25) to calculate the variance of the likelihood function expressed in terms of the state parameter:

$$\tilde{\sigma}_{\theta,LF}^2 = \left( \frac{\partial f}{\partial \hat{y}} \right)^2 \sigma_{y|\theta}^2 = 1.0017 \cdot 10^{-2} \text{ MN}^2 . \tag{7.9}$$

Finally, we can calculate the expected value of the variance using (5.26):

$$\tilde{\sigma}_{\theta(y)}^2 = \frac{1}{\tilde{\sigma}_{\theta,LF}^{-2} + \sigma_{\theta}^{-2}} = 9.8556 \cdot 10^{-3} \text{ MN}^2 , \tag{7.10}$$

where  $\sigma_{\theta} = (7.818 \text{ MN}) \cdot 0.20 = 1.564 \text{ MN}$  is the standard deviation of the prior distribution.

The expected value of variance resulted  $\tilde{\sigma}_{\theta(y)}^2 = 0.01 \text{ MN}^2$ , corresponding to a standard deviation of  $\tilde{\sigma}_{\theta(y)} = 0.1 \text{ MN}$ , 100 kN, by following both the Monte Carlo and the uncertainty propagation approach. I can conclude the monitoring system design by saying that the monitoring system is expected to be satisfactory because the expected variance of the posterior distribution is lower than the required monitoring effectiveness:  $\tilde{\sigma}_{\theta(y)}^2 = 0.01 \text{ MN}^2 \leq \bar{\sigma}_{\theta(v)}^2 = 0.04 \text{ MN}^2$ .

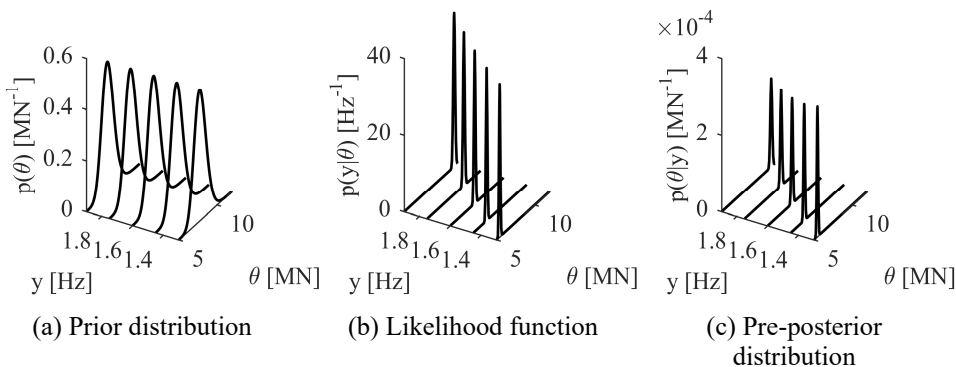


Figure 7.5. Distributions used in the pre-posterior analysis for the prediction of the uncertainty that affects the tension force of stay cable 1BZ.

## 7.5 Discussion of results and conclusions

In this chapter, I applied the performance-based monitoring system design method to a real-life case study. The stay cables of Adige Bridge are long between 46.51 m and 95.06 m, and pinned at the ends. In the monitoring system concept, the tension of the cables is calculated from their first natural frequency, which is measured through an accelerometer installed on the cables themselves. Based on the precision with which we can measure the frequency and on the prior distribution of the cable forces, I predicted the variance of the posterior distribution using the performance-based monitoring system design method proposed in §5.3 of this dissertation. The monitoring system design was carried out using both the propagation of uncertainty and a Monte Carlo algorithm. Uncertainty propagation works with the assumption that the model of the structure is linear and the probability distributions are normal. The concept proposed in this chapter is based on a non-linear model and the prior distribution of the cable tension is log-normal. However, the expected precision of the cable force obtained using the Monte Carlo algorithm is essentially the same as that obtained through uncertainty propagation. This could have been predicted by observing the results of the Monte Carlo algorithm. Indeed, Figure 7.6b showed that the empirical probability density of the variance calculated using the samples of the Monte Carlo simulation is symmetric. Performance-based monitoring system design for cable 1BZ showed that the expected precision of the cable force, which is the capacity of the monitoring solution, satisfies the demand. The monitoring system design of the other stay cables led to similar conclusions.

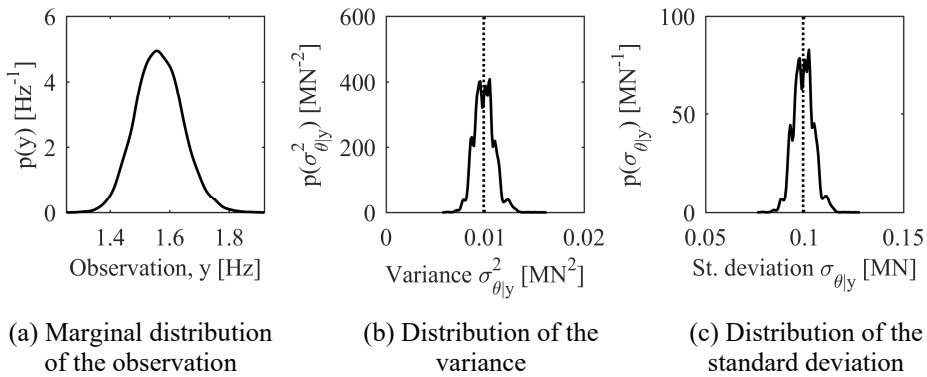


Figure 7.6. Marginal distribution of the observation and distribution of the pre-posterior variance, resulted from the pre-posterior analysis; dotted lines represent the value of expected variance and standard deviation calculated by following the uncertainty propagation approach.

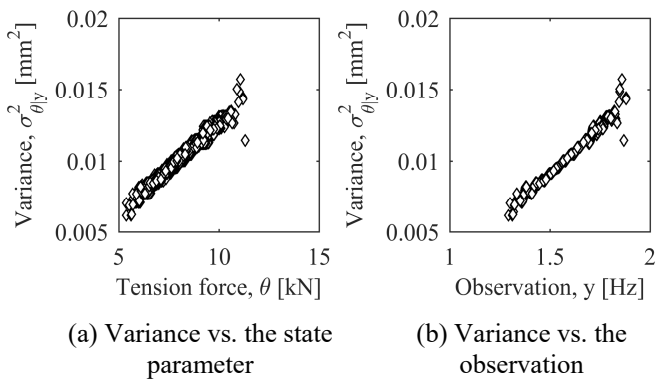


Figure 7.7. Influence of the state parameter and of the observation to the variance of the posterior distribution.

# 8 Multi-parameter monitoring system design: the case study of Wayne Overpass

In this chapter, I show how performance-based monitoring system design can be applied to a problem in which two state parameters have to be estimated based on two observations. Unlike in the monitoring problem of Adige Bridge, in this case study many state parameters have to be estimated through Bayesian inference from multiple observations. The Monte Carlo simulation of §5.3.6 is used to calculate the expected covariance matrix of the state parameters – the capacity of the monitoring system concept – and check whether the expected monitoring precision is greater than the demand. Like in the preceding chapter, I first introduce the case study – the Wayne Overpass, located in Wayne, New Jersey, USA – then I formalize the monitoring problem, show the structural model and the probability distributions. In this example, the model is more complex than the model used for the example of the preceding chapter, however, it is still encoded by an analytical function. This chapter ends with the results of the performance-based monitoring system design process and a discussion of the results.

## 8.1 Wayne Overpass

I worked on the monitoring system of Wayne Overpass during my one-year visit to Princeton University. SHM was applied to this structure as a part of the International Bridge Study within the Long-term Bridge Performance program carried out by the US Federal Highway Administration [131]. The SHMlab of the Department of Civil and Environmental Engineering, at Princeton University, developed the monitoring system concept and installed the monitoring solution, which is based on long-gauge FBG FOSs. Here I show how the monitoring system design process could have been reproduced using the method proposed in §5.3.2 of this dissertation.

The overpass, depicted in Figure 8.1, is located in the town of Wayne, New Jersey, USA. It consists of several spans and each span is made of a concrete slab casted on a set of steel girders, which are simply-supported by the piers. The girders are in composite action with the concrete slab thanks to shear studs welded on the top of the girders. SHM was applied to span 2, which has total width of about 19.50 m. The deck of span 2 is made of eight built-up steel beams of variable length: from 32.08 m to 39.62 m, as shown by Figure 8.2. The beams are approximately 1,610 mm high and a concrete slab 241 mm thick was casted on the steel beams. The thickness and the width of the steel flanges change along each girder and from one girder to another. The deck is also stiffened by several perpendicular diaphragms, as depicted in Figure 8.3.

The objective of SHM was to analyze the structural health of the deck. The girders are visible to the naked eye and can be easily checked by visual inspections. However, the condition of the concrete slab and of the connection between the girders and the slab are difficult to assess. Intrusion of chloride ions due to deicing salts and carbonation may corrode the reinforcement bars within the concrete slab and the connection between the slab and the girders. If the connection between the slab and the girders is lost, the two elements behave separately and the total capacity of the deck considerably drops.



(a) Map with the position of Wayne Overpass



(b) Lateral view, span 2 [131]

Figure 8.1. Position and view of Wayne Overpass.





Figure 8.3. Monitored girders, span 2 [131].

## 8.2 Monitoring system concept

The condition of the connection between the concrete slab and the steel girders influences the position of the neutral axis along the height of the girder section. If the effectiveness of the connection drops, the neutral axis measured on the steel girders lowers. I assume that, with the monitoring system concept, we can calculate the position of the neutral axis from the strain of the flanges. The monitoring system design presented in this chapter focuses on the section in position 5.2 of Figure 8.2, but the same approach can be followed for the other sections – 2.1, 2.2, 2.3, 5.1 and 5.3. In section of position 5.2, the strain of the flanges due to traffic crossing the overpass is maximum and it is probably affected by both southbound and northbound traffic. In the monitoring system concept, two strain sensors are installed on this section, namely “5.2 Up” and “5.2 Down”, for the top flange and bottom flange respectively. The sensors of choice are long-gauge FBG FOSs, which must be glued to the top flange and bottom flange. Sensor “5.2 Down” and sensor “5.2 Up” provide respectively the observations of strain  $y_b$  and  $y_t$ . I define the vector of the observations  $\mathbf{y} = \{y_t, y_b\}$ . In the monitoring system concept, the strain measurements are assumed to be acquired over short periods of time – each interval shorter than two minutes. With this hypothesis, thermal compensation should not be performed because it

would introduce further uncertainty without giving appreciable advantages [131]. From  $\mathbf{y}$ , we want to estimate the position of the neutral axis in section 5.2.

### 8.3 Structural model and distributions

With the monitoring system, we want to estimate two state parameters: the position of neutral axis  $\theta_\alpha$  and the curvature  $\theta_\chi$  in section 5.2, based on a single set of two relative strains  $\mathbf{y} = \{y_b, y_t\}$ . For obvious reasons, I assume that the two measurements  $y_b, y_t$  will be acquired at the same time. The structural model that links the state parameters to the observations  $\mathbf{y}$  is given by the equations below, which are based on the linear model of the cross section illustrated in Figure 8.4. The state parameters are merged in a single vector  $\boldsymbol{\theta} = \{\theta_\alpha, \theta_\chi\}$ . All the other parameters are assumed to be deterministic and are described in Table 8.1. The position of neutral axis  $\theta_\alpha$  is defined as the distance between the neutral axis and the bottom flange (Figure 8.4). Based on the model, the values of strain  $\hat{\mathbf{y}}$  are calculated with the following expression:

$$\hat{\mathbf{y}}(\boldsymbol{\theta}) = \begin{bmatrix} \hat{y}_t \\ \hat{y}_b \end{bmatrix} = \theta_\chi \cdot \begin{bmatrix} \theta_\alpha - h_t \\ \theta_\alpha - h_b \end{bmatrix}, \quad (8.1)$$

where  $\hat{y}_t$  is the theoretical strain that should be measured where the top sensor is installed and  $\hat{y}_b$  is the theoretical strain that should be measured where the bottom sensor is installed.

The prior distribution of the state parameters can be calculated from the properties of the materials and the geometry of the cross section. I assume that: (1) the behavior of steel and concrete in the cross section is linear and elastic; (2) the section has the geometry described by Figure 8.4; (3) the value of the model variables are those of Table 8.1. With these hypotheses, the position of neutral axis is:

$$\theta_\alpha = \frac{A_{sb}z_{sb} + s_w b_w z_{sw} + A_{st}z_{st} + A_{rt}z_{rt} + A_{rb}z_{rb} + s_c b_c z_c E_c / E_s}{A_{sb} + s_w b_w + A_{st} + A_{rt} + A_{rb} + s_c b_c E_c / E_s}. \quad (8.2)$$

We can also calculate the moment of inertia  $J$ :

$$\begin{aligned}
 J = & A_{sb} [z_{sb} - \theta_\alpha]^2 + A_{st} [z_{st} - \theta_\alpha]^2 + A_{rt} [z_{rt} - \theta_\alpha]^2 + A_{rb} [z_{rb} - \theta_\alpha]^2 + \\
 & + \left[ b_c s_c [z_c - \theta_\alpha]^2 + \frac{b_c s_c^3}{12} \right] \frac{E_c}{E_s} + b_w s_w [z_{sw} - \theta_\alpha]^2 + \frac{b_w s_w^3}{12},
 \end{aligned} \quad (8.3)$$

where the moment of inertia of the steel flanges and reinforcement bars, with respect to their centroid, is neglected – only the contribution due to their position is taken into account. Then, I can calculate the curvature of the section:

$$\theta_\chi = \frac{B}{E_s J}. \quad (8.4)$$

These equations enable us to calculate the prior distribution of the position of neutral axis  $\theta_\alpha$  and of the curvature  $\theta_\chi$  from the normal distributions of the effective width of the concrete slab  $b_c$ , the Young's modulus of steel  $E_s$  and the Young's modulus of concrete  $E_c$ . The bending moment  $B$  was assumed to be equal to 500 kNm, which is reasonable given the structure and the loads on the bridge. In mathematical terms:

$$p(b_c) = \mathcal{N}(2,438.4 \text{ mm}, 731 \text{ mm}), \quad (8.5)$$

$$p(E_s) = \mathcal{N}(200,000 \text{ MPa}, 10,000 \text{ MPa}), \quad (8.6)$$

$$p(E_c) = \mathcal{N}(35,000 \text{ MPa}, 7000 \text{ MPa}). \quad (8.7)$$

I performed a Monte Carlo simulation to calculate the mean vector and covariance matrix of the state parameters, *a priori*:

$$\begin{aligned}
 \boldsymbol{\mu}_0 &= \begin{bmatrix} 1343 \text{ mm} \\ 3.37 \cdot 10^{-2} \text{ } \mu\text{E/mm} \end{bmatrix}, \\
 \boldsymbol{\Sigma}_0 &= \begin{bmatrix} 9501 \text{ mm}^2 & -0.311 \text{ mm} \cdot \mu\text{E/mm} \\ -0.311 \text{ mm} \cdot \mu\text{E/mm} & 1.385 \cdot 10^{-5} (\mu\text{E/mm})^2 \end{bmatrix}.
 \end{aligned} \quad (8.8)$$

The position of neutral axis in case the connection between the steel girder and the concrete slab becomes completely ineffective is

$$\theta_{\alpha,f} = \frac{A_{sb}z_{sb} + s_w b_w z_{sw} + A_{st}z_{st}}{A_{sb} + s_w b_w + A_{st}}. \quad (8.9)$$

Using (8.2) and (8.9), I can calculate the expected variation in the neutral axis position after a complete loss of the connection between the steel girder and the concrete slab:

$$\mu_{\theta_{\alpha}-\theta_{\alpha,f}} = -661 \text{ mm}, \quad \sigma_{\theta_{\alpha}-\theta_{\alpha,f}} = 97 \text{ mm}.$$

With the performance-based monitoring system design, I want to check whether the monitoring system concept is expected to provide an estimation of the state parameters *a posteriori* with a covariance matrix that is, in the worst case:

$$\bar{\Sigma}_{\theta|y} = \begin{bmatrix} 5625 \text{ mm}^2 & 0 \\ 0 & 1.385 \cdot 10^{-5} (\mu\epsilon/\text{mm})^2 \end{bmatrix}. \quad (8.10)$$

The value of  $5625 \text{ mm}^2$  corresponds to a standard deviation of the marginal posterior distribution of  $75.0 \text{ mm}$ , while the marginal prior distribution has a standard deviation of  $97.5 \text{ mm}$ . The value of  $1.385 \cdot 10^{-5} (\mu\epsilon/\text{mm})^2$  is the same of the prior distribution because we are not interested in improving our information about the curvature.

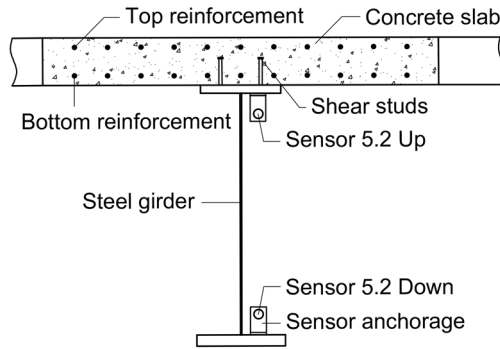
If the strains are calculated using (8.1) given the state parameters  $\theta$ , the results are the theoretical values of strain  $\hat{y}$ . Instead, if the strains are measured by the monitoring system, the values that we obtain are observations, i.e. a value that may be different from  $\hat{y}$  because it is affected by two independent values of random noise  $\mathcal{E}(\sigma_{y|\theta}^2)$  that I assume to be normally distributed with mean zero and standard deviation  $\sigma_{y|\theta}$ ; in mathematical terms:

$$\mathbf{y} = \hat{\mathbf{y}} + \begin{bmatrix} \mathcal{E}(\sigma_{y|\theta}^2) \\ \mathcal{E}(\sigma_{y|\theta}^2) \end{bmatrix}. \quad (8.11)$$

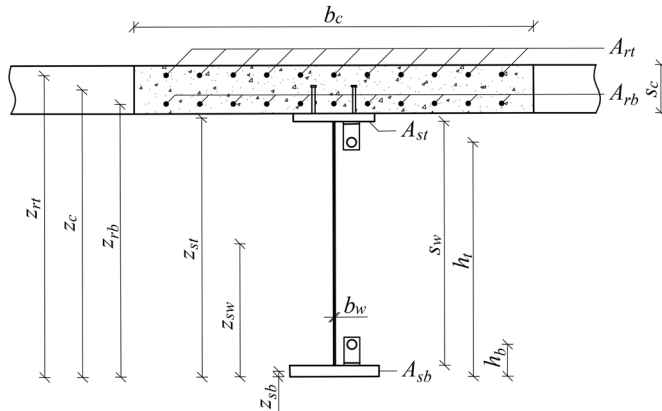
Based on our experience with FBG sensors, I assume that every relative strain measurement is characterized by a noise of standard deviation  $\sigma_{y|\theta} \cong 3 \mu\epsilon$ . I can therefore say that the probability of observing a realization  $\mathbf{y}$  given a set of state parameters  $\theta$  is

$$p(\mathbf{y} | \boldsymbol{\theta}) = \mathcal{N}_m \left( \begin{bmatrix} \hat{y}_t(\boldsymbol{\theta}) \\ \hat{y}_b(\boldsymbol{\theta}) \end{bmatrix}, \begin{bmatrix} \sigma_{y|t}^2 & 0 \\ 0 & \sigma_{y|b}^2 \end{bmatrix} \right), \quad (8.12)$$

where the generic notation  $\mathcal{N}_m(\boldsymbol{\mu}, \boldsymbol{\Sigma})$  denotes a multivariate normal probability density function with mean vector  $\boldsymbol{\mu}$  and covariance matrix  $\boldsymbol{\Sigma}$ . The distribution of (8.12) is the likelihood function of our inference problem and, in the pre-posterior analysis, it depends on both  $\mathbf{y}$  and  $\boldsymbol{\theta}$ .



(a) Section 5.2



(b) Geometrical features of section 5.2 involved in the structural model

Figure 8.4. Geometry of the composite section in position 5.2.

**Table 8.1. Prior information about the parameters of the structural model**

Description	Variable	Mean	COV
Area of the bottom steel flange	$A_{sb}$	29,032 mm <sup>2</sup>	–
Area of the top steel flange	$A_{st}$	18,085 mm <sup>2</sup>	–
Area of bottom reinforcement	$A_{rb}$	2,819 mm <sup>2</sup>	–
Global area of the top reinforcement	$A_{rt}$	2,109 mm <sup>2</sup>	–
Centroid* of the bottom steel flange	$z_{sb}$	31.8 mm	–
Centroid* of the top steel flange	$z_{st}$	1,609.8 mm	–
Centroid* of the bottom reinforcement	$z_{rb}$	1,667.0 mm	–
Centroid* of the top reinforcement	$z_{rt}$	1,800.0 mm	–
Centroid* of the steel web	$z_{sw}$	825.5 mm	–
Centroid* of the concrete slab	$z_c$	1,752.7 mm	–
Steel web depth	$s_w$	1,524.0 mm	–
Steel web thickness	$b_w$	9.5 mm	–
Concrete slab thickness	$s_c$	241.3 mm	–
Position* of the bottom sensor	$h_b$	80.5 mm	–
Position* of the top sensor	$h_t$	1,570.5 mm	–
Effective width of the concrete slab	$b_c$	2,438.4 mm	0.30
Young's modulus of steel	$E_s$	200 GPa	0.05
Young's modulus of concrete	$E_c$	35,000 MPa	0.20
Bending moment	$B$	500.0 kNm	–

\* The position of sensors and the centroids are measured from the bottom steel flange.

Due to the nature of this case study, I cannot show the likelihood function and the pre-posterior distribution because they depend on two state parameters and two observations (four variables). Nevertheless, I can still carry out the Monte Carlo algorithm of §5.3.6 to obtain the expected pre-posterior covariance matrix, which represents the monitoring capacity.

## 8.4 Pre-posterior analysis and results

The pre-posterior analysis was performed using the Monte Carlo algorithm described in §5.3.6 above. However, unlike in the preceding chapter, in this case the state parameters and the observations are multiple variables, which are grouped in vector  $\theta$  and  $y$ , respectively. The algorithm was used to obtain  $N = 1.1 \cdot 10^5$  sets of state

parameters  $\theta_{(n)}$  from their prior distribution. Then, the last  $M = 1.0 \cdot 10^4$  samples were used to calculate  $M$  sets of observations  $\mathbf{y}_{(m)}$ , using the model of (8.1) and by adding a zero-mean sensor noise of standard deviation  $\sigma_{y|\theta} = 3 \mu\epsilon$ . Figure 8.5a depicts a histogram of the  $N$  samples of state parameters and Figure 8.5b shows a histogram of the  $M$  samples of observations.

For each sample of observations, I calculated the mean vector and the covariance matrix of the corresponding posterior distribution. The average covariance matrix was used to plot the expected posterior distribution of Figure 8.6c. Figure 8.6a shows the prior distribution characterized by the mean vector and covariance matrix of (8.8), while Figure 8.6b shows a distribution characterized by the target covariance matrix of (8.10) – the demand. The expected posterior distribution of Figure 8.6c can be marginalized in order to see how much the monitoring system concept is expected to improve the information on each state parameter. Figure 8.7 shows, for each state parameter, a comparison between the marginal prior distribution and the expected marginal posterior distribution. Since the observations are generated from a population of state parameters that comes from the prior distribution, the expected mean of the posterior distribution is the same as the mean of the prior distribution. However, since I simulated the analysis of additional pieces of information, the standard deviation of the expected marginal posterior distributions is smaller than that of the marginal prior distributions, which is correct. The expected covariance matrix calculated from the samples of observations is

$$\Sigma_{\theta(y)} = \begin{bmatrix} 3446 \text{ mm}^2 & -0.096 \text{ mm} \cdot \mu\epsilon/\text{mm} \\ -0.096 \text{ mm} \cdot \mu\epsilon/\text{mm} & 5.866 \cdot 10^{-6} (\mu\epsilon/\text{mm})^2 \end{bmatrix}, \quad (8.13)$$

and must be compared with the covariance matrix, *a priori*, of (8.8) and with the demand of (8.10).

In order to carry out the comparison, I chose to manipulate the expected covariance matrix of the posterior distribution like in (5.18) and (5.21), respectively to see whether the prior distribution and the distribution corresponding to the target covariance matrix dominate the expected posterior distribution. If both the prior distribution and the distribution corresponding to the target covariance matrix dominate the expected posterior distribution, which they do, the monitoring system concept is satisfactory. Using (5.18) and (5.21), we obtain the dimensionless covariance matrices  $\Sigma'_{\theta(y)}$  and  $\bar{\Sigma}'_{\theta(y)}$ , respectively. If the eigenvalues of  $\Sigma'_{\theta(y)}$  are

both less than 1.0, the prior distribution dominates the expected posterior distribution. If the eigenvalues of  $\bar{\Sigma}'_{\theta(y)}$  are both less than 1.0, the distribution corresponding to the target covariance matrix dominates the expected posterior distribution. The graphical representation of the eigenvalues and eigenvectors of the two matrices is shown in Figure 8.8. Table 8.2 presents the eigenvalues and the eigenvectors of  $\Sigma'_{\theta(y)}$  and  $\bar{\Sigma}'_{\theta(y)}$ . Since the maximum eigenvalue is smaller than 1.0, the monitoring system concept is expected to be satisfactory being the capacity of the monitoring system greater than the demand of monitoring precision.

## 8.5 Discussion of results and conclusions

In this chapter, I showed the application of the proposed performance-based monitoring system design method to a real-life case study. In this case, the monitoring problem required two observations for the estimate of two state parameters. I could not perform monitoring system design using the propagation of uncertainty because the state parameters could not be calculated separately from the observations. In the monitoring system concept, a steel girder of Wayne Overpass is instrumented with two FBG FOSs for the measurement of strain. With the two measurements, we wanted to calculate the position of the neutral axis and the curvature of the girder – the state parameters. In the performance-based monitoring system design, I calculated the joint prior distribution of the state parameters using the properties of the structure and a mechanical model. The Monte Carlo algorithm that implements performance-based monitoring system design enabled me to estimate the expected covariance matrix of the posterior distribution – the capacity of the monitoring system concept. The pre-posterior analysis evidenced that a reduction of the uncertainty in the marginal distribution of each state parameter is expected. In this example, I could also use the methods proposed in §5.3.3 and §5.3.4 to check whether the predicted monitoring capacity satisfied the required precision. The expected covariance matrix of the state parameters was rotated and scaled with respect to the covariance matrix that represented the required precision, and then I checked that the eigenvalues of the resulting matrix were less than one. The monitoring system design confirmed that the predicted monitoring capacity satisfied the demand.

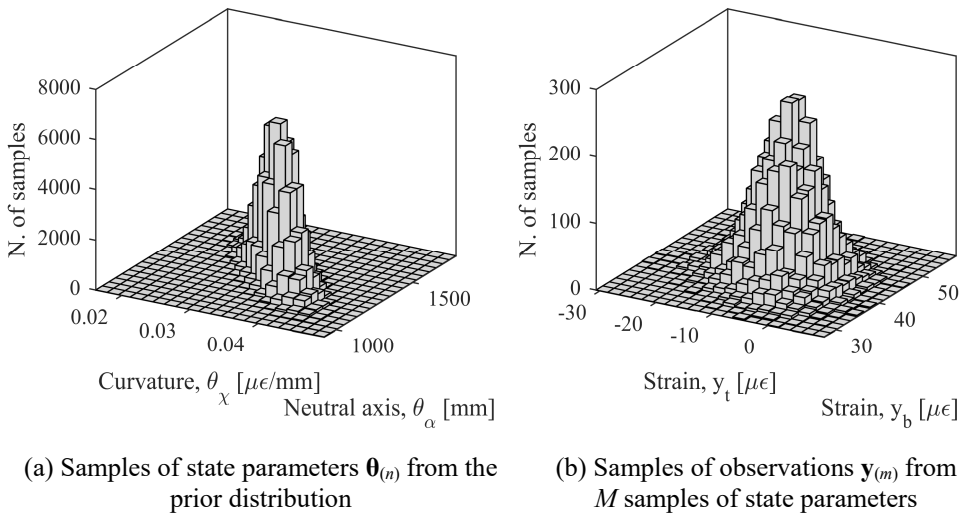


Figure 8.5. Samples of state parameters and observations obtained from the Monte Carlo algorithm for performance-based monitoring system design.

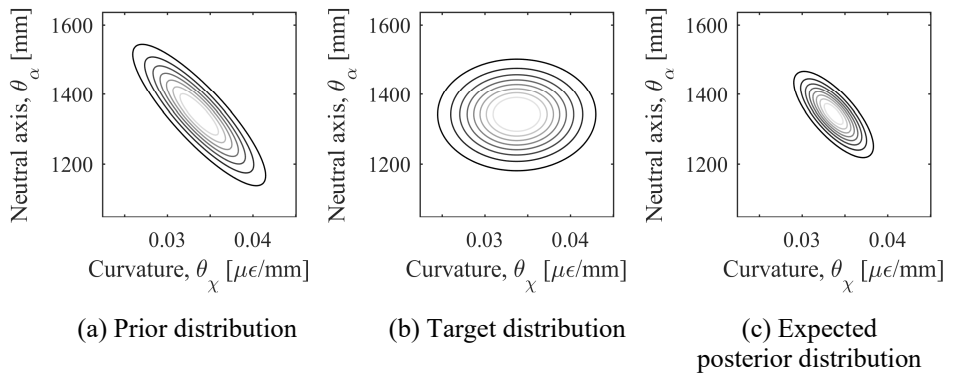


Figure 8.6. Contour plots of the distributions involved in the performance-based monitoring system design.

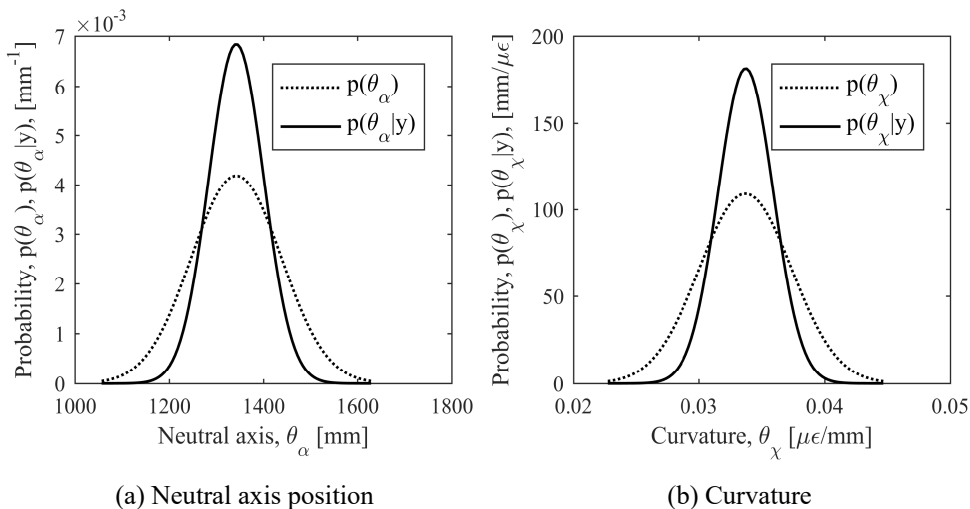


Figure 8.7. Marginal distributions of the prior distribution and the expected posterior distribution.

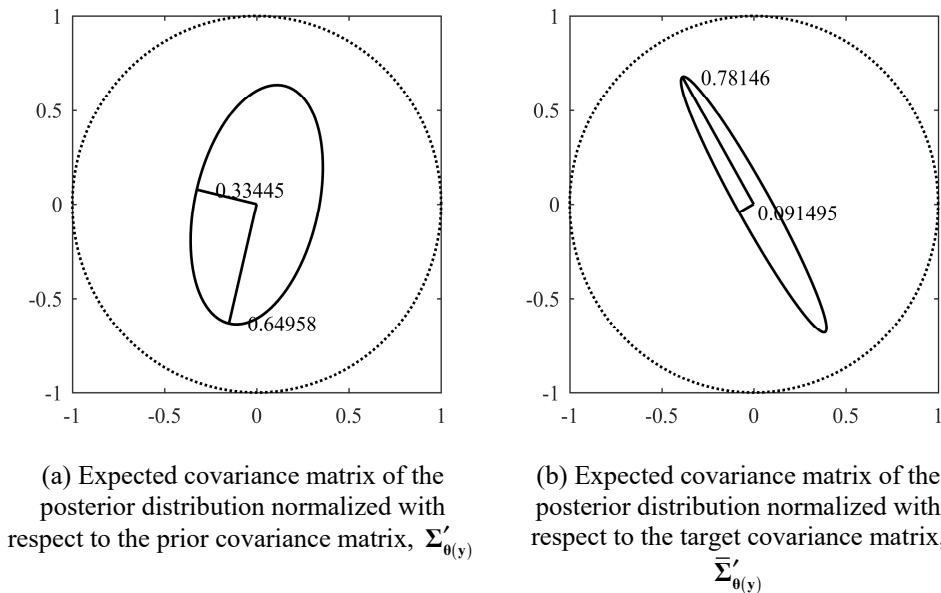


Figure 8.8. Eigenvalues and eigenvectors of the covariance matrices corresponding to the distributions involved in the performance-based monitoring system design.

**Table 8.2. Eigenvalues and eigenvectors of the expected posterior distribution normalized with respect to the prior distribution and to the target covariance matrix**

<b>Matrix</b>	<b>Matrix variable</b>	<b>Eigenvalues</b>	<b>Eigenvectors</b>
Expected covariance matrix normalized with respect to the prior distribution	$\Sigma'_{\theta(y)}$	$\lambda'_{\theta(y),1} = 0.3345$ $\lambda'_{\theta(y),2} = 0.6496$	$\mathbf{v}'_{\theta(y),1} = [-0.9726, 0.2323]$ $\mathbf{v}'_{\theta(y),2} = [-0.2323, -0.9726]$
Expected covariance matrix normalized with respect to the target covariance matrix	$\bar{\Sigma}'_{\theta(y)}$	$\bar{\lambda}'_{\theta(y),1} = 0.0915$ $\bar{\lambda}'_{\theta(y),2} = 0.7815$	$\bar{\mathbf{v}}'_{\theta(y),1} = [-0.8691, -0.4947]$ $\bar{\mathbf{v}}'_{\theta(y),2} = [-0.4947, 0.8691]$



## 9 Summary and conclusions

In this doctoral thesis, I presented an implementation of expected utility theory (EUT) in structural health monitoring (SHM). EUT enables us to identify financially optimal actions in decision problems that are subjected to uncertainty. The management of civil structures and the design of structural health monitoring systems are problems that can be optimized by application of EUT. Currently, most of the management decisions that should be based on data acquired from monitoring systems are taken based on experience and heuristics. The reason for this inconvenience is that most often the output of SHM includes only raw data or an estimate of the structural reliability. Instead, if we want SHM to assist decision-making, the SHM process must include also a formal evaluation of the management strategies and of the consequences that concern the decision problem. With the implementation of Bayesian logic and EUT in the process of SHM, we obtain a decision support system (DSS) that automatically suggests financially optimal action based on monitoring data. In this SHM-based DSS, the probability of structural state (e.g. the probability of damage) is identified through Bayesian inference. Bayesian inference merges monitoring data with information available *a priori*. Then, with the application of EUT, the probability of structural states and the costs of the management strategies are used to identify financially optimal choices. The result is function that maps the monitoring data to provide optimal actions. This classifier is influenced by: (1) the value of the measurements; (2) the structural model used in Bayesian inference; (3) the prior probability of the structural states; (4) the financial consequences of each state-action combination; (5) the risk aversion of the stakeholders. In the development of the SHM-based DSS for Colle Isarco Viaduct, the monitoring data included the long-term acceleration of four cantilevers, which was calculated by fitting the last 14 days of displacement measurements with a quadratic function. These cantilevers can be in two structural states: “damaged” or “undamaged”. Every day, the bridge manager in charge of the structure can decide among three options: “do nothing”, “send inspector” and “close the bridge”. Using Bayesian inference and EUT, I obtained the classifier that indicates the most convenient action for each realization

of the long-term acceleration. Since the costs (direct and indirect) that can follow different combinations of actions and structural states are different from one another, the financially optimal action to take does not necessarily change when the probability of damage exceeds 50%. Instead, the actions “send inspector” and “close the bridge” become optimal for much lower values of the probability of damage because the costs of using a damaged structure are very high. In general, the calculation of a lookup table that replaces the classifier enables SHM-based DSSs to provide optimal actions immediately after new monitoring data are available.

The application of EUT in monitoring system design enables designers to predict, with the information available in the design stage, if the installation of the monitoring system concept is convenient from the financial point of view. Monitoring system design can be seen as a multi-stage decision problem in which we have to choose whether to carry out a monitoring system concept that will assist an operator in the management of the monitored structure. EUT enables us to calculate a value of expected utility for both the decision of installing the monitoring system concept and proceeding without monitoring. If we can choose among multiple monitoring systems, the optimal monitoring strategy is the one that corresponds to the maximum expected utility, while monitoring should not be performed if managing the structure without monitoring data corresponds to the maximum expected utility. The calculation of these expected utilities also provides the value of information (VOI) that is contained in the monitoring data. The framework for VOI-based monitoring system design is already available in the literature, but it is too complicated and burdensome to be applied by practitioners in real-life. Practitioners such as civil engineers are used to structural design but they are not used to the application of EUT. In this thesis, I analyzed the formulation of VOI-based monitoring system design and I developed a performance-based monitoring system design method that follows the scheme of the semi-probabilistic structural design currently prescribed by design codes. In the proposed method, the designer can avoid the use of EUT in the calculation of the capacity of a monitoring system concept, while EUT must be applied in the calculation of the required monitoring precision. The calculation of the monitoring capacity is performed using Bayesian pre-posterior analysis based on the information available in the design stage such as the expected sensor noise. The demand, which will be compared to the capacity, is the monitoring effectiveness that makes SHM convenient from the financial point of view. Like in structural design, the demand can be the same for different monitoring problems. Therefore, it can be

calculated once and then prescribed by design codes, releasing practitioners from the task of implementing EUT. Moreover, capacity and demand are defined as the covariance matrix of the state parameters that represent the structural state, such as structural stiffness or natural frequencies. Thus, practitioners can judge the capacity using their engineering experience.

The proposed performance-based monitoring system design method was applied to two case studies. In the first, the monitoring problem was the estimation of a single state parameter based on a single observation using an analytical model. This application enabled me to show the probability distributions used in the calculation of the monitoring capacity. In addition, the calculation of the monitoring capacity could be carried out both by propagation of uncertainty and using a Monte Carlo simulation. The capacity obtained using uncertainty propagation is reliable when the relationship between state parameters and observations, defined by the model, is approximately linear in the range where the prior distribution of the state parameters is significant. In the second case study, the monitoring problem was the estimation of two state parameters based on two observations. Since the model did not permit the calculation of each state parameter based on the measurements only, the uncertainty propagation approach could not be applied. However, in this case I could apply the methods that I proposed for the comparison of multi-parameter capacity and demand. In both the two case studies, the precision of the monitoring system concept was satisfactory because the capacity was better than the monitoring demand.

The proposed monitoring system design method is a formal procedure for the prediction of monitoring effectiveness in the design stage. Therefore, the validation was considered concluded with the application of the formulation to the monitoring problems of the two case studies. There is no need to prove that the formulation works by checking that the predicted monitoring effectiveness is the same as the effectiveness obtained after the acquisition of real data. In fact, as structural design is effective provided we assume the correct material properties, monitoring system design is effective as long as our assumptions on the uncertainty is accurate.

The implementation of Bayesian inference and EUT in monitoring data analysis and monitoring system design financially optimizes SHM-based decisions and reduces the risk with respect to heuristic decision-making, which often occurs in practice. If the management of a monitored structure follows the suggestions of a DSS that was developed using EUT, with the correct data, models and assumptions, the utility related to the service of the structure is maximized. The use of SHM-based

DSSs that suggest management strategies in real-life settings enables operators of civil structures to take full advantage of monitoring data and prior information such as inspection reports. Performance-based monitoring system design enables practitioners that are not familiar with EUT to design effective monitoring systems using their experience. Moreover, since it was developed based on the VOI-based approach, it guarantees that the installation of the chosen monitoring system is financially convenient.

---

# References

- [1] H. Sohn, C. R. Farrar, F. M. Hemez, J. J. Czarnecki, D. D. Shunk, D. W. Stinemat and B. R. Nadler, "A Review of Structural Health Monitoring Literature: 1996–2001," Los Alamos National Laboratory, Los Alamos, 2004.
- [2] C. R. Farrar and K. Worden, "An introduction to structural health monitoring," *Philosophical Transactions of the Royal Society A*, vol. 365, p. 303–315, 2007.
- [3] J. M. Brownjohn, "Structural health monitoring of civil infrastructure," *Philosophical Transactions of the Royal Society A*, vol. 365, p. 589–622, 2007.
- [4] S. K. Lee, "Current state of bridge deterioration in the US – part 1," *NACE International*, vol. 51, no. 1, p. 62–67, 2012.
- [5] D. M. Frangopol, J. S. Kong and E. S. Gharaibeh, "Reliability-Based Life-Cycle Management of Highway Bridges," *Journal of Computing in Civil Engineering*, vol. 15, no. 1, p. 27–34, 2001.
- [6] C. R. Farrar and N. A. Lieven, "Damage prognosis: the future of structural health monitoring," *Philosophical Transactions of the Royal Society A*, vol. 365, p. 623–632, 2007.
- [7] H. Sohn, *A Bayesian Probabilistic Approach to Damage Detection for Civil Structures*, Stanford: Stanford University, 1999.
- [8] M. H. DeGroot, *Optimal Statistical Decisions*, New York City: Wiley, 1970.
- [9] C. R. Farrar, S. W. Doebling and D. A. Nix, "Vibration-based structural damage identification," *Philosophical Transactions of the Royal Society A*, vol. 359, no. 1778, p. 131–149, 2001.
- [10] H. Raiffa and R. Schlaifer, *Applied Statistical Decision Theory*, Boston: Clinton Press, 1961.

- [11] JCGM, "JCGM 200:2012. International vocabulary of metrology – basic and general concepts and associated terms (VIM)," BIPM, 2012.
- [12] J. P. Lynch, "An overview of wireless structural health monitoring for civil structures," *Philosophical Transactions of the Royal Society of London A*, vol. 365, p. 345–372, 2007.
- [13] D. H. Sigurdardottir, *Strain-Based Monitoring Methods for Beam-Like Structures*, Princeton: Princeton University, 2015.
- [14] A. E. Aktan, F. N. Catbas, K. A. Grimmelsman and C. J. Tsikos, "Issues in infrastructure health monitoring for management," *Journal of Engineering Mechanics*, vol. 126, no. 7, p. 711–724, 2000.
- [15] B. Glisic and D. Inaudi, *Fiber Optic Methods for Structural Health Monitoring*, Chichester: John Wiley & Sons, 2007.
- [16] P. Hayton, S. Utete, D. King, S. King, P. Anuzis and L. Tarassenko, "Static and dynamic novelty detection methods for jet engine health monitoring," *Philosophical Transactions of the Royal Society A*, vol. 365, p. 493–514, 2007.
- [17] D. M. Powers, "Evaluation: from precision, recall and F-measure to ROC, informedness, markedness and correlation," *Journal of Machine Learning Technologies*, vol. 2, no. 1, p. 37–63, 2011.
- [18] D. Sivia and J. Skilling, *Data Analysis: a Bayesian Tutorial*, Oxford: Oxford University Press, 2006.
- [19] M. W. Vanik, J. L. Beck and S. K. Au, "Bayesian probabilistic approach to structural health monitoring," *Journal of Engineering Mechanics*, vol. 126, no. 7, p. 738–745, 2000.
- [20] J. L. Beck and S. Au, "Bayesian updating of structural models and reliability using Markov chain Monte Carlo simulation," *Journal of Engineering Mechanics*, vol. 128, no. 4, p. 380–391, 2002.
- [21] M. P. Enright and D. M. Frangopol, "Condition prediction of deteriorating concrete bridges using Bayesian updating," *Journal of Structural Engineering*, vol. 125, no. 10, p. 1118–1125, 1999.
- [22] H. Sohn and K. H. Law, "A Bayesian probabilistic approach for structure damage detection," *Earthquake Engineering and Structural Dynamics*, vol. 26, no. 12, p. 1259–1281, 1997.

- 
- [23] C. Cappello, D. Zonta, M. Pozzi and R. Zandonini, "Impact of prior perception on bridge health diagnosis," *Journal of Civil Structural Health Monitoring*, vol. 5, no. 4, p. 509–525, 2015.
- [24] M. Cesare, J. C. Santamarina, C. J. Turkstra and E. Vanmarcke, "Risk-based bridge management," *Journal of Transportation Engineering*, vol. 119, no. 5, p. 742–750, 1993.
- [25] M. H. Faber and M. G. Stewart, "Risk assessment for civil engineering facilities: critical overview and discussion," *Reliability Engineering and System Safety*, vol. 80, p. 173–184, 2003.
- [26] M. H. Faber, "Risk assessment and decision making in civil engineering," in *AMAS Course on Reliability-Based Optimization*, Warsaw, 2002.
- [27] D. Bernoulli, "Specimen theoriae novae de mensura sortis," *Commentarié Academiæ Scientiarum Imperialis Petropolitanae*, vol. 5, 1738.
- [28] D. Bernoulli, "Exposition of a new theory on the measurement of risk," *Econometrica*, vol. 22, no. 1, p. 23–36, 1954.
- [29] N. E. Jensen, "An introduction to Bernoullian utility theory: I. Utility functions," *The Swedish Journal of Economics*, vol. 69, no. 3, p. 163–183, 1967.
- [30] J. von Neumann and O. Morgenstern, *Theory of Games and Economic Behavior*, New York: John Wiley & Sons, 1944.
- [31] R. E. Melchers, *Structural Reliability Analysis and Prediction*, Chichester: John Wiley & Sons, 1999.
- [32] S. Thons, R. Schneider and M. H. Faber, "Quantification of the value of structural health monitoring information for fatigue deterioration structural systems," in *12th International Conference on Applications of Statistics and Probability in Civil Engineering*, Vancouver, 2015.
- [33] D. Zonta, B. Glisic and S. Adriaenssens, "Value of information: impact of monitoring on decision-making," *Structural Control and Health Monitoring*, vol. 21, no. 7, p. 1043–1056, 2014.
- [34] M. Pozzi and A. Der Kiureghian, "Assessing the value of information for long-term structural health monitoring," *Proceedings of SPIE*, vol. 7984, 2011.

- [35] S. Mussi, "Putting value of information theory into practice: a methodology for building sequential decision support systems," *Expert Systems*, vol. 21, no. 2, p. 92–103, 2004.
- [36] A. Der Kiureghian and O. Ditlevsen, "Aleatory or epistemic? Does it matter?," *Structural Safety*, vol. 31, no. 2, p. 105–112, 2009.
- [37] M. Meckesheimer, A. Booker, R. Barton and T. Simpson, "Computationally inexpensive metamodel assessment strategies," *AIAA Journal*, vol. 40, no. 10, p. 2053–2060, 2002.
- [38] M. H. Faber and M. A. Maes, "Issues in societal optimal engineering decision making," *Structure and Infrastructure Engineering*, vol. 4, no. 5, p. 335–351, 2008.
- [39] New Jersey Department of Transportation, "Road User Cost Manual," 2001.
- [40] M. H. Faber and R. Rackwitz, "Sustainable decision making in civil engineering," *Structural Engineering International*, vol. 14, no. 3, p. 237–242, 2004.
- [41] F. Partnoy, *Wait: The Art and Science of Delay*, New York City: PublicAffairs, 2012.
- [42] O. Ashenfelter and M. Greenstone, "Using Mandated Speed Limits to Measure the VSL," *Journal of Political Economy*, vol. 112, no. S1, p. S226–S267, 2004.
- [43] D. Kahneman and A. Tversky, "Prospect theory: an analysis of decision under risk," *Econometrica*, vol. 47, no. 2, p. 263–292, 1979.
- [44] A. Tversky and D. Kahneman, "Advances in prospect theory: cumulative representation of uncertainty," *Journal of Risk and Uncertainty*, vol. 5, p. 297–323, 1992.
- [45] D. Kahneman and A. Tversky, "Choices, values, and frames," *American Psychologist*, vol. 39, no. 4, p. 341–350, 1984.
- [46] D. V. Lindley, "On a measure of the information provided by an experiment," *Annals of Mathematical Statistics*, vol. 27, no. 4, p. 986–1005, 1956.
- [47] D. J. MacKay, *Information Theory, Inference and Learning Algorithms*, Cambridge: Cambridge University Press, 2003.

- 
- [48] T. M. Cover and J. A. Thomas, *Elements of Information Theory*, New York: Wiley, 2006.
- [49] I. A. Papazoglou, "Bayesian decision analysis and reliability certification," *Reliability Engineering and System Safety*, vol. 66, p. 177–198, 1999.
- [50] M. H. Faber, "Chapter 7: Bayesian decision analysis," in *Statistics and Probability Theory*, Berlin, Springer, 2012, p. 143–154.
- [51] JCSS, *Probabilistic Model Code*, JCSS Joint Committee on Structural Safety, 2006.
- [52] C. Papadimitriou, J. L. Beck and S. Au, "Entropy-based optimal sensor location for structural model updating," *Journal of Vibration and Control*, vol. 6, no. 5, p. 781–800, 2000.
- [53] C. Papadimitriou, "Optimal sensor placement methodology for parametric identification of structural systems," *Journal of Sound and Vibration*, vol. 278, no. 4, p. 923–947, 2004.
- [54] C. Papadimitriou, and G. Lombaert, "The effect of prediction error correlation on optimal sensor placement in structural dynamics," *Mechanical Systems and Signal Processing*, vol. 28, p. 105–127, 2012.
- [55] F. E. Udawadia, "Methodology for optimum sensor locations for parameter identification in dynamic systems," *Journal of Engineering Mechanics (ASCE)*, vol. 120, no. 2, p. 368–390, 1994.
- [56] E. Heredia-Zavoni and L. Esteva, "Optimal instrumentation of uncertain structural systems subject to earthquake ground motions," *Earthquake Engineering and Structural Dynamics*, vol. 27, no. 4, p. 343–362, 1998.
- [57] V. Fedorov and P. Hackl, "Optimal experimental design: spatial sampling," *Calcutta Statistical Association Bulletin*, vol. 44, 1994.
- [58] M. Meo and G. Zumpano, "On the optimal sensor placement techniques for a bridge structure," *Engineering Structures*, vol. 27, p. 1488–1497, 2005.
- [59] E. Flynn and M. Todd, "Optimal placement of piezoelectric actuators and sensors for detecting damage in plate sensors," *Journal of Intelligent Materials Systems and Structures*, vol. 21, no. 3, p. 265–274, 2010.
- [60] E. Flynn, M. Todd, A. Croxford, B. Drinkwater and P. Wilcox, "Enhanced detection through low-order stochastic modeling for guided-wave structural

- health monitoring," *Structural Health Monitoring*, vol. 11, no. 2, p. 149–160, 2011.
- [61] E. Flynn and M. Todd, "A Bayesian approach to optimal sensor placement for structural health monitoring with application to active sensing," *Mechanical Systems and Signal Processing*, vol. 24, no. 4, p. 891–903, 2010.
- [62] G. Parmigiani and L. Inoue, *Decision Theory: Principles and Approaches*, Chichester: John Wiley & Sons, 2009.
- [63] M. Mitchell, *An Introduction to Genetic Algorithms*, London: MIT Press, 1996.
- [64] S. Madanat, "Optimal infrastructure management decisions under uncertainty," *Transportation Research*, vol. 1, no. 1, p. 77–88, 1993.
- [65] J. D. Sorensen, "Framework for risk-based planning of operation and maintenance for offshore wind turbines," *Wind Energy*, vol. 12, p. 493–506, 2009.
- [66] H. O. Madsen, S. Krenk and N. C. Lind, *Methods of Structural Safety*, Englewood Cliffs: Prentice Hall, 1986.
- [67] J. Qin, S. Thons and M. H. Faber, "On the value of SHM in the context of service life integrity management," in *12th International Conference on Applications of Statistics and Probability in Civil Engineering*, Vancouver, 2015.
- [68] M. Memarzadeh and M. Pozzi, "Value of information in sequential decision making: component inspection, permanent monitoring and system-level scheduling," *Reliability Engineering and System Safety*, vol. 154, p. 137–151, 2016.
- [69] D. L. Hall and A. H. McMullen, *Mathematical Techniques in Multisensor Data Fusion*, Norwood: Artech Print on Demand, 2004.
- [70] A. S. Morris and R. Langari, *Measurement and Instrumentation: Theory and Application*, Oxford: Butterworth-Heinemann, 2012.
- [71] K. Worden and G. Manson, "The application of machine learning to structural health monitoring," *Philosophical Transactions of the Royal Society A*, vol. 365, p. 515–537, 2007.

- 
- [72] T. Bayes, "An essay toward solving a problem in the doctrine of chances," *Philosophical Transactions of the Royal Society of London*, vol. 53, p. 370–418, 1763.
- [73] C. Bishop, *Pattern Recognition and Machine Learning*, Berlin: Springer, 2006.
- [74] N. Srivastava, G. Hinton, A. Krizhevsky, I. Sutskever and R. Salakhutdinov, "Dropout: a simple way to prevent neural networks from overfitting," *Journal of Machine Learning Research*, vol. 15, p. 1929–1958, 2014.
- [75] C. Cappello, D. Zonta and B. Glisic, "Expected utility theory for monitoring-based decision making," *Proceedings of the IEEE*, vol. 104, no. 8, p. 1647–1661, 2016.
- [76] W. M. Bolstad, *Introduction to Bayesian Statistics*, New York City: Wiley, 2007.
- [77] P. Gregory, *Bayesian Logical Data Analysis for the Physical Sciences*, Cambridge: Cambridge University Press, 2005.
- [78] H. Kantz, T. Schreiber, I. Hoffman, T. Buzug, G. Pfister, L. G. Flepp, J. Simonet, R. Badii and E. Brun, "Nonlinear noise reduction: a case study on experimental data," *Physical Review E*, vol. 48, no. 2, p. 1529–1538, 1993.
- [79] G. Park and D. J. Inman, "Structural health monitoring using piezoelectric impedance measurements," *Philosophical Transactions of the Royal Society A*, vol. 365, p. 373–392, 2007.
- [80] H. Sohn, "Effects of environmental and operational variability on structural health monitoring," *Philosophical Transactions of the Royal Society A*, vol. 365, p. 539–560, 2007.
- [81] B. Peeters and G. De Roeck, "One-year monitoring of the Z24-Bridge: environmental effects versus damage events," *Earthquake Engineering & Structural Dynamics*, vol. 30, no. 2, p. 149–171, 2000.
- [82] C. Y. Kim, D. S. Jung, N. S. Kim and J. G. Yoon, "Effect of vehicle mass on the measured dynamic characteristics of bridges from traffic-induced vibration test," in *Proceedings of IMAC-XIX*, Orlando, 2001.
- [83] G. De Roeck, J. Maeck, T. Michielsen and E. Seynaeve, "Traffic-induced shifts in modal properties of bridges," in *Proceedings of IMAC-XX*, Los Angeles, 2002.

- [84] Q. W. Zhang, L. C. Fan and W. C. Yuan, "Traffic-induced variability in dynamic properties of cable-stayed bridge," *Earthquake Engineering & Structural Dynamics*, vol. 31, no. 11, p. 2015–2021, 2002.
- [85] M. Abe, Y. Fujino, M. Yanagihara and M. Sato, "Monitoring of Hakucho suspension bridge by ambient vibration measurement," in *Proceedings of SPIE 3995*, Newport Beach, 2000.
- [86] J. A. Quintana, F. J. Carrion, S. E. Crespo, V. Bonilla, P. Garnica and A. Perez, "SHM and evaluation of a continuous reinforced concrete pavement," *Journal of Civil Structural Health Monitoring*, vol. 6, no. 4, p. 681–689, 2016.
- [87] W. M. Bolstad, *Understanding Computational Bayesian Statistics*, New York City: Wiley, 2010.
- [88] J. L. Beck and L. S. Katafygiotis, "Updating models and their uncertainties. I: Bayesian statistical framework," *Journal of Engineering Mechanics*, vol. 124, no. 2, p. 455–461, 1998.
- [89] G. L. Bretthorst and G. Larry, "An introduction to model selection using probability theory as logic," in *Maximum Entropy and Bayesian Methods*, Dordrecht, Kluwer Academic, 1990, p. 53–79.
- [90] M. Evans and T. Swartz, "Methods for approximating integrals in statistics with special emphasis on Bayesian integration problem," *Statistical Science*, vol. 10, no. 3, p. 254–272, 1995.
- [91] N. Metropolis, A. Rosenbluth, M. Rosenbluth, A. Teller and E. Teller, "Equation of state calculation by fast computing machines," *Journal of Chemical Physics*, vol. 21, p. 1087–1092, 1953.
- [92] W. K. Hastings, "Monte Carlo sampling methods using Markov chains and their applications," *Biometrika*, vol. 57, p. 97–109, 1970.
- [93] J. Ching and Y. C. Chen, "Transitional Markov chain Monte Carlo method for Bayesian model updating, model class selection, and model averaging," *Journal of Engineering Mechanics*, vol. 133, no. 7, p. 816–832, 2007.
- [94] J. Ching and J.-S. Wang, "Application of the transitional Markov chain Monte Carlo algorithm to probabilistic site characterization," *Engineering Geology*, vol. 203, p. 151–167, 2016.

- 
- [95] P. Angelikopoulos, C. Papadimitriou and P. Koumoutsakos, "X-TMCMC: Adaptive kriging for Bayesian inverse modeling," *Computer Methods in Applied Mechanics and Engineering*, vol. 289, p. 409–428, 2015.
- [96] A. Owen and Y. Zhou, "Safe and effective importance sampling," *Journal of the American Statistical Association*, vol. 95, no. 449, p. 135–143, 2000.
- [97] R. Y. Rubinstein and D. P. Kroese, *Simulation and the Monte Carlo Method*, 2nd ed., New York: Wiley, 2011.
- [98] J. A. Bucklew, *Introduction to Rare Event Simulation*, New York: Springer-Verlag, 2004.
- [99] W. H. Press, S. A. Teukolsky, W. T. Vetterling and B. P. Flannery, *Numerical Recipes: the Art of Scientific Computing*, Cambridge: Cambridge University Press, 2007.
- [100] V. Dubourg, B. Sudret and F. Deheeger, "Metamodel-based importance sampling for structural reliability analysis," *Probabilistic Engineering Mechanics*, vol. 33, p. 47–57, 2013.
- [101] K. Worden and J. M. Dulieu-Barton, "An overview of intelligent fault detection in systems and structures," *Structural Health Monitoring*, vol. 3, no. 1, p. 85–98, 2004.
- [102] O. Cappé, R. Douc, A. Guillin, J.-M. Marin and C. P. Robert, "Adaptive importance sampling in general mixture classes," *Statistics and Computing*, vol. 18, p. 447–459, 2008.
- [103] D. Straub, "Value of information analysis with structural reliability methods," *Structural Safety*, vol. 49, p. 75–86, 2014.
- [104] D. Zonta, C. Cappello, A. Beltempo, A. Bonelli, D. Bolognani, O. S. Bursi, C. Costa and W. Pardatscher, "Structural retrofit and health monitoring of Colle Isarco viaduct," in *Structural Faults + Repair 2016*, Edinburgh, 2016.
- [105] Autostrada del Brennero SpA, "Disegno di Contabilità," Autostrada del Brennero SpA, Trento, 1974.
- [106] P. Joris, "Risultati di Livellazioni e di Controlli Strumentali Periodici dell'Opera: Viadotto Colle Isarco," Autostrada del Brennero SpA, Trento, 2013.

- [107] Autostrada del Brennero SpA, "Consolidamento Strutturale dell'Impalcato del Viadotto Colle Isarco a Progresiva km 8+957: Perizia di Variante," Trento, Italy, 2013.
- [108] B. Gentilini and L. Gentilini, "Il viadotto di Colle Isarco per l'Autostrada del Brennero," *L'Industria Italiana del Cemento*, vol. 5, p. 318–334, 1972.
- [109] P. Moyo and J. M. Brownjohn, "Application of Box–Jenkins models for assessing the effect of unusual events recorded by structural health monitoring systems," *Structural Health Monitoring*, vol. 1, no. 2, p. 149–160, 2002.
- [110] P. Moyo, P. Omenzetter and J. M. Brownjohn, "Detection of bridge anomalous behavior and assessment of their impact on structural performance," in *1st European Workshop on Structural Health Monitoring*, Paris, 2002.
- [111] P. Omenzetter and J. M. Brownjohn, "Application of time series analysis for bridge monitoring," *Smart Materials and Structures*, vol. 15, no. 1, p. 129–138, 2006.
- [112] P. Omenzetter, J. M. Brownjohn and P. Moyo, "Identification of unusual events in multi-channel bridge monitoring data," *Mechanical Systems and Signal Processing*, vol. 18, no. 2, p. 409–430, 2004.
- [113] D. Guizzetti, "Sistema di Monitoraggio Geodetico Automatico con Due Stazioni Totali Leica TM50 Completo di Piattaforma di Gestione Leica GeoMoS," Leica Geosystems, Trento, 2014.
- [114] L. Kirkup and R. Frenkel, *An Introduction to Uncertainty in Measurement*, Oxford: Cambridge University Press, 2010.
- [115] Battan Ivan SrL, "Scheda Approvazione Materiali 22-2016: Sensori RTD PT100 a 4 Fili," Autostrada del Brennero SpA, Trento, 2016.
- [116] Battan Ivan SrL, "Scheda Approvazione Materiali 18-2016: Modulo di Input Analogico RTD 4 Canali PT100," Autostrada del Brennero SpA, Trento, 2016.
- [117] Battan Ivan SrL, "Scheda Approvazione Materiali 17-2016: Chassis a 8 Slot per il Montaggio delle Schede di Misura," Autostrada del Brennero SpA, Trento, 2016.
- [118] M. D. Todd, J. M. Nichols, S. T. Trickey, M. Seaver, C. J. Nichols and L. N. Virgin, "Bragg grating-based fibre optic sensors in structural health

- monitoring," *Philosophical Transactions of the Royal Society A*, vol. 365, p. 317–343, 2007.
- [119] Battan Ivan SrL, "Scheda Approvazione Materiali 23-2016: Sensore di Deformazione FBG," Autostrada del Brennero SpA, Trento, 2016.
- [120] B. Glisic and D. Inaudi, "Long-gage fiber optic sensors for global structural monitoring," in *The First International Workshop on Structural Health Monitoring of Innovative Civil Engineering Structures*, 2002.
- [121] Battan Ivan SrL, "Scheda Approvazione Materiali 30-2016: Reading Unit per 56 Sensori di Deformazione in Fibra Ottica BFG," Autostrada del Brennero SpA, Trento, 2016.
- [122] Battan Ivan SrL, "Scheda Approvazione Materiali 25-2016: Gruppo UPS 8 kVA," Autostrada del Brennero SpA, Trento, 2016.
- [123] E. Alpaydin, *Introduction to Machine Learning*, 2nd ed., Boston: The MIT Press, 2009.
- [124] European Committee for Standardization, *Eurocode: basis of structural design*, 2002.
- [125] D. Tonelli, *Solving Decision Problems through a Mechanical Equivalent of Expected Utility Theory*, Trento: University of Trento, 2016.
- [126] H. B. Mitchell, *Multi-Sensor Data Fusion: an Introduction*, Berlin: Springer, 2010.
- [127] D. Zonta, F. Bruschetta, R. Zandonini, M. Pozzi, M. Wang, B. Glisic, D. Inaudi, D. Posenato and Y. Zhao, "Sensor fusion on structural monitoring data analysis: application to a cable-stayed bridge," *Key Engineering Materials*, vol. 569, p. 812–819, 2013.
- [128] B. H. Kim, T. Park, H. Shin and T. Yoon, "A comparative study of the tension estimation methods for cable supported bridges," *Steel Structures*, vol. 7, no. 1, p. 77–84, 2007.
- [129] D. J. Ewins, *Modal Testing, Theory, Practice, and Application*, 2nd ed., New York: Wiley, 2000.
- [130] B. H. Kim and T. Park, "Estimation of cable tension force using the frequency-based system identification method," *Journal of Sound and Vibration*, vol. 304, no. 3–5, p. 660–676, 2007.

- [131] D. H. Sigurdardottir and B. Glisic, "Neutral axis as damage sensitive feature," *Smart Materials and Structures*, vol. 22, no. 7, 2013.



The average age of strategic constructions in the Western world is becoming higher and higher. Many of these structures need inspection, maintenance or replacement, resulting in significant costs. The accurate estimate of structural condition can make operators optimize the allocation of resources. Nowadays, the progress of technology and machine learning has made structural health monitoring appealing to the agencies that manage important structures. This has encouraged the research community in the study of new structural health monitoring methods. In spite of this, the use of monitoring data is often disregarded by practitioners, who still prefer to gather more information and then act based on experience. Similarly, unlike the design of civil structures, the design of structural health monitoring systems is carried out based on heuristics rather than on rigorous evaluations of the expected monitoring system effectiveness. In this doctoral thesis, I apply expected utility theory for the development of decision support systems to be used in structural health monitoring and I develop a procedure for the design of structural health monitoring systems that follows the scheme of semi-probabilistic structural design. The use of monitoring data in a decision support system that implements expected utility theory financially optimizes the management of civil structures. The proposed monitoring system design method enables practitioners to design monitoring systems using their experience and guarantees that the installation of a monitoring solution is financially convenient. I present the mathematical formulation for monitoring-based decision support systems and monitoring system design. Then, I propose the numerical algorithms for the development of monitoring-based decision support systems and solutions for monitoring data analysis. Finally, the proposed methods are applied to three case studies, which enabled me to discuss the application in real life and the hypotheses. The applications show also the feasibility of the proposed approaches and test the numerical algorithms.

Carlo Cappello received his master's degree in civil engineering from the University of Trento, Italy. He was a doctoral student at the same university from January 2014 to June 2017 and was a visiting student research collaborator at Princeton University from September 2014 to August 2015. His major research interests included Bayesian data analysis, statistical decision-making, pattern recognition, structural reliability and design of structural health monitoring systems. He regularly attended the main conferences in his field of interest. In 2015, he won the young researcher best paper award of the 7th International Conference on Structural Health Monitoring of Intelligent Infrastructure (Torino, Italy) and the third place in the student competition of Asia-Pacific Summer School 2015 (University of Illinois at Urbana-Champaign, IL, USA).